Ladder Polymers for Photonic Applications

Dissertation

Zur Erlangung des akademischen Grades
Doktor der Naturwissenschaften
(Dr. rer. nat.)
in der Wissenschaftsdisziplin Makromolekulare Chemie

eingereicht im
Fachbereich Chemie
der Bergischen Universität Wuppertal

Satish Amrutrao Patil

geb. am 01.07.1974
in Warwatti (B), India

Wuppertal, im Februar 2004

Devoted to my beloved parents

Satish

Die vorliegende Arbeit wurde in der Zeit von März 2001 bis Januar 2004 an der Universität Potsdam und an der Bergischen Universität Wuppertal unter der Anleitung von Herrn Prof. Dr. U. Scherf angefertigt.

Herrn Prof. Dr. U. Scherf danke ich sehr für die Überlassung des Themas dieser Arbeit, für seine stete Diskussionsbereitschaft sowie für seine persönliche Unterstützung.

Table of Contents:

List of Symbols and Abbreviations

OLED	Organic light emitting diodes
EL	Electroluminescence
FET	Field effect transistor
PPV	Poly(*para*-phenylene vinylene)
CVD	Chemical vapour deposition
ROMP	Ring opening metathesis polymerisation
MEHPPV	Poly[2-methoxy-5-(2-ethoxyhexyloxy)-*para*-phenylenevinylene]
HOMO	Highest occupied molecular orbital
LUMO	Lowest unoccupied molecular orbital
PPP	Poly(*para*-phenylene)
PF	Polyfluorene
PDHF	Poly(9,9-di-*n*-hexylfluorene)
lm/W	Lumens/Watt
δ	Chemical shift
PVK	Poly(N-vinylcarbazole)
LPPP	Ladder-type poly(*para*-phenylene)
PL	Photoluminescence
Me-LPPP	Methylated-ladder poly(*para*-phenylene)
DP	Degree of polymerization
$\overline{M}_n$	Number average molecular weight
$\overline{M}_w$	Weight average molecular weight
NMR	Nuclear magnetic resonance
ITO	Indium tin oxide
Ca	Calcium
Al	Aluminium
ASE	Amplified spontaneous emission
DFB	Distributed feedback configuration
PET	Poly(ethylene terephthalate)
Ph-LPPP	Diphenylated ladder poly(*para*-phenylene)
PEDOT/PSS	Poly(3,4-ethylenedioxythiophene)/poly(styrene-sulfonate)
ICP-OES	Inductively coupled plasma optical emission spectrometry
PFCB	Poly[N-(3,7,11-trimethyldodecyl)carbazole-2,7-diyl]

COD	Cyclooctadiene
LPPPC	Ladder poly(*para*-phenylene carbazole-2,7-diyl)
SEC	Size exclusion chromatography
LPPPMC	Ladder poly(*para*-phenylene carbazole-3,6-diyl)
PF	Prompt fluorescence
TSL	Thermally stimulated luminescence
DOS	Density of states
MDP	Molecularly doped polymers
PC	Polycarbonate
TPA	Tripenyl amine
SAM	Self-assembled monolayer

1. Introduction to conjugated polymers

1.1 History of conjugated polymers

Polymers were known as insulating materials before 1970 with a wide range of applications in various fields. In electronics and electrical applications they have been mainly used for insulating purpose due to their very high resistivity. Needless to say, polymers touch our lives as does no other class of materials in almost every kind of products.

The new advance in the field of polymer chemistry was the discovery of organic polymers with metallic properties. For many years the properties of long chain polyenes have been investigated as potential conductor or semiconductors[1]. However, the longest available polyenes chain showed a length of less than 20 vinylene units. In 1958, polymerization of acetylene to essentially infinite polyene chains had been successfully carried out in the presence of Ziegler-Natta catalysts[2]. The product of these early reactions was a fine powder of polyacetylene, the conductivity of a pellet was found to increase substantially on exposing to strong acceptors such as I_2 or AsF_5[3]. At the beginning of the 1970s, the Japanese chemist Shirakawa found that it was possible to synthesize polyacetylene films in a new way, in which he could control the ratio of *cis*- and *trans*-isomers as well as the morphology of the black coloured polyacetylene that appeared on the inside of the reaction vessel. Once by mistake a thousand-fold excess of catalyst was added. To Shirakawa's surprise, this time a beautiful silvery film appeared on the surface of the catalyst solution. Shirakawa was stimulated by this discovery. The silvery film was *trans*-polyacetylene film and the corresponding reaction at another temperature (-78 °C) gave a copper-coloured film instead. The latter film appeared to consist of almost pure *cis*-polyacetylene. This way of varying temperature and concentration of catalyst was decisive for the development ahead. In collaboration with MacDiarmid and Heeger at the University of Pennsylvania doping experiments with I_2 on these polyacetylene films leads to an increase in ten million times of the electrical conductivity. In 1977, Heeger, MacDiarmid, Shirakawa, and co-workers published their discovery in the article "Synthesis of electrically conducting organic polymers: Halogen derivatives of polyacetylene $(CH)_n$" in *The Journal of the Chemical Society, Chemical Communications*[4]. The discovery was considered as a major breakthrough. Since then the field has grown immensely, and also given rise to many new and exciting applications. These significant results have initiated a lot of further research on the physical and electrical properties of conjugated polymers. The essential structural characteristic of all conjugated polymers is their extended conjugated π-electron

system extending over a large number of monomer units. This feature results in materials with directional conductivity, preferably along the axis of the chain. However, interchain electron transfer is also necessary and can be limiting factor for the macroscopic dc conductivity.

Π-conjugated macromolecules are believed to possess a spatially delocalised band-like electronic structure[5,6]. The mechanism of electrical conductivity in these polymers is based on the motion of charged defects within the conjugated framework[7], the charge carriers have to jump from one chain to the next by hopping. The charge carriers, either positive p-type or negative n-type, are the products of oxidising or reducing certain segments of the polymer chain, the so-called effectively conjugated segments. The knowledge of the chemical nature of the interactions between conjugated polymer and the various dopants is fundamental for a real understanding of the electronic properties. Some of the well known conjugated polymers shown in Figure 1.1.

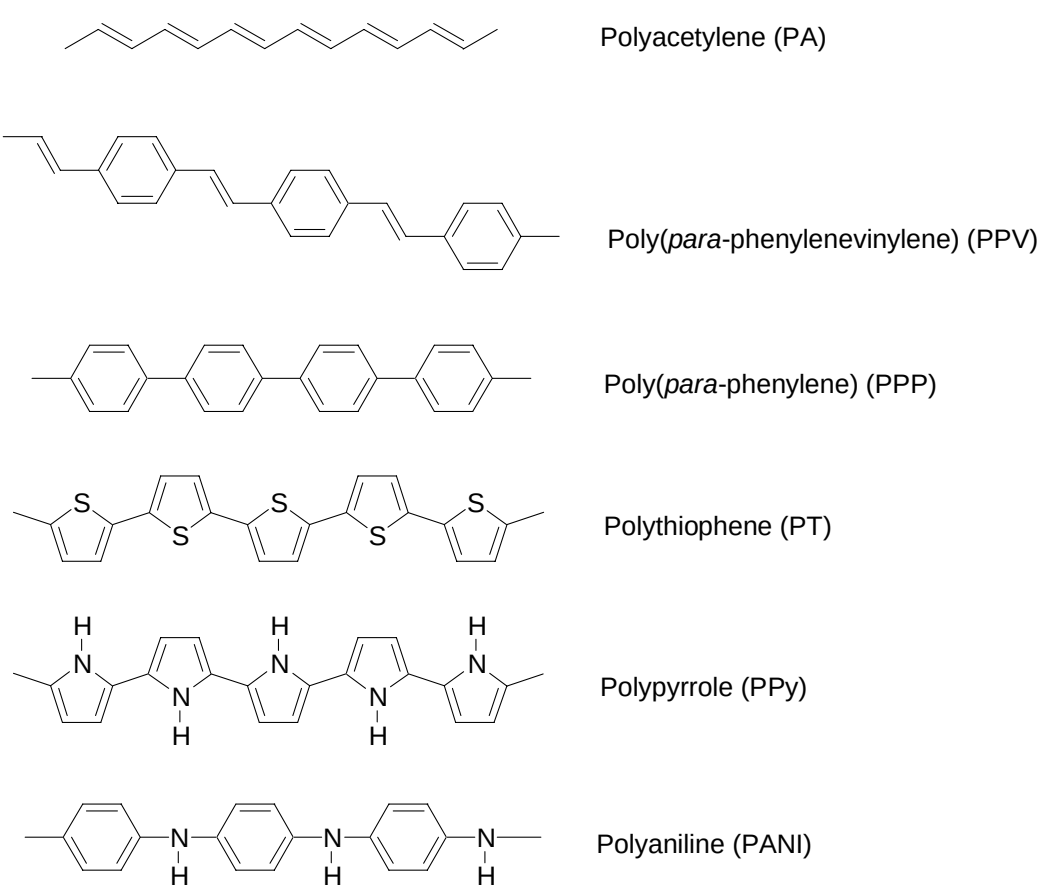

Figure 1.1 : Chemical structures of well known conjugated polymers [polyaniline is depicted in its non-conjugated, insulating state (leucoemeraldine)]

1.2 Applications of conjugated polymers

The hope for possible applications has always been one of the strong motivations behind the research in conjugated polymers. A basic idea was to combine the electronic and optical properties of conductors or semiconductors with the attractive mechanical properties and the processing advantages of organic polymers[8]. The initial interest in conjugated polymers dates from the report of metallic properties in chemically doped polyacetylene[3]. Polyacetylene and many of the other polymers that were studied at an early stage, such as polypyrrole[9] and polyaniline[10], have proved to be particularly suitable for applications as conductive materials in their doped state, but for a number of reasons were less promising as semiconductors in their non-doped, pristine state. The development of other conjugated polymers with useful semiconducting properties took almost another decade, although there were early reports of diodes made of polyacetylene[11,12]. The first report of devices with potentially useful properties date from the mid-1980s, with field effect transistors (FETs) reported by Koezuka *et al.*[13] based on electrochemically deposited poly(3-methylthiophene) films. With the availability of solution processable conjugated polymers, the scope for investigation of conjugated polymers with respectable semiconducting properties advanced rapidly. Conjugated polymers have recently received much attention due to their potential applications in electroluminescence (EL) devices. Polymeric EL materials offer a number of advantages, such as fast response time, high device performance and ease of device processability as compared to inorganic semiconductors.

1.3 Electroluminescent polymers

Electroluminescence is a non-thermal emission of light, from a solid material subjected to an external electric field. The basic requirement for organic electroluminescent materials is the capability of injection of both holes and electrons from suitable electrodes, and the ability to transport these charges efficiently. Recombination of the charged species leads to excited states (excitons), their radiative relaxation into the ground state produces the EL photons. This phenomenon have been seen in a wide range of inorganic semiconductors, and for organic semiconductors it was first reported for anthracene single crystals in the 1960[14]. Since the efficiencies and lifetimes of the resulting devices were significantly lower than those obtained for inorganic systems at the same time, research activities have been focused on inorganic materials. In the late 1980s, Tang and Van Slyke[15] as well as Saito and

Tsutsui *et al.*[16,17] demonstrated efficient electroluminescence in organic fluorescent dyes in a two-layer device with subsequently vacuum deposited organic layers. More recently, organic light-emitting diodes (OLEDs) based on semiconducting polymers have been reported, first in 1990 using poly(*para*-phenylene vinylene) (PPV) as a single semiconductor layer[18] as illustrated in Fig. 1.2. The progress in light emitting polymers have been impressive after this initial findings. Single-layer polymer light emitting diode (PLED) displays will soon be commercially available[19]. In comparison with these research and development activities, much progress have been made in the understanding of the underlying science that controls the properties of these devices. In comparison with inorganic semiconductors, relatively little is known about the fundamental optical and electronic properties of these materials, even the nature of organic semiconductor excitations remains controversial. There has been considerable progress made recently in resolving some of those issues which determine the limits of device performance e.g. related to the intrinsic electronic structure of the polymers. Some of the issues addressed are the occurrence of triplet excitons, the engineering of high luminescence efficiency in the presence of strong intermolecular interactions and also the coupling between the electronic excitations. The requirement that, the organic material should serve both as charge carrier transporting and luminescent material in high quantum efficiency OLEDs has imposed strong demand of a comprehensive understanding of the basic principle of the OLED operation.

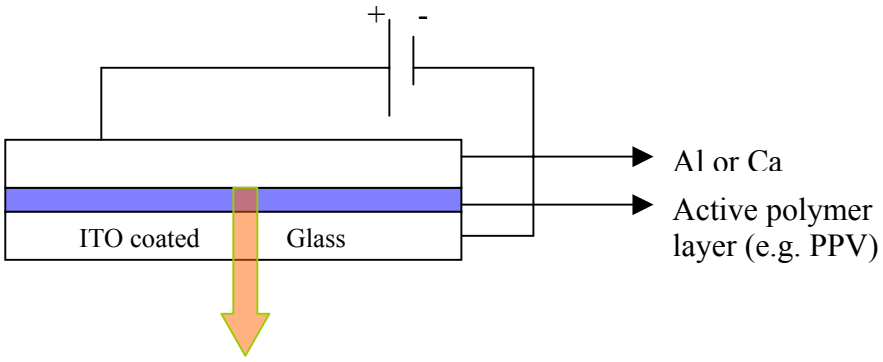

Figure 1.2 : Single-layer organic light emitting diode (OLED)

In a single-layer electroluminescent device (Fig. 1.2) the thin film of an organic light-emitting material is sandwiched between two electrodes, one of which has to be semitransparent (ITO). The operation of the device involves several steps, including charge injection, transport, capture and radiative recombination of positive and negative charge

carriers inside the organic layer to yield an efficient light emission. Under an applied voltage oppositely charged carriers (electrons and holes) are injected into the layer from the cathode and anode, and capture one another within the polymer film to form excitons. The spin wave function of the exciton, formed from two spin ½ electronic charges can be either singlet and triplet. Spin allowed radiative (fluorescence) emission is possible from singlet only, and when the exchange energy is large, as in most of the organic semiconductors, cross-over from triplet to singlet is unlikely, so that triplet excitons do not produce light emission, other than by indirect processes such as triplet-triplet annihilation[20].

The basic work mentioned above have stimulated huge academic and industrial research in organic electroluminescent material. PPV, which have been used as the first polymeric LED material shows a HOMO-LUMO energy gap of about 2.5 eV and produces yellow-green luminescence[21]. PPV itself is insoluble, intractable and infusible, any synthesis of PPV directly from a monomer produces a insoluble material, which cannot be solution processed, particularly desirable to produce high quality transparent thin films. The synthetic route most commonly used towards PPV is the so called sulfonium precursor route[22,23], a soluble non-conjugated precursor is conveniently processed from solution (methanol) and is converted to PPV by thermal treatment in the solid state (film) at temperatures of 200-300 ^{o}C. Since the quality of the resulting PPV films strongly depends on the individual processing steps, the synthetic sequence has been carefully elaborated and revised[24], in particular the influence of the conversion temperature on the film properties has been studied[25].

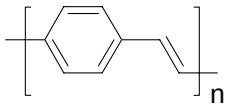

PPV **1**

PPV films have been also generated starting from soluble PPV precursors by other procedures such as layer-by-layer deposition processes taking advantage of self-assembling[26] or Langmuir-Blodgett techniques[27] in order to increase the molecular order the charge carrier transport, and consequently the efficiency of the corresponding OLED devices. Chemical vapour deposition (CVD) in combination with ring opening metathesis polymerisation (ROMP) of suitable cyclophane precursors have been also suggested as a potential alternative to the conventional sulfonium precursor route of PPV synthesis[28]. The introduction of substituents into the PPV skeleton allows for a modification of the electronic properties e.g.

band gap energy, electron affinity (EA), and ionisation potential (IP) as well as enables the solution processing of PPVs that are now soluble in organic solvents. In 1991, Heeger and Braun reported red-orange emitting PLEDs based on an unsymmetrical substituted soluble dialkoxy PPV derivative poly[2-methoxy-5-(2-ethoxyhexyloxy)-*para*-phenylenevinylene] (**MEH-PPV 2**) in a simple single-layer device configuration (ITO/MEH-PPV/Ca) with an external quantum yield of 1 %[29]. MEH-PPV **2** has been synthesized by the base-induced dehydrochlorination polymerisation of the corresponding bis(chloromethyl) derivatives (Gilch procedure).

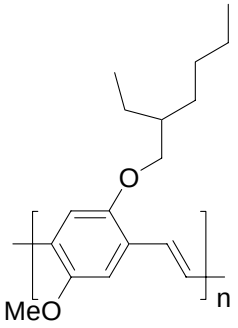

MEH-PPV **2**

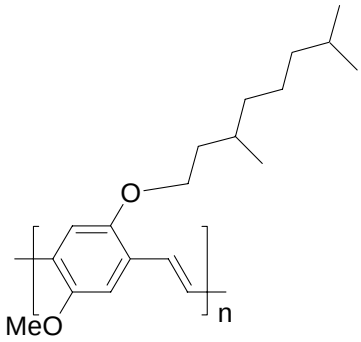

OC_1C_{10}-PPV **3**

A variety of other PPV derivatives containing alkyl[30] and alkoxy[31,32] side chains or cholestanyloxy[33] and oligoethyleneoxy[34] substituents have been synthesized by the Gilch method or Wittig and Heck-type polycondensations. PPV derivatives with at least one long solubilizing alkyl or alkoxy side chain are soluble in organic solvents such as chloroform or THF providing sufficient processability with respect to electrooptical applications[35]. In comparison to PPV, the emission maximum of dialkoxy PPVs such as MEH-PPV **2** is typically bathochromically shifted. Furthermore, long side chains separate the polymer chains from each other and hence impede the formation of non-emissive relaxation sites (aggregates or excimers). This effect seems to be advantageous with regard to high photo- and electroluminescence quantum efficiencies of corresponding PLEDs. The highest external quantum efficiency that has obtained by using soluble PPV´s reached a value of 2.1 %[37]. PPV-based single layer PLED developed at Philips in 1996 are based on a dialkoxy-substituted PPV derivative called OC_1C_{10}-PPV **3** and revealed a brightness of 100 cdm^{-2} typical for screen displays with a luminous efficiency of 1 lm/W at a low operation voltage of 2.8 V.

It is well known that in conjugated polymers electron injection is more difficult than the hole injection. One strategy to overcome this problem is the use of metals with low work functions as the cathode. Indeed, the replacement of aluminium contacts by calcium electrodes in a conventional PPV-diode typically increases the PLED efficiency of analogous devices by a factor of 10[32,36]. However, calcium is highly susceptible to atmospheric degradation. Therefore, it seems to be more advantageous to alternatively improve the electron affinity of the semiconducting polymer. Researchers at Cambridge Display Technology (CDT) first introduced this concept in 1993[37]. They attached electron withdrawing cyano groups to the vinylene bonds an dialkoxy-substituted PPVs, (MEH-CN-PPV **4** or CN-PPV **5**) which were synthesized by a Knoevenagel polycondensation of suitable monomers. A bright red fluorescent material was obtained **(CN-PPV 5)**. Internal efficiencies of 0.2 % were reported for a single-layer configuration Al/CN-PPV/metal, independent of the cathode material used for the device fabrication (Al or Ca).

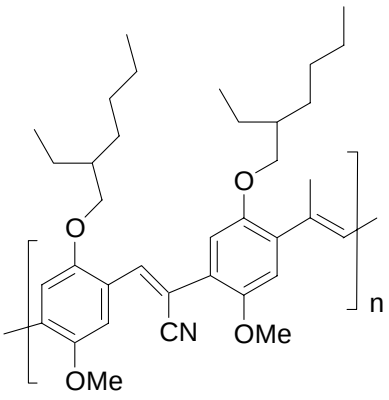

MEH-CN-PPV **4**

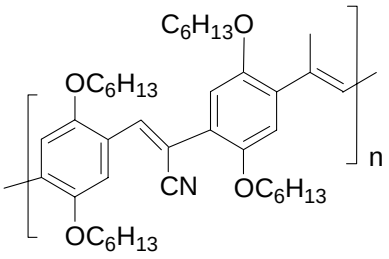

CN-PPV **5**

Multicolour display applications require at least three basic colours: red, green and blue. Although all three principle colours have been demonstrated in PLEDs, only green and red PLEDs materials currently meet the requirements for commercial uses. Blue light-emitting polymers for commercial use are still under developed. Blue emission is already difficult to achieve with inorganic semiconductors because of the high HOMO-LUMO energy gap and has been problematic in the case of semiconducting polymers too[38]. The design of blue emitting electroluminescent polymers based on PPV-type structures with interrupted main-chain conjugation suffers from the drawback that the emission occurs usually from the longest conjugated segments. The emission spectrum is therefore often broadened.

1.4 Blue light emitting polymers

1.4.1 Poly(*para*-phenylene) and derivatives

As mentioned above a high HOMO-LUMO gap is required for blue light emission. Leising *et al.*[39] were the first to describe the use of poly(*para*-phenylene) **(PPP 6)** as a blue light emitter in PLEDs [λ_{max}= 459 nm]. PPP is (similar to PPV) insoluble and difficult to process. The synthesis of PPP again requires a precursor route. A major task for semiconducting polymer researcher was to make PPPs soluble in common organic solvents without loosing the characteristic electronic and optical properties. Several research groups introduced suitable alkyl, aryl or alkoxy groups onto the PPP backbone (Fig.1.3). Monoalkoxy substituted PPPs, poly[2(2´-ethylhexyloxy)-1,4-phenylene] **(EHO-PPP 7)**, poly(2-decyloxy-1,4-phenylene) **(DO-PPP 8)** and poly[2-(6´-cyano-6´-methylheptyloxy)-1,4-phenylene] **(CN-PPP 9)** are soluble in common organic solvents[40,41].

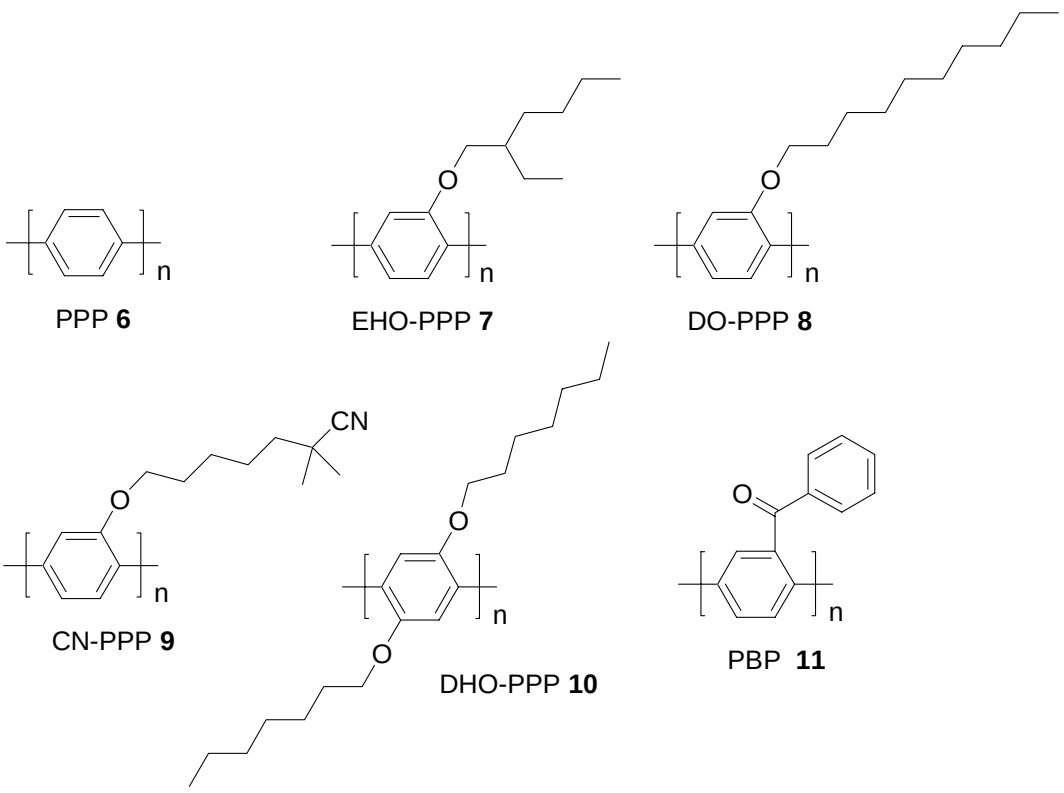

Figure 1.3: Poly(*para*-phenylene) and its derivatives

The polymers CN-PPP, EHO-PPP and DO-PPP show very similar absorption and PL spectra, with PL and EL maxima around 420 nm. The conjugation length of these polymers is shortened compared to that of PPP due to distortion of the main chain caused by the *ortho*-substituents. Other PPPs with alkoxy substituents (octyl, dodecyl or heptadecyl) on position 2 of the phenylene unit also show very similar absorption and PL spectra[42]. The side chain length of the alkoxy groups does not give a significant effect on the length of the effectively conjugated segment of the alkoxy substituted PPPs. Poly(2,5-diheptyloxy-1,4-phenylene) **(DHO-PPP 10)** obtained by an oxidative coupling of 1,4-diheptoxybenzene with $FeCl_3$ shows a PL maximum in the film at 400 nm with a strong second peak at 500 nm[33]. These results suggests that the preparation of this polymer by oxidative coupling polymerisation produces a defect rich polymer, causing a second emission component in the long wavelength region.

The benzoyl substituted poly(2-benzoyl-1,4-phenylene) **(PBP 11)** is also soluble in common organic solvents (e.g. toluene, chloroform-etc) and thermally stable up to 400 ^{0}C[43]. A thin film of PBP shows the PL maximum at 433 nm, slightly shifted to higher energy than that of unsubstituted PPP but shifted to lower energy as compared to alkoxy substituted PPPs. The quantum yield for the solution PL of PBP **11** in chloroform was measured to be 15 %.

1.4.2 Polyfluorenes

Because of their good solubility, high solid state fluorescence quantum yields and high chemical stability, alkyl substituted polyfluorenes (PFs) (Fig. 1.4) have attracted considerable interest as a semiconducting blue light emitter[44]. 9,9-Dialkyl–2,7-dibromofluorene monomers have been coupled by the nickel(0) mediated reductive polycondensation after Yamamoto to the desired poly(9,9-dialkylfluorene)s[45]. The first PLED of blue emission colour was fabricated in 1991 by using poly(9,9-di-*n*-hexylfluorene) PDHF **12** by spin casting a film from a solution in chloroform[46]. The EL spectrum of PDHF exhibited an emission maximum at 470 nm with a shoulder at 420 nm and a FWHM of ca 200 nm. However, the broad emission spectrum indicates multiple emission components from different chromophores including defects. The alkyl chains at position 9 of the fluorine unit do not influence the absorption, PL and EL spectra but improve the solubility of the polymer in organic solvents.

Poly(9,9-di-*n*-hexylfluorene) **12** have been used as a blue light emitter in multicolour devices[47]. The dioctyl substituted analogue **13** has been employed in a highly efficient blue emitting PLED with luminous efficiencies up to 8.2 lm/W[48]. But, unfortunately films of polyfluorene derivatives reveal an unstable blue electroluminescence, as operation time increases a yellow componenent is emerging that can be assigned to the formation of keto (fluorenone) defects[49,50].

12 **13**

Figure 1.4: Fluorene based polymers

1.4.3 Polymers with carbazole units

Carbazole based polymers (Fig. 1.5) are attractive materials for blue light emitting diodes. Non-conjugated poly(N-vinylcarbazole) (PVK **14**) have been used as a hole transporting and emissive material and emits light in the blue region at 410 nm[51]. PVK can be generated by both free radical and cationic polymerization of N-vinylcarbazole[52]. But, since PVK is a non-conjugated polymer the PLEDs fabricated with PVK emissive layers show poor quantum yields[51].

Non-conjugated poly(N-alkyl-3,6-carbazole)s **15** have been also studied in PLED[53,54]. The synthesis of conjugated N-alkyl–2,7-carbazoles **16** have been developed recently by Leclerc *et al.*[55]. These polymers are soluble in organic solvents and emit blue light in PLED devices without excimer formation[56].

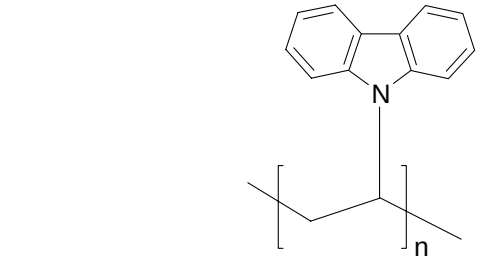

14

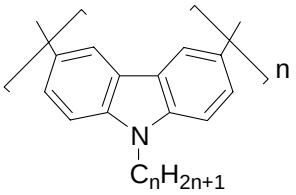

15

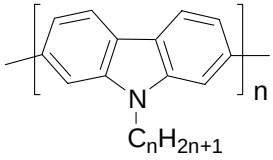

16

Figure 1.5: Carbazole-based polymers

1.4.4 Ladder-type poly(*para*-phenylene)s

A ladder-type poly(*para*-phenylene) (LPPP) have been first synthesized by Scherf *et al.*[57] in 1991, the PPP backbone is here incorporated into a rigid, double-stranded ladder structure. All benzene rings in this ladder structure are arranged in the same plane, the polymer exhibits a good solubility in organic solvents. Both absorption and PL maxima of the polymer solution in toluene are between 450-460 nm with a very small Stokes shift due to the rigid structure of the conjugated backbone. The history, synthesis and physical properties of this promising class of blue emitting polymer is described in more detail in the following chapter.

2 History and synthesis of ladder polymers

2.1 History of ladder polymers

A ladder polymer is defined as a "uninterrupted series of rings connected by sterically restrictive links around which rotation cannot occur without the breaking of a bond"[64].

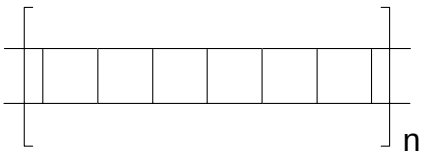

"Classical" ladder Polymer

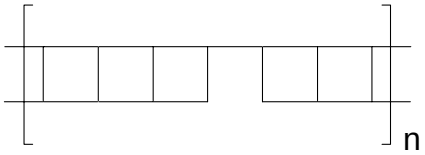

"Imperfect" ladder or step ladder polymer

Conjugated ladder polymers possess a planarized π-electron system which ensures optimum electron delocalization. Theory predicts that such materials will exhibit outstanding electronic properties including siginificant third-order susceptibilities[58]. Ladder polymers are predicted to show a high thermal stability and a high resistance to chemical degradation[59]. In order to have all these unique properties perfect ladder polymers are required. However, in practice, it is often difficult to bring nearly perfect ladder structures for experimental realization. There are many reasons for these difficulties. First, many ladder polymers are insoluble in common solvents and precipitate from solutions before reactions are complete. This deficiency not only leads to the formation of low molecular-weight products but also leads to incompletely cyclized structures. Without a doubt, the synthesis of a perfect ladder polymer is a real synthetic challenge. In the case of ladder polymers, two independent strands have to be generated without defects or crosslinking. In the early 1970s poly(benzimidazobenzophenanthroline) (BBL **17**) was synthesized and it was discovered that this ladder polymer is readily processible into durable films using casting or spraying techniques[60,61].

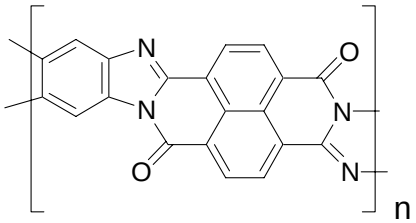

BBL **17**

Several other ladder polymers were than synthesized and a few ladder polymers gained some industrial importance as materials for high-temperature applications such as heat-resistant coatings e.g. in aerospace vehicles.

2.2 Synthesis of ladder polymers

Attempts to generate ladder polymers have a long history, but ladder polymers prepared at the initial stage showed a poor solubility, due to their rigid structure. Many synthetic efforts have been made to bring soluble ladder polymer to an experimental realization. A new generation of substituted, soluble ladder polymer have been made using the following improved approaches:

1. Novel polycondensation methods e.g. repetative Diels-alder reaction[62]
2. Polymer-analogous cyclization of single-stranded linear prepolymers[63-64]

Most of the known synthesis of ladder polymers fall into the these two methods. But it is essential to prevent side-reactions and to take care of an almost quantitative conversion of the starting materials. It is beyond the scope of this chapter to cover all the history of ladder polymers. We will deal with the conjugated poly(*para*-phenylene)-type (LPPP) ladder polymers. The polymer-analogous cyclization of suitable single-stranded precursors have been successfully applied to synthesize such polyphenylene-based conjugated ladder polymers.

2.3 Polymer-analogous cyclization of single-stranded linear prepolymers

This synthetic approach to conjugated ladder polymers of the LPPP-type involves a two-step procedure in which (1) a soluble precursor polymer is synthesized via polycondensation of suitable monomers, followed by (2) polymer-analogous cyclization with generation of the double stranded structure. By optimization of the substitution pattern and the reaction conditions it was possible to control the regiochemistry of the final reaction step (see LPPP synthesis on page 16). The key to defect poor structures are transformations with complete regioselectivity. This is essential for the synthesis of structurally defined ladder polymers[57]. The successful route have been extended to the synthesis of a other arylene ladder polymers (Fig. 2.1) composed of different building blocks.

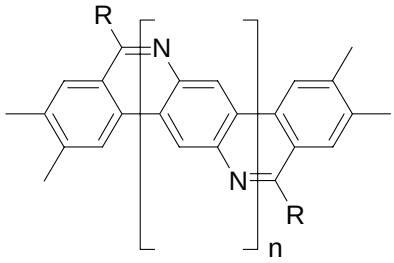

R: -C_nH_{2n+1}

18

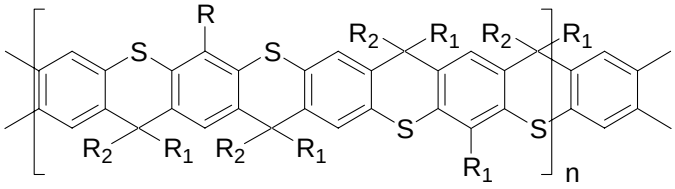

R: -1,4-C_6H_4-C_nH_{2n+1}
R_1: -CH_3, -H
R_2: -CH_3

19

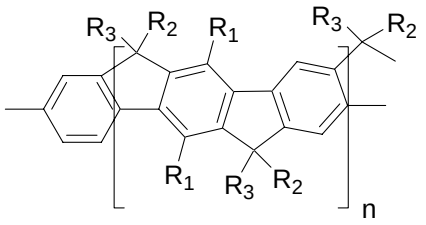

R_1: n-C_6H_{13}
R_2: -1,4-C_6H_4-n-$C_{10}H_{21}$
R_3: H

20

Figure 2.1: Arylene-type ladder polymers

2.4 Polyphenylenes (PPPs)

Poly(*para*-phenylene) (PPP) is an interesting class of conjugated polymers from both an academic as well as an industrial point of view because of its excellent chemical resistance (due to the lack of functional groups), considerable thermal and photostability, high electrical conductivity in the oxidized (doped) state and its blue electroluminesence[65,66]. The structure of PPP consists of a rigid aromatic backbone of linearly arranged *para*-phenylene moities. PPP can be readily synthesized e.g. by the oxidative coupling of benzene with $CuCl_2/AlCl_3$ after Kovacic or by the reductive dehalogenation of 1,4-dibromobenzene (see fig. 2.2). However, PPP is insoluble, intractable and very difficult to process. One way to overcome this shortcoming is to introduce flexible alkyl or alkoxy chains onto the backbone of PPP.

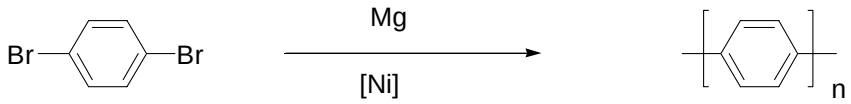

Figure 2.2: Synthesis of PPP

Schlüter *et al.* first synthesized soluble alkyl substituted PPPs (see fig. 2.3) by a Suzuki cross-coupling method with a molecular weight $\overline{M}_n$ of ca. 10,000 which corresponding to chain of ca. 100 phenylene rings[67].

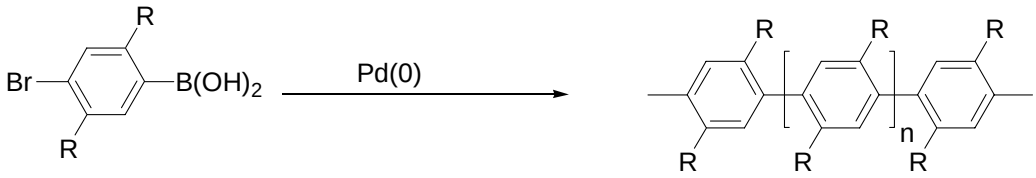

Figure 2.3 : Synthesis of soluble PPP (R= alkyl, alkoxy)

However, the final product behaves remarkably different from unsubstituted PPP. The material obtained was soluble in common organic solvents, which enables a thorough analysis of its structure and molecular weight. NMR spectroscopy and vapor pressure osmometry showed that the alkyl chain substituted PPP has degree of polymerization (DP) of approximately 100[68]. However, the attachment of alkyl side chains onto the main PPP backbone has some serious drawbacks. The introduction of the alkyl side chains onto the PPP backbone force a distortion of neighbouring phenylene rings out of planarity. The dihedral angle between the two neighbouring phenylene rings increases due to the repulsive interaction of the *ortho* hydrogens. The optical and electronic properties however strongly depend on the conformation of the main chain. Although small deviations from coplanarity (<30-40°) do not considerably affect the optical and electronic properties of such conjugated polymers a higher mutual distortion of the main chain phenylene units e.g. induced by *ortho* alkyl substituents leads to drastic changes, e.g. a hypsochromic shift of the longest wavelength absorption maximum (λ_{max}), a reduction of the photoluminescence quantum yield, and a reduced charge carrier mobility[69,70].

However, as already mentioned, the flexible side chains guarantee the solubility of the polymers in common organic solvents. Therefore, the challenge is to synthesize a PPP-type

polymer by combining both good processibility and minimum conformational twisting. Scherf *et al.* were the first to solve this synthetic problem[71]. They demonstrated that a careful design of functionalized monomers allows the generation of fully conjugated ladder polymers (LPPP) with maximum π-conjugation in the main chain. In the first step a Suzuki-type cross coupling of an aromatic dibromodiketone with an aromatic diboronic acid in the presence of a palladium catalyst leads to an open chain precursor polymer. The Suzuki-type condensation is a very efficient method for the coupling of the starting materials. Dibromonomers containing electron-withdrawing functional groups such as nitro or keto can be condensed with high efficiency. In order to increase the solubility of the final polymer, flexible *n*-hexyl side chains were introduced into the aromatic diboronic acid, the benzoyl groups of the dibromonomer have been decorated with *n*-decyl side chains. The open chain PPP precursor (polyketone) produced by the Suzuki-type cross coupling possesses a number average molecular weight ($\overline{M}_n$) of around 10,000-20,000 (Fig. 2.4), which corresponds to the chain of ca. 25-50 phenylene rings. Moreover, the two alkyl substituents of the boronic acid building block guarantee a regioselective ring closure in the last reaction step since there are no structural alternatives to the two remaining positions.

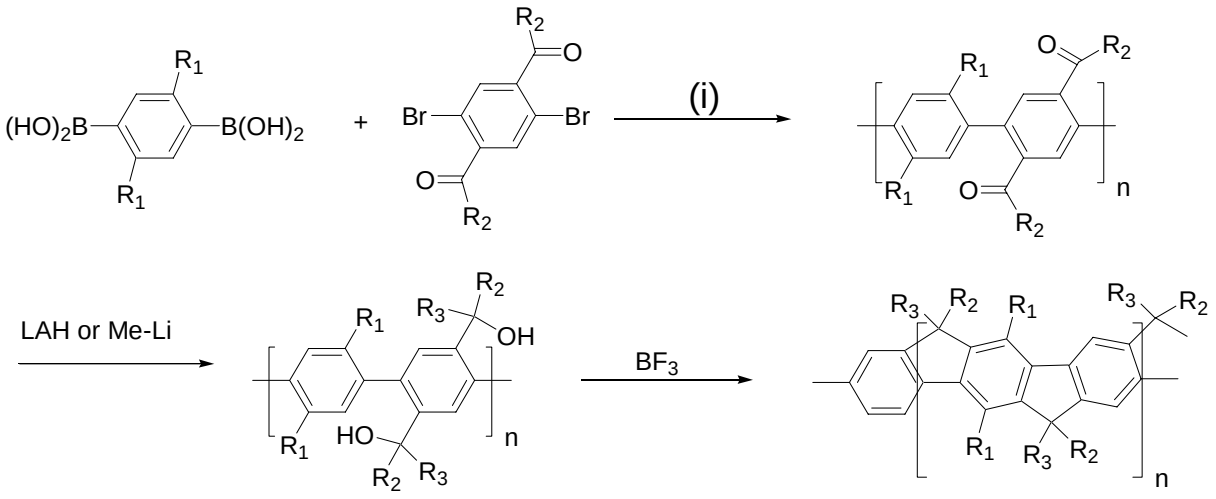

(i) $Pd(PPh_3)_4$, toluene/H_2O/Na_2CO_3 ; (R_1 = *n*-C_6H_{13}; R_2 = -1,4-C_6H_4-*n*-$C_{10}H_{21}$ and R_3 = H) (LPPP) or CH_3 (Me-LPPP)

Figure 2.4 : Reaction scheme towards poly(*para*-phenylene) ladder polymers (LPPP)

A general catalytic cycle for the Suzuki-type cross-coupling reaction involves (1) oxidative addition, and (2) transmetalation followed by (3) elimination of the product as shown in Fig. 2.5. The oxidative addition is often the rate determining step in the catalytic cycle [72]. Electron withdrawing groups on the aryl halide increases the reactivitiy towards the palladium(0) catalyst. The mechanism of the transmetalation step is not well understood as it is highly dependent on reaction conditions used for the coupling. It is known that the transmetalation between the organopalladium halide and the organoboron compound normally does not occur readily due to the low nucleophilicity of organic group at the boron center. However, the above reaction is carried out under basic conditions so that the nucleophilicity of the boron atom is enhanced via the formation of so-called *"ate"* complexes with negatively charged base. When a Lewic acid combines with a base to give an anion in which the central atom has a "higher than-normal" valence the resulting species is called *"ate"* complex (e.g. $Ar\text{-}BL_3^{\ominus}$) Such *"ate"* complexes can undergo a clean coupling reaction with organic halides.

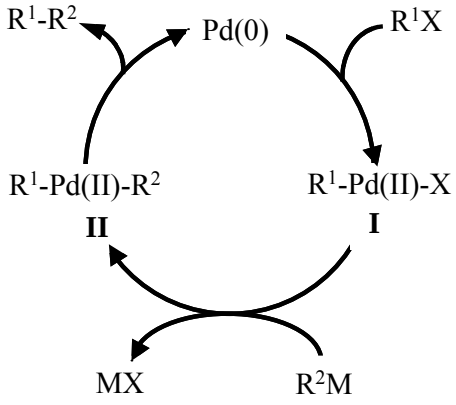

Figure 2.5: A general catalytic cycle for Suzuki cross-coupling

As mentioned above, it was found that electron accepting keto substituents on the aromatic dibromo monomer increase the rate of aryl-aryl coupling. In order to synthesize the final planar ladder polymer the open precursor was first transformed into a polyalcohol by reduction with lithium aluminium hydride (LAH) in a mixture of toluene/THF or preferably, by the addition of Me-Li. The final ring closure reaction was carried out in dichloromethane with boron trifluoride etherate as Lewis-acid catalyst, under formation of LPPP (R_3 = H) or Me-LPPP ($R_3 = CH_3$).

Immediately after the addition of BF_3 a strongly blue fluorescent solution of the ladder polymer is generated. The final ladder polymer is deep yellow in colour and shows a very intense blue photoluminescence in solution. This polymer has been fully characterized by means of ^{1}H and ^{13}C NMR-spectroscopy and has no sign of structural ir-regularities within the detection limit of the methods, such as incomplete cyclization or intermolecular crosslinking. The challenge in the intramolecular cyclization step is the suppression of side reactions (crosslinking), or a quantitative conversion of the functional groups is needed to obtain perfect ladder polymers. There have been many serious doubts raised in the literature concerning feasibility of the concept[62]. However, a carefuly selection of the starting compounds e.g. with bulky *n*-alkylated phenyl substituents suppresses any intermolecular crosslinking. It is noteworthy that the cyclization reaction is not successful in the absence of the bulky aryl substituents at the benzylic bridge position. In such cases cross-linked, insoluble products are formed via intermolecular Friedel-Crafts reaction upon treatment with the Lewis acid. To increase the chromphorically active part of the ladder polymer the synthesis have been modified. Instead of using an aromatic dibromodiketone, 2,5-dibromoterephthalic dialdehyde was used to couple with the dialkylated phenylene diboronic acid. This leads to a open chain polymer precursor with main chain aldehyde functional groups (Fig. 2.6).

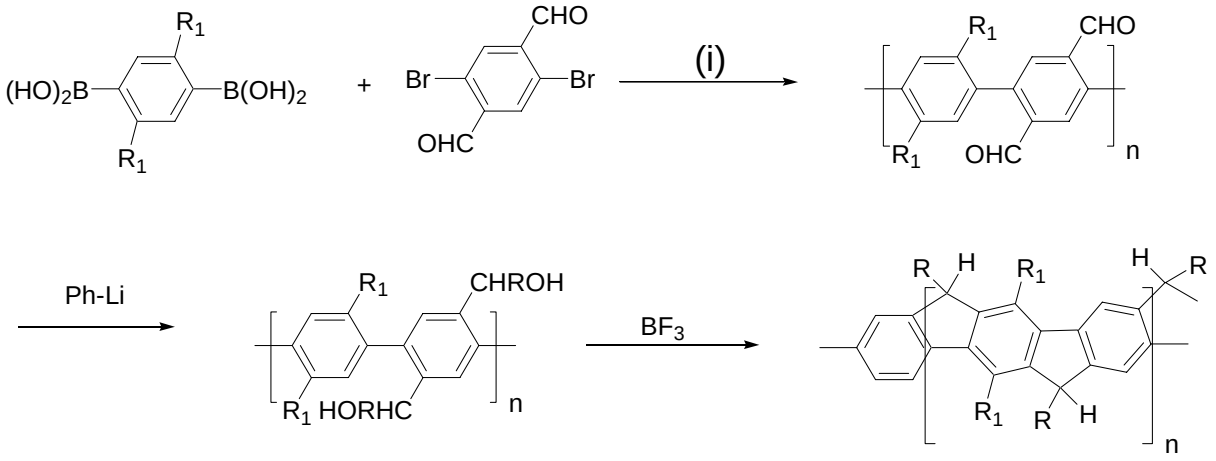

(i) $Pd(PPh_3)_4$, toluene/H_2O/Na_2CO_3; (R = H and R_1 = *n*-C_6H_{13})

Figure 2.6: Synthetic scheme for the formation of ladder-type poly(*para*-phenylene) (modified procedure)

The aldehyde precursor has a number average molecular weight of ca. 7,000 corresponding to ca. 40 phenylene rings per chain. The next two steps are similar to the

preperation of LPPP/Me-LPPP in converting the open chain precursor into the final ladder polymer. The main advantage of this modified route lies in the great variety of side groups which can be attached to the macromolecule. Thus an increase in the chromophorically active part of the molecule can be obtained. Also following this protocol unwanted side-reactions can occur leading to an incomplete ladder formation, especially if aliphatic substituents are introduced. Outstanding features of LPPP-type polymers are their photo- and electroluminescence properties. Due to the fixed and rigid geometry of the macromolecule, they show an extraordinarlly small Stokes shift with a mirror-symmetrical shape of absorption and emission (Fig. 2.7). In solid state often an additional low energy emission feature at ca. 2.2 eV is detectable in the yellow region. The origin of this emission is up to now not fully understood, there have been many controversial remarks regarding this feature in the literature[73].

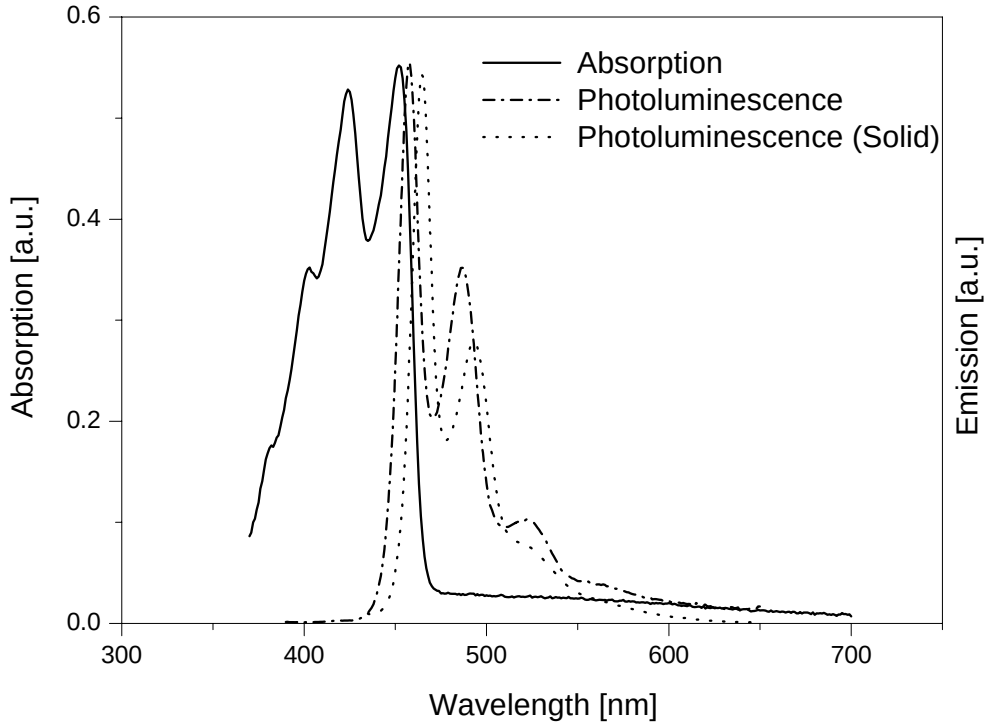

Figure 2.7: Absorbption and emission spectra of Me-LPPP

Solid state aggregation as well as defect formation have been used to explain the behaviour. Recent experiments however, supports the presence of emissive defects (keto

defects)[74]. LPPP-type polymers show the occurance of a highly efficient electroluminescence[75]. The outstanding optical properties of the LPPP-type polymers tempted strongly for detailed investigation of the photophysical properties. The photoconductivity of the poly(*para*-phenylene) ladder polymers is nearly as high as that of unsubstituted poly(*para*-phenylenevinylene) (PPV) one of the best polymeric photoconductors yet known[76].

2.5 Device Fabrication for LED

Tasch *et al.* were the first to fabricate efficient blue PLEDs by using Me-LPPP as an active layer. They used the single layer device structure (ITO/Me-LPPP/Ca) to fabricate the device. They found high external EL quantum yields of up to 4 % with blue emission at a relatively low electrical field of ca. 0.5 MV cm^{-1}[77].

Me-LPPP is also characterised by a high charge carrier mobility which is not at all common in amorphous conjugated polymers. The reason for the often observed low charge carrier mobilities is the conformational disorder leading to a trapping of charges at defects. A value of more than 10^{-3} cm^2 Vs^{-1} was measured for Me-LPPP (hole mobility μ at room temperature) with an external electric field E of 4-6 MV/cm using time-of-flight measurements[78]. This high value is quite significant as compared to other conjugated polymers like PPV and its derivatives and is only two orders of magnitude below that of crystalline anthracene[78]. The explanation for this unusal characterstic of Me-LPPP is its defect-poor structure. Photoconductivity of Me-LPPP films have also been investigated by using the xerographic technique [79]. The energy of half discharge of thin Me-LPPP films is about 2.5 $\mu J/cm^2$ which is comparable to commercially availiable red light sensitive double-layer photoactive systems. Thus, Me-LPPP could be a promising candidate as a active layers in blue laser printers[76].

The occurance of the two above mentioned properties, namely high EL efficiencies and the defect free structure makes this material a promising candidate for a solid state organic polymer laser. Optically pumped solid state dye lasers had been realized long before in the form of dye molecules doped into different matrices[80]. A key ingredient for any laser is a sufficiently high effective stimulated emission cross section. In most of the conjugated polymers the stimulated emission is rather weak due to a competition with photoinduced

absorption processes[81]. The efficient stimulated emission of Me-LPPP was first observed in "pump and probe" experiments in 1995[82], a amplified spontaneous emission (ASE) could be observed for spin coated Me-LPPP films on quartz substrates during continous increase in the excitation energy. A considerable narrowing of the PL spectrum was observed above a threshold energy of ca. 25 μJ/cm^2, when a Me-LPPP film was optically pumped with fs laser pulses at 400 nm[83].

In order to realise real lasing it is necessary to apply appropriate resonator geometries. That could be demonstrated for Me-LPPP films using two different resonator geometries. In a first device lasing was observed in an open cavity configuration, whereby the polymer film was spin coated onto one of the two mirrors. With an optimally adjusted mirror distance an opticaly pumped single-mode laser emission at ca. 585 nm resulted which was characterised by a linewidth of less than 1 nm[84]. In the second case the lasing was demonstrated by using nanostructured PET foils as distributed feedback (DFB) resonators.

The organic substrate allows the generation of flexible devices. Nanostructured poly(ethylene terephthalate) (PET) foils have been coated with Me-LPPP films (see fig. 2.8). For this geometry under optical pumping at 400 nm an unusally low lasing threshold energy of about 1.5 nj/pulse was measured in attaining a single-mode blue laser emission at ca. 487 nm with a line width of less than 0.4 nm[85]. As next step experiments towards electrical pumping of the laser device are planned.

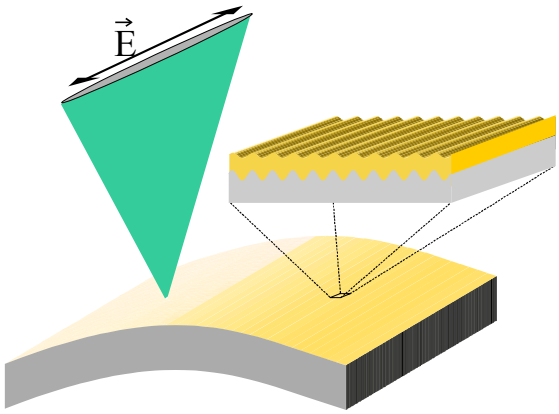

Figure 2.8: Flexible polymer laser device where a nanostructured PET film acts as a distributed feedback (DFB) resonator is coated with a Me-LPPP film

In addition to the lasing properties, Me-LPPP have been extensively investigated for other different potential applications e.g as two photon absorber or in photovoltaics[86]. Me-LPPP have recently gained much interest for its high two photon absorption cross section[87]. Me-LPPP shows a two-photon absorption cross-section which is one of the highest reported for conjugated polymers or oligomers[88]. But there are still some unsolved problems: One is the yellow emission component in the solid state due to formation of defects via oxidation or photoxidation[89]. The synthetic challenge is to modify the Me-LPPP basic structure to end up with materials which show pure blue light emission. A second problem is related to the presence of triplet excitations in all PLED devices. We have synthesized a new LPPP derivative which astonishgly shows an intense steady-state electrophosphorescence at room temperature. The synthetic details as well as optical and electronic properties of this polymer will be described in the next chapter (chapter 3).

3. Electrophosphorescence in a novel ladder type poly(*para*-phenylene) derivative

3.1 Introduction

Recently conjugated polymer-based light emitting diodes (PLEDs) are rapidly emerging in display technology. A large number of light emitting polymers have been introduced during the last ten years. In parallel with the development of new polymers, much progress has been made in understanding of the underlying science of PLED devices. Although, a lot of research have been carried out to understand the device physics of inorganic or molecular crystal-based LEDs, it is not possible to adopt the principles developed for these systems to PLEDs. The most polymeric materials used in organic light emitting diodes form disordered, amorphous films without a macroscopic crystal lattice. In contrast to inorganic semiconductors, impurities usally act as traps rather than sources of mobile charge carriers. There has been considerable progress made in resolving some of the issues which determine the limits of PLED device performance.

In a single-layer electroluminescent device the thin film of the light emitting material is sandwiched between two electrodes. If an external voltage is applied, oppositely charged carriers (electrons and holes) are injected into the organic layer beyond a specific threshold voltage depending on the HOMO and LUMO of the organic material applied. The oppositely charged electrons and holes combine within the emissive material to form triplet as well as singlet excited states, so-called excitons. According to the Franck-Condon principle, only singlet excitons contribute to the light emission[90]. This is because the transition of singlet excited state (S_1) to singlet ground state (S_0) (fluoroscence) is spin-allowed but the transition of triplet excited state to ground state (phosphorescence) is forbidden[91]. The greatest puzzle relates to the role of triplet excitons in conjugated polymers. The ratio of triplet to singlet exciton generated by charge carrier recombination of electrons and holes should be 3:1 due to spin stastics rules. Although, the precise ratio of triplet to singlet excitons is currently debated very controversely and may affect the electroluminescence quantum efficiency of conjugated polymers[92]. Since the phosphorescence is very weak the only way to observe triplets in conjugated polymers directly is to study their phosphorescence spectra with time gated spectroscopic methods. Hereby, the longer living phosphorescence is detected after the decay of most of the short living fluorescence (spontaneous photoluminescence). It is difficult to observe intrinsic phosphorescence in conjugated polymers under steady-state conditions

because (i) the triplets are populated via intersystem crossing (ISC) and the ISC rate is very low in conjugated polymers due to the high energy gap (ca.1 eV) between singlet and triplet states and (ii) the triplets can be efficiently quenched at traps (defects). It has been proposed that it should not be possible to observe intrinsic triplet emission in polymer light emitting diodes (PLEDs)[93]. The following energy level diagram (Fig. 3.1) illustrates the process of fluorescence and phosphorescence in conjugated polymers.

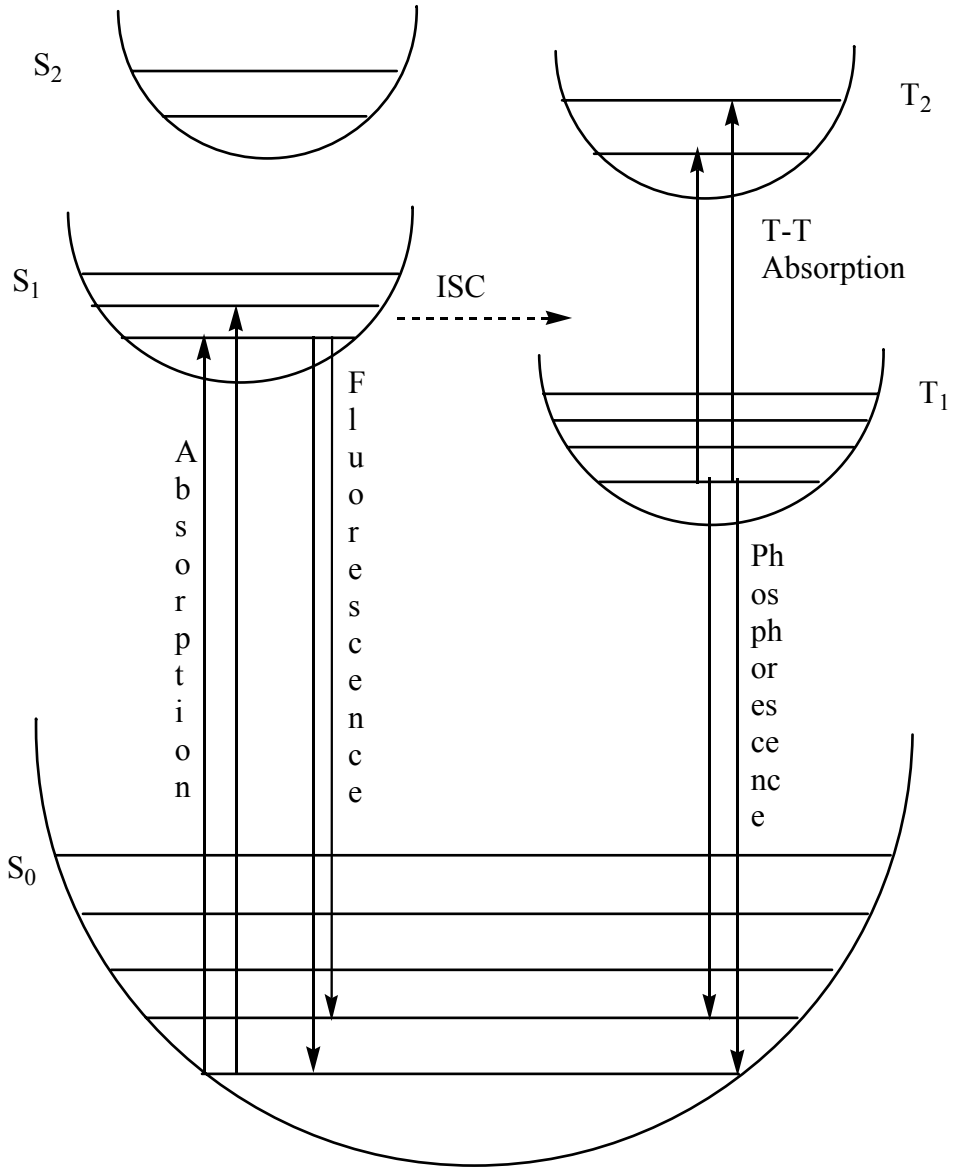

Figure 3.1: Electronic structure and photophysics of excitations in a semiconducting polymer

Several routes have been developed in order to design devices which show triplet emissions based on conjugated polymers. One approach is to dope the polymers with species

that show an efficient phosphorescence. This can be done by doping with metal complexes with a strong spin-orbit coupling. Platinum-containing porphyrins (e.g. platinum octaethyl porphyrin, PtOEP) have been successfully used as a dopant in both molecular and polymeric hosts[94]. Both singlet and triplet excitons generated in the host material are collected at the porphyrin, which shows efficient phosphorescence. The second approach is based on the chemical modification of the conjugated polymer. Heeger *et al.*[95] synthesized conjugated polymers containing iridium complexes (Fig. 3.2), the iridium complexes in the main chain serve as a triplet harvesting centers. The potential drawback with both approaches is that one disturbs the original intrinsic electronic properties of the conjugated polymers. The triplet emission colour is determined by the metal complex generally red-shifted.

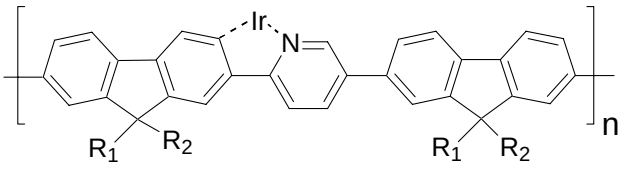

Figure 3.2: Structure of polyfluorenes containing main chain iridium complexes

We have synthesized a new poly(*para*-phenylene) ladder polymer which shows intrinsic electrophosphorescence at room temperature without a significant alternation of the original electronic properties of the polymer. Ladder-type polyphenylenes (LPPPs) are well-suited due to their high degree of purity and low level of structural disorder and were the first conjugated polymers to show weak intrinsic phosphorescence at low temperatures in time gated spectroscopical investigations[93]. We have now synthesized a novel LPPP derivative with two aryl substituents (Ph-LPPP; R_2, R_3 = aryl, see Fig. 3.3) at the methylene bridge positions, which shows very surprising emission properties.

3.2 Synthesis of Ph-LPPP

The Pd(0)-catalysed Suzuki coupling have been applied to synthesize the corresponding single chain polyarylene precursor similar to Me-LPPP[71] (as shown in fig. 3.3). The condensation reaction of 2,5-dihexyl-1,4-phenylene diboronic acid **21** with 1,4-bis(4´-decylbenzoyl)-2,5-dibromobenzene **22** provide the polyketone **23** with a number average molecular weight ($\overline{M}_n$) of ca. 7,500, which corresponds to a PPP chain composed of

ca. 20 phenylene units. The intermediate open chain precursor was characterized by NMR. The ^{1}H NMR shows broad signals of the aromatic hydrogen atoms at 7.0-8.0 ppm and signals of the aralkyl substituents at 2.53 and 2.32 ppm. The ^{13}C NMR-spectrum exhibits 10 signals of nonequivalent aromatic carbons with an additional peak of the keto group at 196.8 ppm. The single-stranded precursor have been further converted to polyalcohol **24** by reacting with phenyl lithium (Ph-Li). The final ring closure reaction of **24** to the planar ladder polymer **25** was carried out in dichloromethane with boron trifluoride etherate as the Lewis-acid catalyst. The number-average molecular weight ($\overline{M}_n$) of **25** was 10,000 (after soxhlet extraction with acetone for three days) determined by gel permeation chromatography using polystyrene as a standard. The increase in $\overline{M}_n$ results from some fractionation during the work-up of the reaction mixtures. The final ladder polymer **25** was fully characterized by ^{1}H and ^{13}C NMR-spectroscopy. The ^{13}C NMR spectrum of **25** displays ca. 10 signals of 14 nonequivalent carbons (Fig. 3.4) in the aromatic region and the signal of the diphenylmethylene bridge carbon at 64.5 ppm. The phenylmethyl-methylene bridge carbon in Me-LPPP for comparision displays a signal at 54.0 ppm[71]. The signals of the keto group of **23** at 196.8 ppm as well the signals of the alcohol group (-Ar-CHOH-Ar-) of **24** at 75.0 ppm are not detectable.

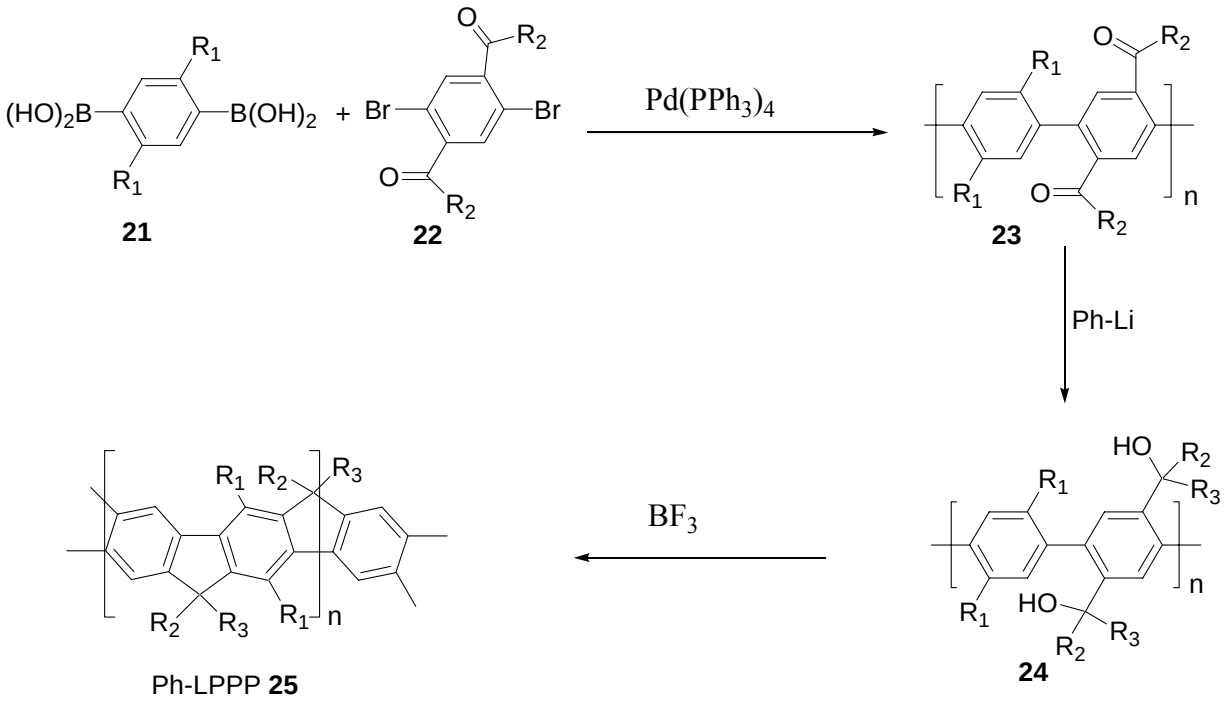

(R_1 = n-C_6H_{13}; R_2 = 1,4-C_6H_4-n-$C_{10}H_{21}$ and R_3 = C_6H_5)

Figure 3.3: Formation of diphenyl-substituted *para*-phenylene ladder polymer (Ph-LPPP)

The ^{1}H NMR-spectrum of the final ladder polymer shows broad signals of the aromatic protons at 7.0-8.0 ppm. The α-methylene group of the main chain hexyl substituents ($-CH_2-C_5H_{11}$) as well as the side chain decyl substituents ($-CH_2-C_9H_{19}$) displays a signal at ca. 2.50 ppm.

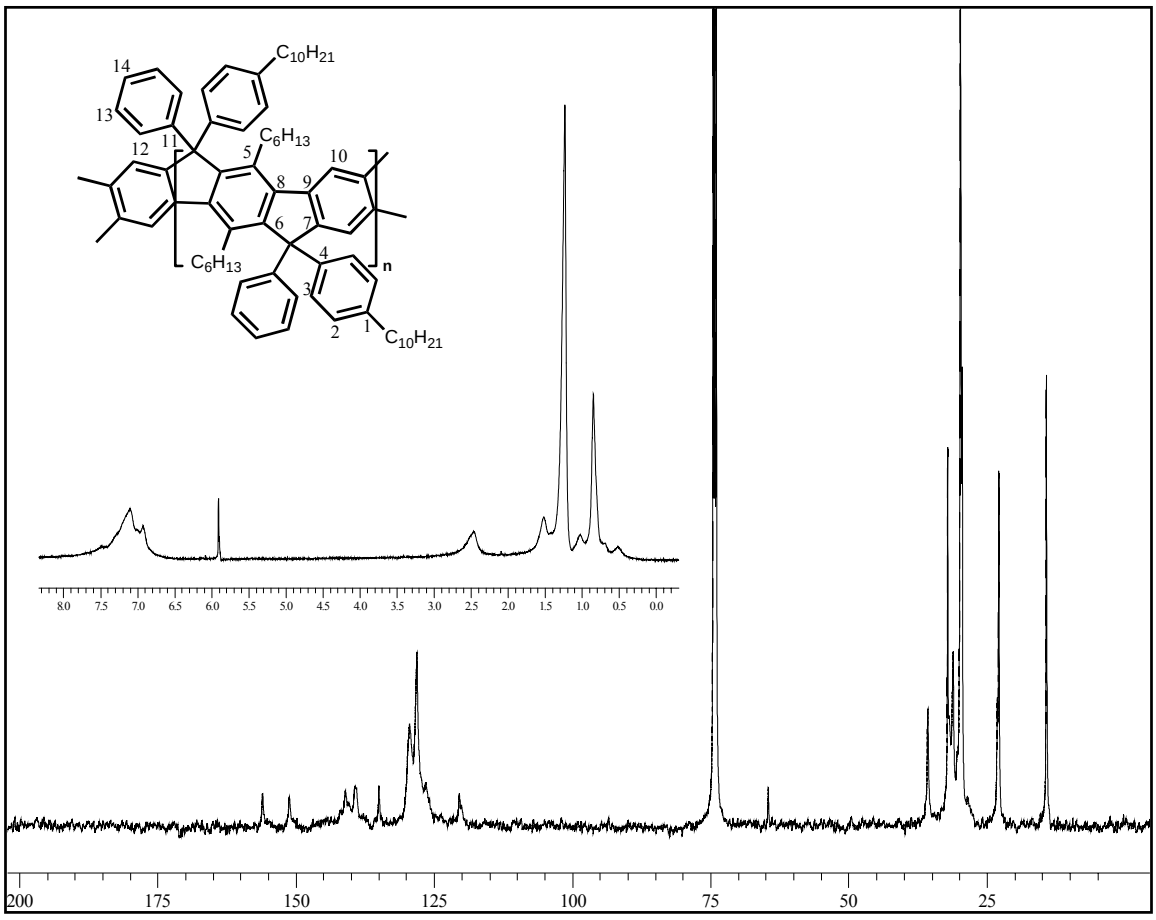

Figure 3.4: ^{1}H and ^{13}C NMR-spectra of Ph-LPPP

3.3 Optical and photophysical properties of Ph-LPPP

Figure 3.5 shows the optical properties of Ph-LPPP (absorption and photoluminescence) in dilute solution (chloroform). The absorption maximum peaks at 455 nm with a vibronic side band at 425 nm. The photoluminescence (PL) of Ph-LPPP is intense blue and peaks at 459 nm upon excitation at 415 nm, with a quantum yield of 80 % (chloroform, at room temperature). The Stokes shift between absorption and emission is extremely small, which indicates a rigid backbone structure with only weak geometrical changes during the transition from the ground into the excited state. In comparision with Me-

LPPP this polymer shows a very similar characteristic, which indicates the occurance of a planar backbone structure.

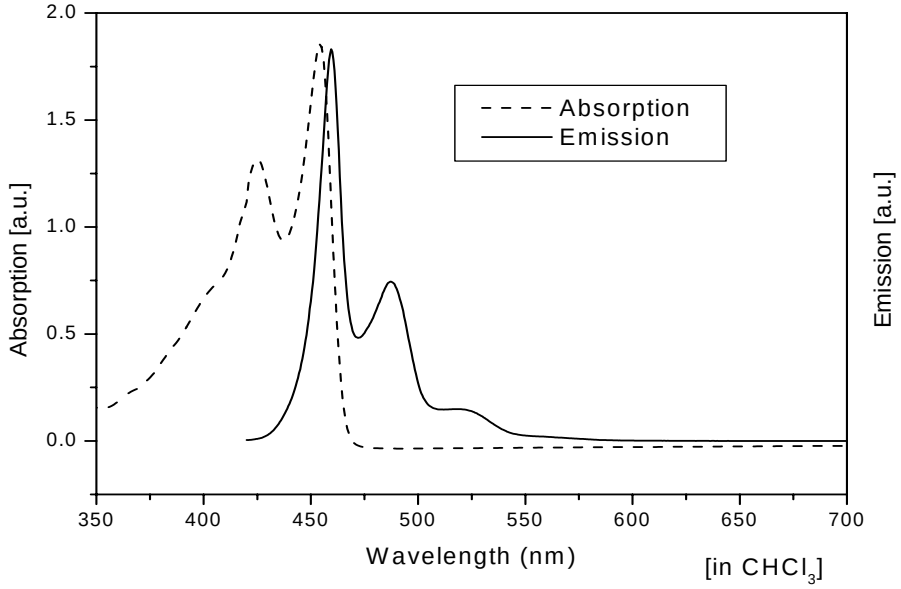

Figure 3.5: Absorption and emission spectra of Ph-LPPP (in solution).

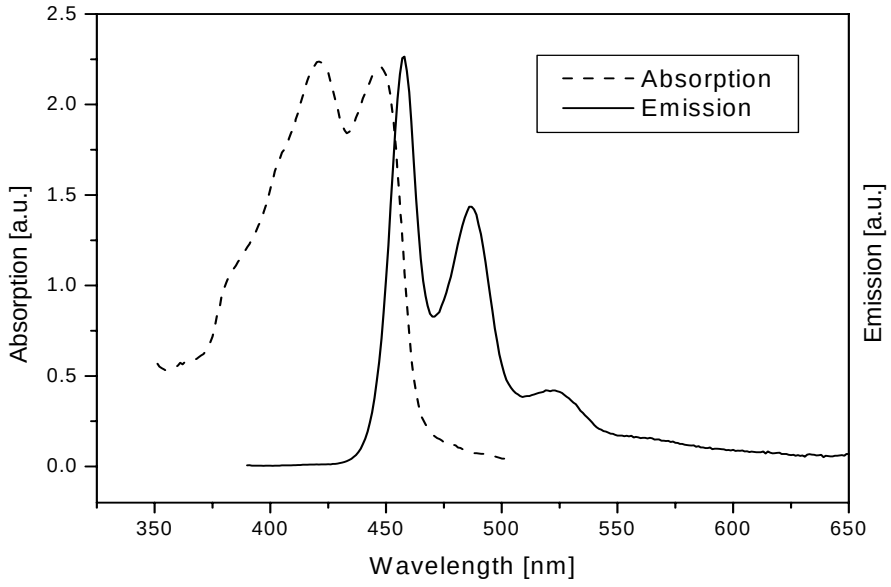

Figure 3.6: Absorption and emission spectra of Ph-LPPP (in film).

However, the optical properties of Ph-LPPP in the solid state (Fig. 3.6) shows one more weak peak in yellow region. In addition to the blue photoluminescence of the Ph-LPPP

chromophore [λ_{max} (emission) 460 nm], a weak second PL component appears. The latter is bathochromically shifted into the yellow region of the spectrum [λ_{max} (emission) 540-600 nm]. The interpretation for this characteristic of Ph-LPPP in the solid state is the presence of a small amount of keto defects similar to what have been previously found in polyfluorenes[50]. The keto defects are probably formed in an oxidative side reaction during the addition of Ph-Li and the ring closing reaction with BF_3.

3.4 Electroluminescence measurment of Ph-LPPP

The electroluminescence of Ph-LPPP was investigated in collabaration with the groups of John Lupton (LMU, Münich) and Emil List (TU, Graz) in simple two layer LED devices as depicted in Figure 3.7. The device configuration was ITO/PEDOT:PSS/Ph-LPPP/Al. A charge transport layer (50 nm) of poly(3,4-ethylenedioxythiophene)/polystyrene sulfonate (PEDOT/PSS) was deposited on the ITO layers in order to improve the device performance.

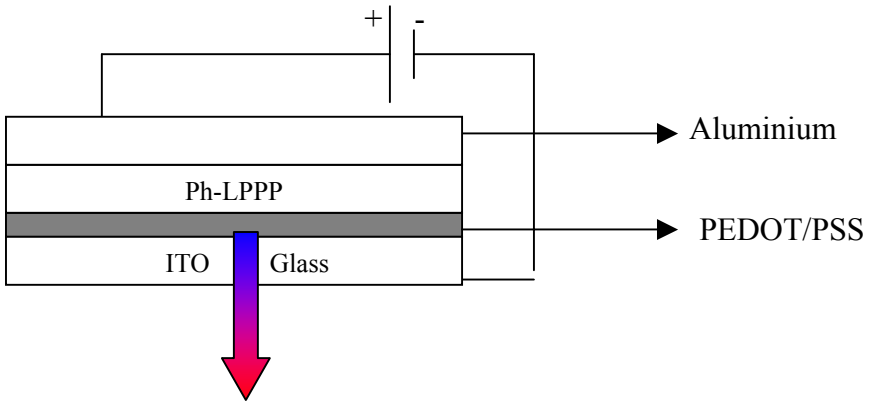

Figure 3.7: LED device by using Ph-LPPP as the active layer

Figure 3.8 shows a comparison of EL and PL spectra of Ph-LPPP layers. Both spectra exhibit the typical spectral PL characteristic of LPPPs. The S_0-S_1 (0-0) transition band of the PL spectrum peaks at 460 nm and is followed by a vibronic feature displaced by 0.2 eV to higher energy. This band is due to spontaneous emission from S_1 (fluorescence) and is short living. The occurrence of a second emission feature in the EL spectrum at 600/650 nm is very surprising. Whereas the high energy EL band coincide with the PL spectrum of the Ph-LPPP singlet exciton[77], the lower energy feature observed only in EL corresponds to the previously observed triplet emission of Me-LPPP reported under gated detection at low temperatures[96].

We found that the ratio between the 600 nm and the 460 nm band depends sensitively on the operating voltage/current and on the sample temperature. The 600 nm band was found to decrease substantially with increasing driving voltage and decreasing temperature.

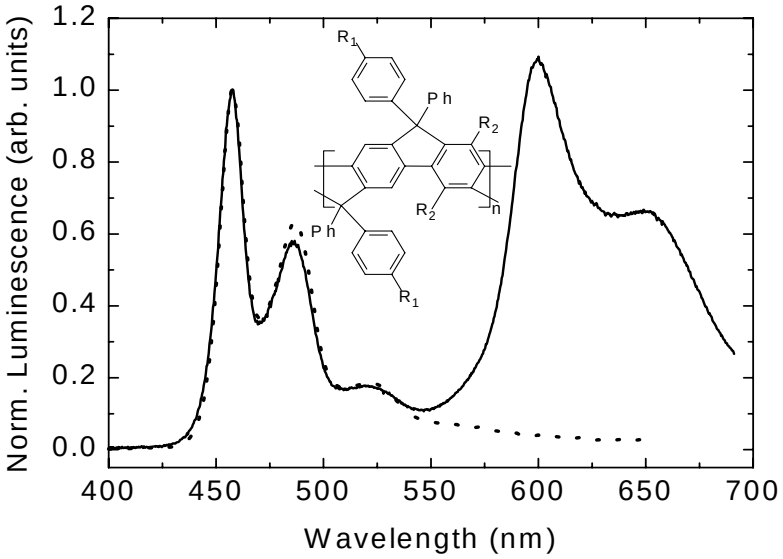

Figure 3.8: EL (——) and PL (···) spectra of the diphenyl-substituted poly(*para*-phenylene) ladder polymer Ph-LPPP.

The above evidence leads us to the conclusion that the 600 nm emission band results from triplet excitations (electrophosphorescence). However, there should be also evidence for phosphorescence at room temperature under optical excitation. Therefore, we performed time-gated PL spectroscopy on thin films of Ph-LPPP. Figure 3.9 shows normalized PL spectra detected at different delay times, which were recorded on thin films of Ph-LPPP using a frequency-doubled mode-locked titanium-sapphire laser operating at 380 nm and a repetition rate of 80 MHz, as well as a Hamamatsu streak camera coupled to a 0.5 m monochromator with a 50 lines/mm grating. The spectrum is found to broaden rapidly within the first 40 ps. After 1 ns delay all of the singlet emission has decayed and a broad band centered at 560 nm with shoulders at 530 nm and 600 nm is observed. After 3 ns delay the broad 560 nm band is overlaid by a narrow band centered at 600 nm, with a vibronic shoulder at 650 nm. A scenario of this behaviour is the following 1) First the short living singlet emission is observed at 460/480 nm; 2) followed by an emission component of keto defects at ca. 560 nm; 3) at longer detection times, the long living phosphorescence peaking at 600/650 nm becomes dominant.

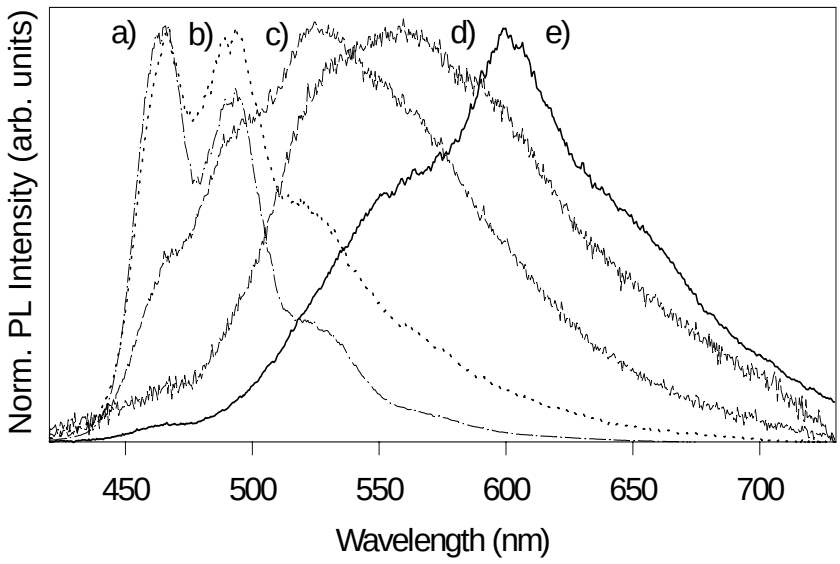

Figure 3.9: Delayed PL spectra of Ph-LPPP excited at 380 nm and detected after a) 0-40 ps; b) 100-140 ps; c) 300-400 ps; d)1-2 ns; e) 3-4 ns.

To clarify the origin of the electrophosphorescence at room temperature, we performed a detailed elemental analysis of our polymers in order to identify heavy metal impurities (especially Pd, since Pd catalysts have been used in the synthesis of Ph-LPPP), which may open a radiative decay route for triplet excitons. The heavy metal (Pd) analysis has been done by inductively coupled plasma optical emission spectrometry (ICP-OES). This technique is popular for elemental analysis of metal traces. ICP is applicable to around 73 elements and provides fast multi-element analysis with superior detection limits to atomic absorption spectrometry (AAS) for many elements. Two ladder polymers (Me-LPPP and Ph-LPPP) were analysed by this technique to compare the palladium content. The palladium concentration in methyl substituted Me-LPPP was < 2 ppm, a distinctly higher concentration of 80-150 ppm was found in Ph-LPPP, also after careful purification by repeated chromatography and reprecipitaion steps[97]. The increased incorporation of Pd in Ph-LPPP is thought to result from the high affinity of Pd impurities present after the first Pd-catalysed coupling steps to phenyl lithium, which is used in the second step of the reaction sequence to Ph-LPPP. Transmetallation to phenyl-palladium species and their subsequent reaction with polymeric intermediates (e.g. the keto precursor **23**) should lead to a covalent incorporation of some palladium centers into the polyphenylene backbone[98]. In contrast, the methyl lithium used in the synthetic sequence towards Me-LPPP possesses a much lower affinity to

palladium incorporation. However, it is difficult to predict the exact structure around the Pd centers because the Pd-content is too low, common characterization techniques (NMR) are not applicable.

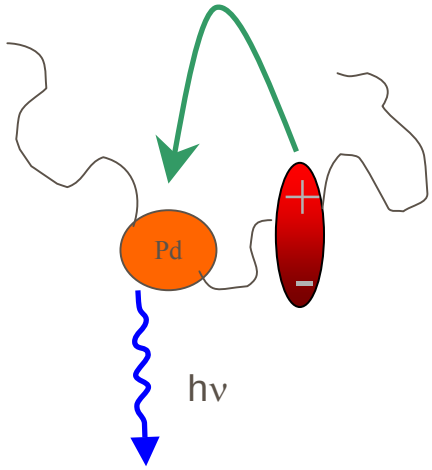

Figure 3.10: Mechanism of triplet harvesting and phosphorescence at palladium sites in Ph-LPPP

In order to further prove that, the emission feature observed at 600/650 nm in the delayed PL spectra is due to phosphorescence, Lupton *et al.* probed the sensitivity to ambient oxygen[99]. Figure 3.11 depicts the change in delayed emission 3 ns after excitation upon purging the vacuum chamber with air and re-evacuating. For an increase in base pressure from 10^{-4} mbar to 1 mbar the 600 nm feature almost vanishes, as seen in Figure 3.11a. As the chamber pressure is increased further, the broad 560 nm feature increases. Upon evacuation the 560 nm feature is found to decrease again, as seen in Figure 3.11b. Below a pressure of 10^{-3} mbar the phosphorescence band partially reappears and increases further in intensity as the pressure is lowered. The insets depict the same spectra on a logarithmic scale normalized to the 560 nm emission. The broad band at 560 nm is also observed in the delayed PL spectra of dilute solution albeit of substantially weaker intensity. It is therefore, as already discussed most likely related to keto defects as in the case of polyfluorenes[50], rather than aggregates or excimers[100].

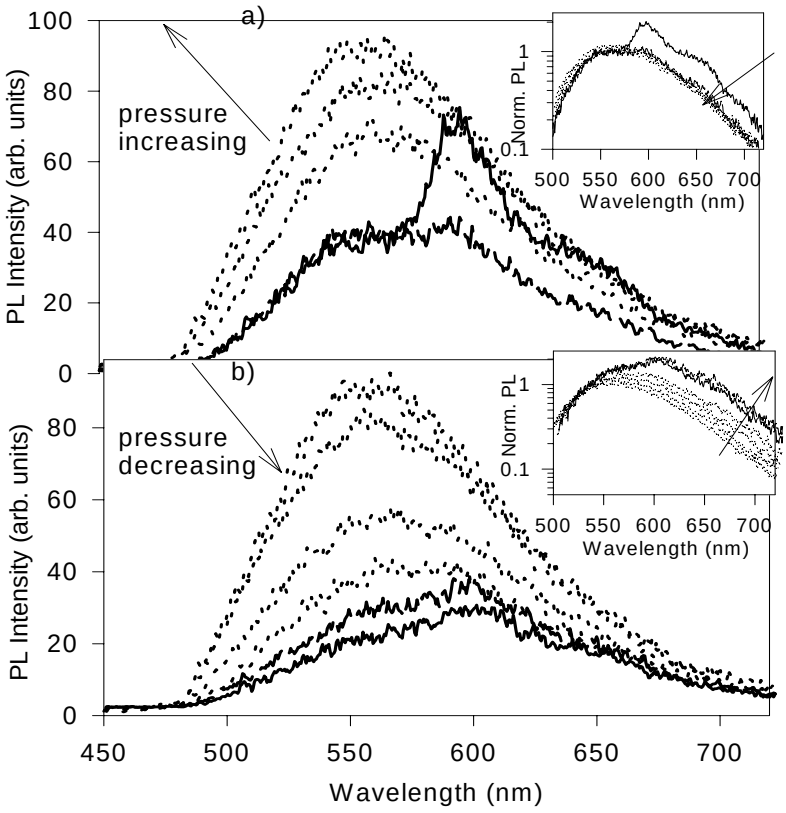

Figure 3.11: Delayed PL spectra of Ph-LPPP detected in a 1 ns window at 3 ns after excitation in dependence of vacuum pressure. a) pressure increasing from bottom to top from 10^{-4} mbar (——), 1 mbar (---) to atmospheric pressure (···). b) decreasing pressure on the same sample spot from top to bottom from atmospheric pressure (···) to 10^{-3} mbar (---) to 10^{-4} mbar (——). The insets show the same spectra normalized to the band at 560 nm.

The results show that, the incorporation of trace amounts of a heavy metal (Pd) to the polymer backbone leads to efficient steady-state phosphorescence at room temperature. The scenario occurring in the OLED device can be explained as follows: electrically generated triplets migrate through the host polymer during their extended lifetime and either relax non-radiatively or recombine radiatively on a Pd containing site as shown in Figure 3.10.

In contrast to previously reported heavy metal (Pt) containing metalorganic polymers, with their limited applicability in optoelectronic devices due to problems with stability and purity as well as due to their low PL quantum yields the Ph-LPPP results are very promising. Towards Ph-LPPP, we did not change the basic chemistry and did not loose the very favorable electronic properties of the LPPP system, but we activated an effective phosphorescence channel [101,102]. Therefore, one can follow the intrinsic properties of triplet

excitons without any addition of external dopants. We thus demonstrate experimentally that the underlying assumption made by Wilson *et al.*[101], that the properties of triplet excitons derived from a polymer system strongly perturbed by the presence of metal atoms in each repeat unit are comparable to those of metal free polymers. The present system provides the energetically most efficient way of harvesting triplet excitons, which has up to now been demonstrated by the incorporation of phosphorescent metal complexes into a polymeric or molecular host[94,90].

In general, these results demonstrate that we can reproducibly synthesize Ph-LPPP successfully with palladium contents of 80-150 ppm as found in three different batches of Ph-LPPP. All these batches show similar electrophosphorescence behaviours. One may intuitively anticipate that this ladder polymer open the doors for further triplet studies and could help in the development of electrically driven polymer lasers.

4. Carbazole containing polymers

4.1 Introduction

Polymers containing carbazole moieties in the main chain have attracted much attention because of their unique properties which allow various photonic applications such as in photoconductive, electroluminescent and photorefractive materials[103]. Some examples of polymers containing carbazole moieties in the main chain include poly(N-vinylcarbazole), poly(carbazole)s[104], poly(carbazolylenevinylene)[105] and poly(carbazolyleneethynylene)[106]. Carbazole-based polymer derivatives have been studied in organic light emitting diodes as a hole transporting material[53,54]. The most widely applied material is poly(N-vinylcarbazole) (PVK) as a vinyl polymer with side chain carbazole functions. Light-emitting devices with PVK as a host and a narrow-band laser dye as a guest have been extensively studied[107].

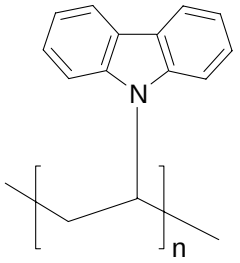

PVK

In the class of poly(carbazole)s, poly(N-alkyl-carbazole-3,6-diyl)s derivatives are described but they don´t possess an uninterrupted π-conjugation. Recently, Leclerc *et al.* reported the first synthesis of conjugated homo and copolymers derived from N-alkyl-2,7-carbazole building blocks[55]. These new conjugated polymer materials are particularly promising as emitters in blue light emitting diodes (PLEDs) because they contain a bridged biphenyl unit without bulky *ortho*-substituents similar to polyfluorene. However, blue light emitting polyfluorenes show problems connected to their poor colour stability of the solid state emission due to the presence of keto defects which produces long wavelength emission components and decreased fluorescence quantum yields[50]. Interestingly, polycarbazoles do not show the formation of keto defects[56]. By considering all these points we have started to synthesize novel carbazole-based homo and copolymers as well as novel ladder-type poly(*para*-phenylene carbazolylenes)s containing the polar carbazole group within the main chain. All these polymers are soluble (or partially soluble) in common organic solvents due to

substitution with long alkyl chains e.g. at the N-position of the carbazole unit. The substituents are introduced at positions which do not lead to significant increase of the steric hindrance in the polymer backbone. The permanent dipole moment of the carbazole moiety is expected to influence the optoelectronic properties e.g. to increase the two photon absorption cross section. This class of new ladder polymers is particularly promising for the future development of light emitting diodes, polymer lasers and optical limiters.

4.2 Synthesis of monomers

4.2.1 N-(3,7,11-trimethyldodecyl)-2,7-dichlorocarbazole

The synthesis of 2,7-carbazole derivatives is difficult due to the presence of 3,6-electron rich positions in carbazole ring. Recent reports on carbazole homopolymers show low molecular weights and a poor solubility in common organic solvents[55]. These relatively modest molecular weight and the poor solubility can be tentatively explained by a low degree of substitution, flexible side chains being required to obtain both soluble and high molecular weight conjugated polymers. We have, therefore synthesized 2,7-dichlorocarbazoles with a long, branched alkyl chain at the N-position of the carbazole ring in order to synthesize soluble carbazole-based polymers. As shown in Figure 4.1, N-(3,7,11-trimethyldodecyl)-2,7-dichlorocarbazole have been synthesized in three steps. In the first step, the Suzuki coupling between 4-chlorophenylboronic acid **26** and 1-bromo-4-chloro-nitrobenzene **27** in the presence of Pd(0) in a mixture of benzene and aqueous K_2CO_3 gives 1-chloro-4-(4´-chlorophenyl)-2-nitrobenzene **28** in a high yield (97 %). Subsequently, it can undergo a reductive Cadogen ring closure using triethyl phosphate to yield 2,7-dichlorocarbazole **29.** Finally, the alkylation of the nitrogen atom in DMF/K_2CO_3/alkyl bromide leads to N-(3,7,11-trimethyldodecyl)-2,7-chlorocarbazole **30** in 87 % yield.

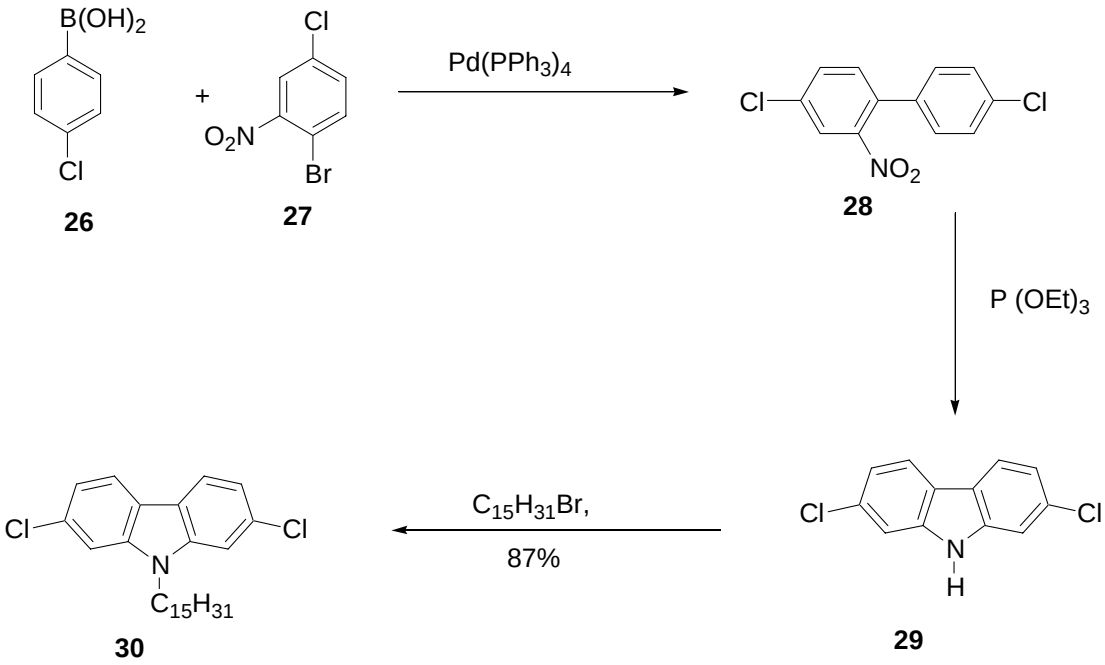

Figure 4.1: Synthesis of N-(3,7,11-trimethyldodecyl)-2,7-chlorocarbazole

The structure of the compounds **28, 29** and **30** have been confirmed by NMR spectroscopy and mass spectrometry. The ^{1}H NMR-spectrum of compound **30** shows two doublets at 7.80 and 7.19 ppm in the aromatic region. These peaks belongs to the protons at positions **b** and **c** of carbazole ring (shown in Figure 4.2) and one singlet at 7.30 for the proton at position **a** of the carbazole ring. A triplet at higher field (δ: 4.07 ppm) belongs to the protons of the α-methylene group of the alkyl chain. The multiplet at 3.4 ppm is due to some remaining alkyl chloride. A complete separation of the final compound **30** from the excess of alkyl chloride was not successful, e.g. by column chromatography. The mixture was used in the following reactions without further purification.

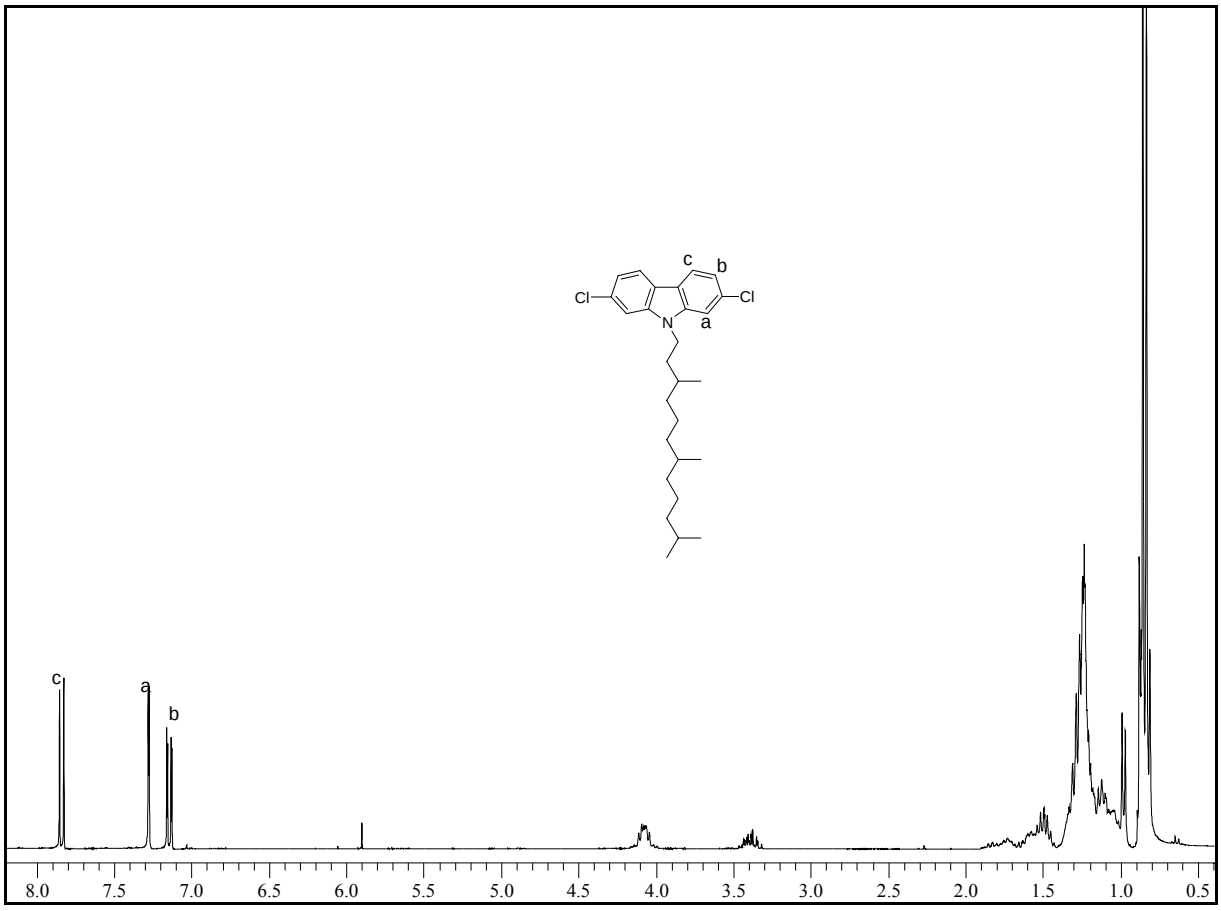

Figure 4.2: ^{1}H NMR-spectrum of N-(3,7,11-trimethyldodecyl)-2,7-dichlorocarbazole

4.2.2 Synthesis of N-alkyl 2,7-bis (4´,4´,5´,5´-tetramethyl-1´,3´,2´-dioxaborolan-2´-yl) carbazole

The palladium-catalyzed Suzuki cross coupling reaction of aryl bromides, aryl iodides and pseudohalides (e.g. triflates) with organoboron reagents has become one of the most utilized methods for the formation of carbon-carbon bonds[108]. Organoboron reagents (e.g. boronic acid, boronic ester) are a prerequisite for Suzuki couplings[72]. In order to synthesize carbazole based polymers by employing Suzuki-type coupling, we have synthesized 2,7-diboronic esters of carbazole. The synthesis of N-alkyl-2,7-bis(4´,4´,5´,5´-tetramethyl-1´,3´,2´-dioxaborolan-2´-yl) carbazole have been carried out in six steps as shown in Figure 4.3. The Suzuki-type coupling between 4-methoxyphenylboronic acid **31** and 4-bromo-3-nitroanisole **32** under standard conditions yields 1-methoxy-4-(4´-methoxyphenyl)-2-nitrobenzene **33** with high conversion (81 %). This step is followed by a Cadogen ring closing reaction in hot triethyl phosphate to give 2,7-dimethoxycarbazole **34**. The alkylation of **34** at

the nitrogen atom leads to N-alkyl-2,7-dimethoxycarbazole **35**. This reaction was carried out under inert atmosphere using finely powdered NaOH, a phase transfer agent (tetrabutylamonium hydrogensulfate), and 1-bromoalkane (1-bromooctane or 1-bromo-3,7,11-trimethyldodecane as shown in Fig. 4.5) in anhydrous acetone. The N-alkyl-2,7-dihydroxycarbazole **36** was generated by using the standard ether cleavage reagent BBr_3 in methylene chloride in 55 % yield. Finally, N-alkyl-2,7-dihydroxycarbazole **36** was converted to N-alkyl-2,7-bis(trifluoromethylsulfonyl)carbazole **37** by reacting **36** with trifluoromethanesulfonic anhydride in cold pyridine with DMAP as catalyst. This N-alkyl-2,7-bis(trifluoromethylsulfonyl)carbazole can be used in Stille- or Suzuki-type polycondensations by reacting with an appropriate partner (e.g. a diboronic acid or a bistannyl compound). Finally, **37** can be further converted to the corresponding diboronic ester **38** by reacting with pinacolborane and a $PdCl_2$(dppf) catalyst. which is more suitable for Suzuki-type couplings with dibromo monomers. The diboronic ester is not stable on common silica gel, it degrades on silica gel while purifying with column chromatography. Therefore, the crude dark red oil was purified by column chromatography on triethyl amine pre-treated silica gel (deactivated silica) with 5 % ethyl acetate in hexane as a eluent.

The structure of all compounds have been confirmed by NMR and mass spectrometry. These analysis confirmed that the N-alkyl-2,7-bis(4′,4′,5′,5′-tetramethyl-1′,3′,2′-dioxaborolan-2′-yl)carbazole monomers (with different alkyl side chain) have been successfully synthesized. The ^{1}H NMR-spectrum of **38** (R_1= $C_{15}H_{31}$) shows two doublets and one singlet at 8.07, 7.89 and 7.69 ppm in the aromatic region (see figure 4.4). The low field triplet (δ; 4.40 ppm) represents the α-methylene protons of the N-alkyl chain. The sharp singlet at 1.3 ppm belongs to the methyl protons of the diboronic ester.

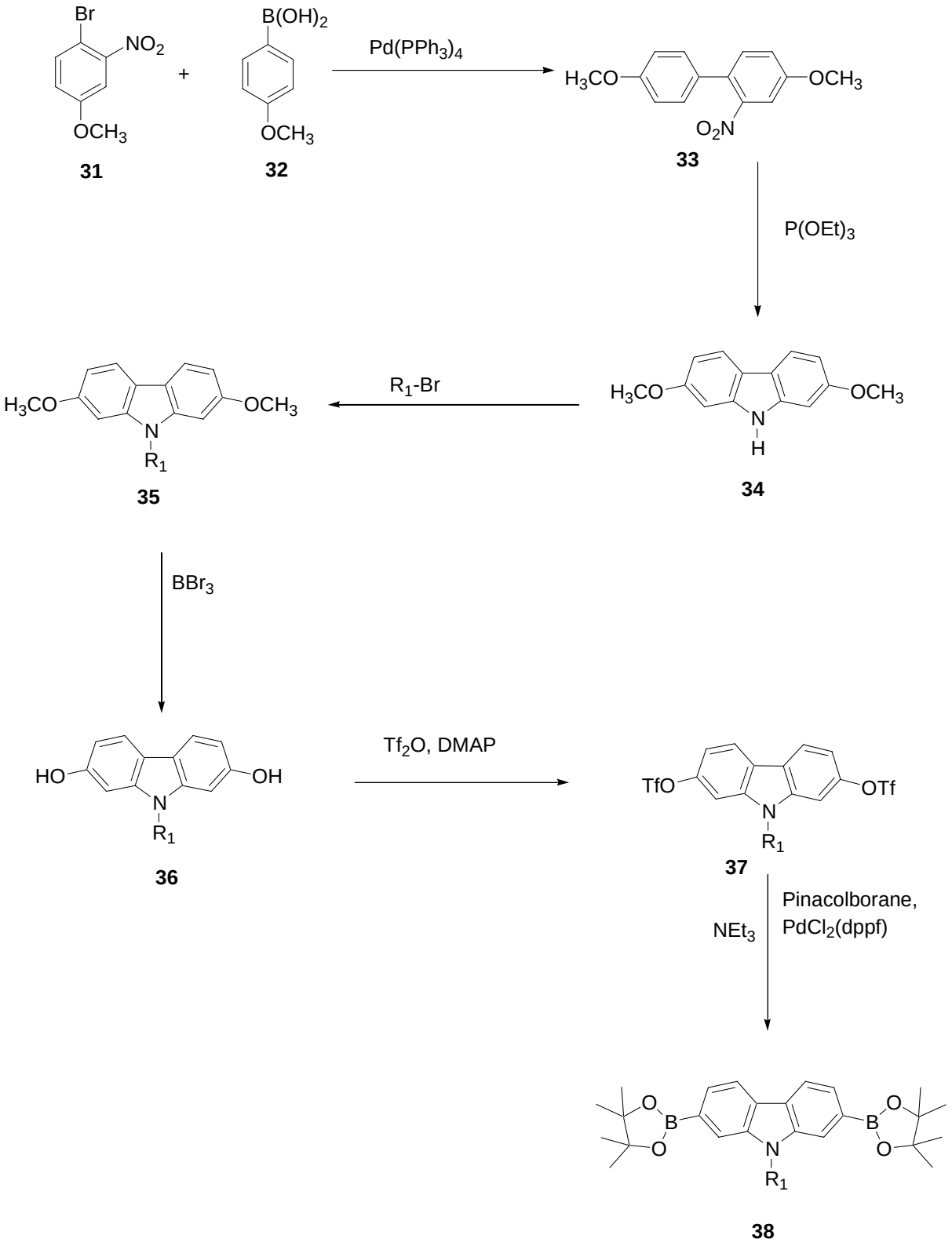

Figure 4.3 : Synthesis of N-alkyl-2,7-bis(4′,4′,5′,5′-tetramethyl-1′,3′,2′-dioxaborolan-2′-yl)-carbazole (R_1= C_8H_{17} and $C_{15}H_{31}$)

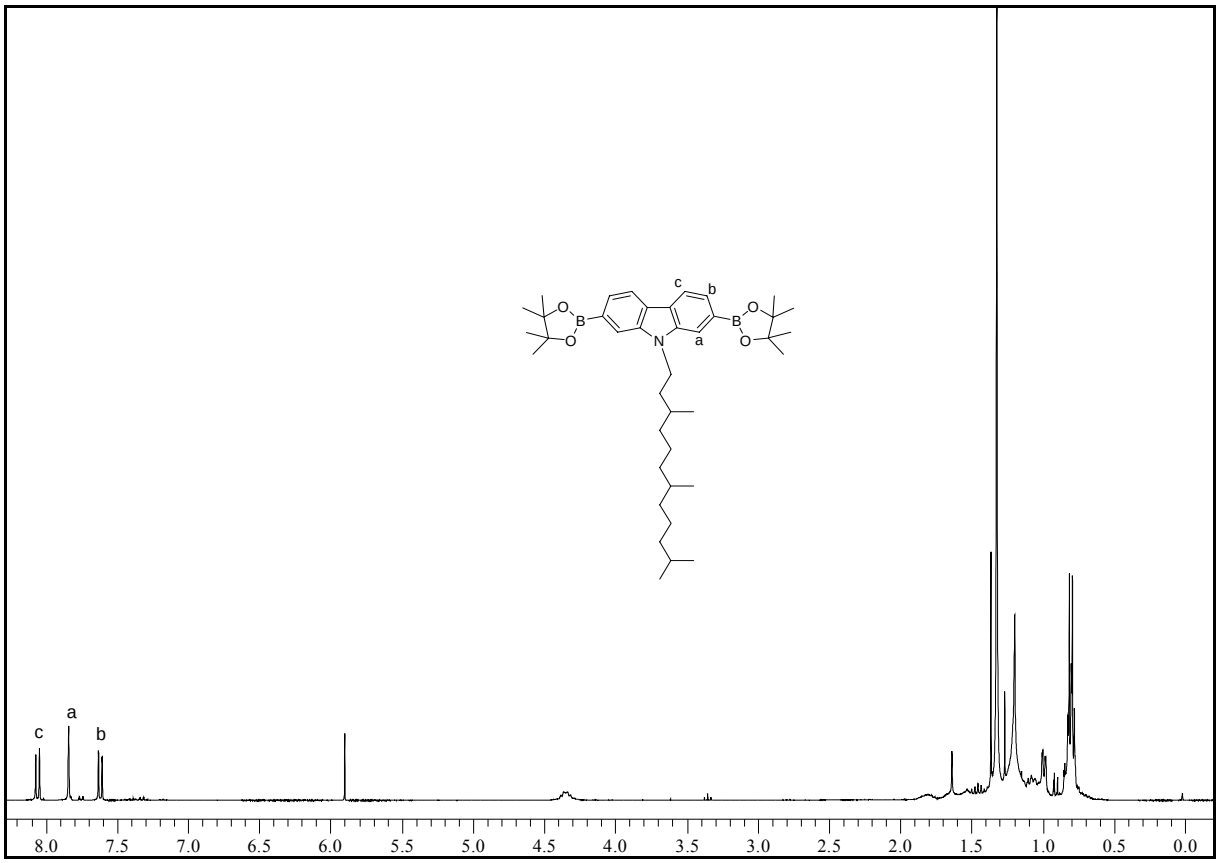

Figure 4.4 : ^{1}H NMR-spectrum of N-(3,7,11-trimethyldodecyl)-2,7-bis(4′,4′,5′,5′-Tetramethyl-1′,3′,2′-dioxaborolan-2′-yl)carbazole in $C_2D_2Cl_4$

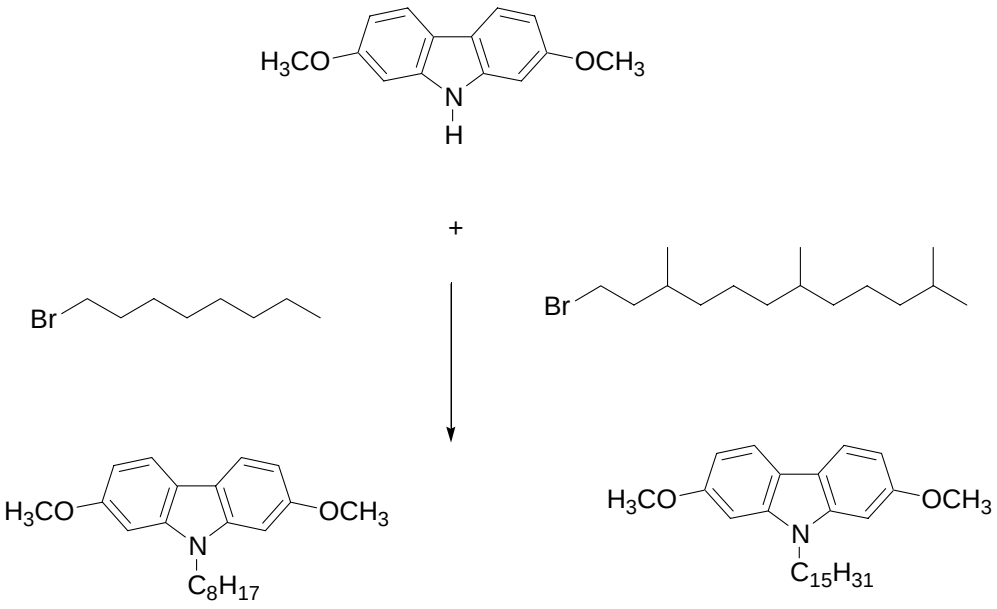

Figure 4.5: Substitution with alkyl chains at the N-atom of the carbazole ring

4.3 Synthesis of polymers

4.3.1 Synthesis of poly[N-(3,7,11-trimethyldodecyl)carbazole-2,7-diyl] (PFCB)

The synthesis of poly[N-(3,7,11-trimethyldodecyl)carbazole-2,7-diyl] PFCB **39** is depicted in Figure 4.6. The condensation was carried out by reductive Yamamoto coupling[45] using N-(3,7,11-trimethyldodecyl)-2,7-dichlorocarbazole **30** as a starting material in presence of cyclooctadiene (COD) ligand and $Ni(COD)_2$ as catalyst. As shown in Table 4.1, PFCB exhibits an increased number average molecular weight $\overline{M}_n$ of ca. 6,000 corresponding to a degree of polymerization of ca. 16, when compared to poly(N-octyl-carbazole-2,7-diyl) ($\overline{M}_n$=2,600) and poly(N-ethylhexyl-carbazole-2,7-diyl) ($\overline{M}_n$= 2,200)[55]. PFCB shows a narrow polydispersity of only ca. 1.1, this may be due to some fractionation during work-up. The resulting conjugated polymer is partially soluble (50 %) in common organic solvents like chloroform, dichloromethane. Nevertheless, the soluble part of PFCB **39** can be easily processed into thin polymer films on various substrates by spin coating.

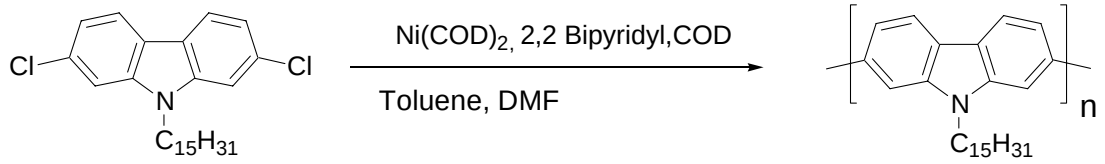

30 **39**

Figure 4.6: Synthesis of poly [N-(3,7,11-trimethyldodecyl)carbazole-2,7-diyl]

4.3.2 Optical characterization of poly[N-(3,7,11-trimethyldodecyl)carbazole-2,7-diyl] (PFCB)

The room temperature absorption and photoluminescence properties of PFCB **39** are shown in Figure 4.7. The absorption maxima, both in chloroform solution and in the solid state, are at 382 and 371 nm respectively. This shift indicates a some what more disordered solid state conformation of PFCB **39**. The solid state absorption maximum is slightly shifted hypsochromically by 9 nm. Photoluminescence spectra of PFCB **39** show a maximum emission around 420 nm in chloroform solution, and 429 nm in solid state. This slight

bathochromic shift might be due to weak interchain interactions or a somewhat modified solid state confirmation.

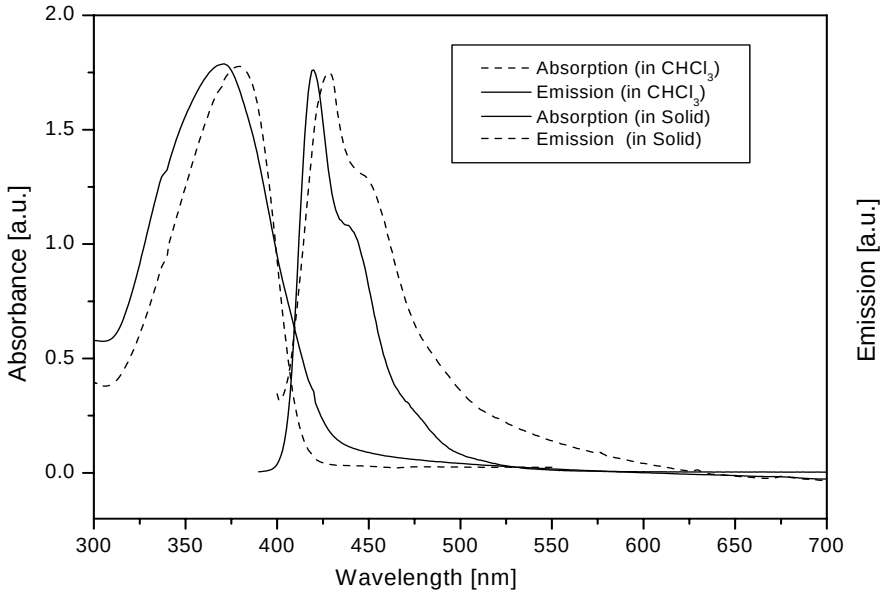

Figure 4.7: Absorption and emission spectra of PFCB **39** in chloroform and in the solid state.

These emission spectra shows also a well-resolved vibronic fine structure, which is associated with a more planar excited state geometry[109]. However, in contrast to polyfluorene[74] derivatives, PFCB **39** does not show any evidence for the formation of emissive defects leading to additional emission bands in the low energy region. These features are particularly promising for the future development of stable blue-light emitting polymers.

4.3.3 Synthesis of ladder-type poly(*para*-phenylene –2,7-carbazolylene) LPPPC

Structurally well-defined polyarylenes have been synthesized via several methods. In particular, Pd(0)-catalysed aryl-aryl couplings developed by Suzuki and Stille or Ni(0)-catalysed couplings according to Yamamoto have been employed most succesfully[110,111,45]. For the synthesis of carbazole-based ladder polymers we have used the Suzuki-type coupling procedure. The carbazole based ladder polymer **8** was synthesized in three steps according to Figure 4.8. The polyketone **40** was synthesized in the first step by using the well-known Suzuki-type coupling reaction. The Pd(0) catalysed polycondenstaion reaction of N-octyl-2,7-bis(4′,4′,5′,5′-tetramethyl-1′,3′,2′-dioxaborolan-2′-yl)carbazole **38** with the 1,4-bis(4′-

decylbenzoyl)-2,5-dibromobenzene derivative **22** in a two-phase solvent system (toluene/1M aq. Na_2CO_3) provides the polyketone **40** in 67 % yield. The number average molecular weight ($\overline{M}_n$) determined by size exclusion chromatography (SEC) and calibrated with polystyrene standards was 10,200 g/mol with a polydispersity of 1.99.

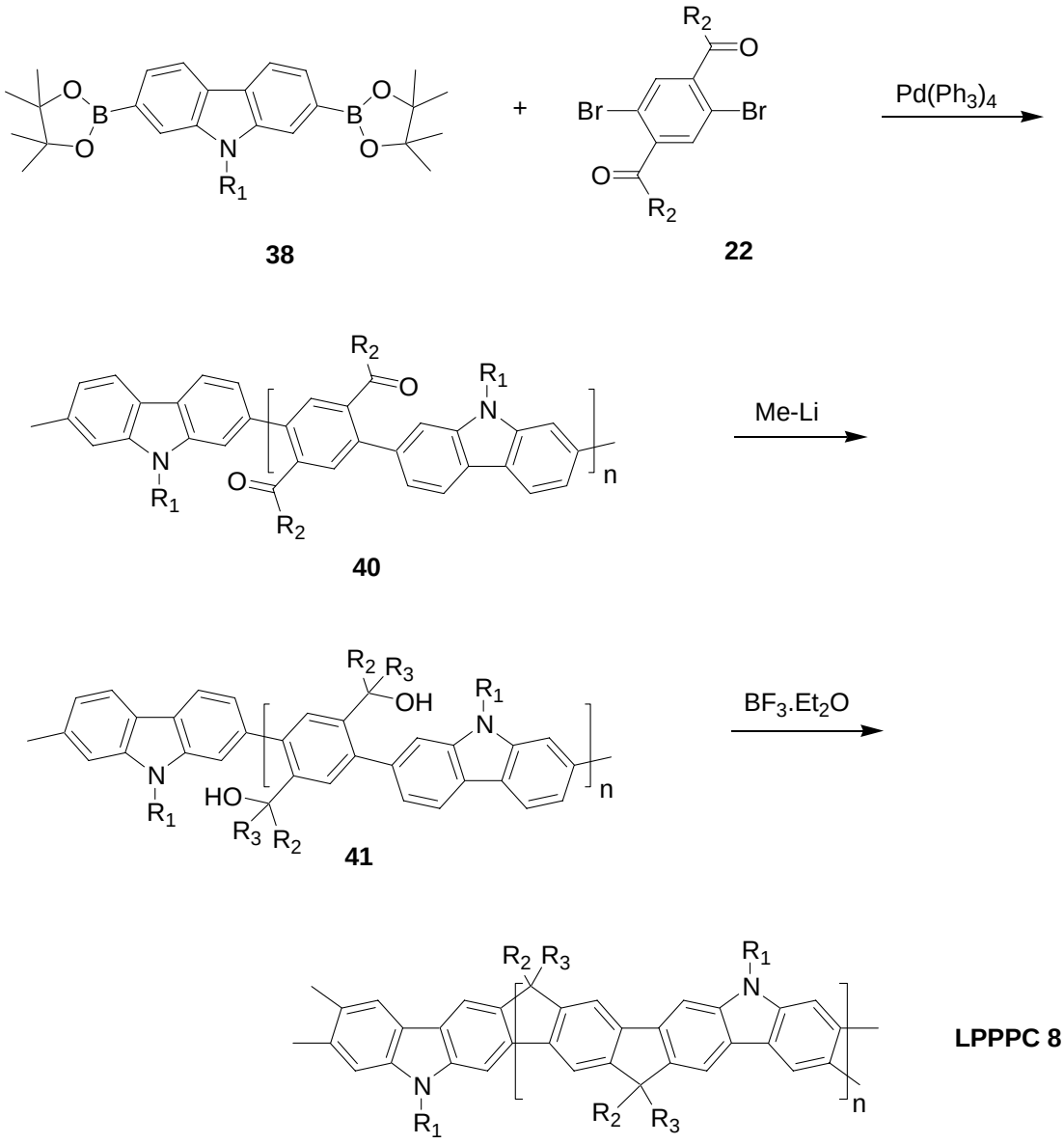

R_1 = *n*-C_8H_{17} and $C_{15}H_{31}$; R_2 = -1,4-C_6H_4-*n*-$C_{10}H_{21}$ and R_3 = CH_3

Figure 4.8: Synthesis of ladder-type poly(*para*-phenylene-2,7-carbazolylene)

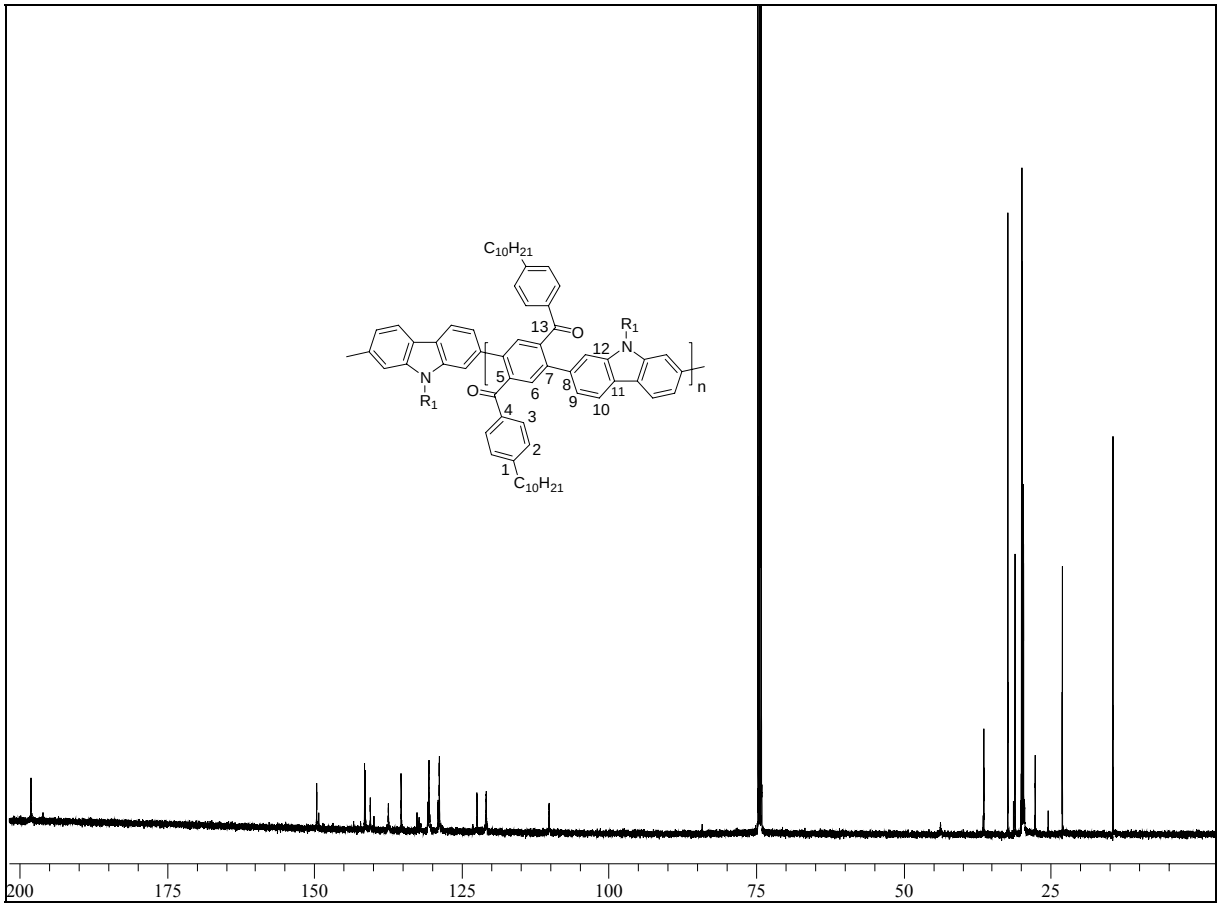

Figure 4.9: ^{13}C NMR-spectra of polyketone **40** (R_1= C_8H_{17})

Since polyketone **40** is soluble in common organic solvents, ^{1}H and ^{13}C NMR-spectroscopy can be used to confirm the structure of the polymer. The ^{13}C NMR-spectrum of polyketone **40** displays 13 major signals of non-equivalent carbons in the aromatic region some minor signals are due to end groups. Additionally, it shows the well resolved peak of the carbonyl group at 198.1 ppm as shown in Figure 4.9. In order to synthesize the desired ladder polymer the polyketone **40** was first transformed into the polyalcohol **41** by reaction with Me-Li. The final ring closure reaction of **41** to the planar ladder polymer (LPPPC **8)** have been carried out in dichloromethane with boron trifluoride etherate as Lewis-acidic catalyst. Immediately after the addition of BF_3 a strong blue fluorescent solution of the ladder polymer is generated.

The ladder polymer LPPPC **8** is completely soluble in common organic solvents (e.g. chloroform, toluene). The ^{13}C NMR-spectrum of LPPPC **8** displays 12 major signals for 13 non-equivalent aromatic carbons (Fig. 4.10). Signals from remaining keto or alcohol groups could not be detected within the limits of detection of the method.

The ^{1}H NMR-spectrum of the ladder polymer **8** shows the typical broad peaks of viscous polymer solutions. The aromatic protons appear between 6.8 and 8.1 ppm. It also show characteristic peaks of the alkyl chains. The peaks at 2.5 ppm belongs to the α-methylene of the hexyl ($-CH_2-C_5H_{11}$) as well as of the dodecyl substituents ($-CH_2-C_9H_{19}$). The signal of α-methylene protons of the N-alkyl substituents at ca. 4.3 ppm is very broad. Comparing the aliphatic region of the ^{1}H NMR-spectrum of LPPPC **8** with that of Ph-LPPP **25** (Fig. 3.4) we assign the peak at 2.0 ppm to the proton of the methyl group ($-CH_3$) at the methylene bridge carbon (Fig. 4.10), which is not present in the ^{1}H NMR-spectrum of Ph-LPPP. The number and weight average molecular weights of LPPPC **8** (GPC, PS calibration) were estimated to 35,300 and 69,100 with a polydispersity 1.95, which corresponds to an average degree of polymerization of ca. 130 arylene units. The reason for the pronounced increase in the molecular weight during the conversion of **41** to LPPPC **8** is not fully clear, however as observed also for Me-LPPP, it may be related to some branching as result of side reactions (single electron transfer and dimerisation during the addition of Me-Li).

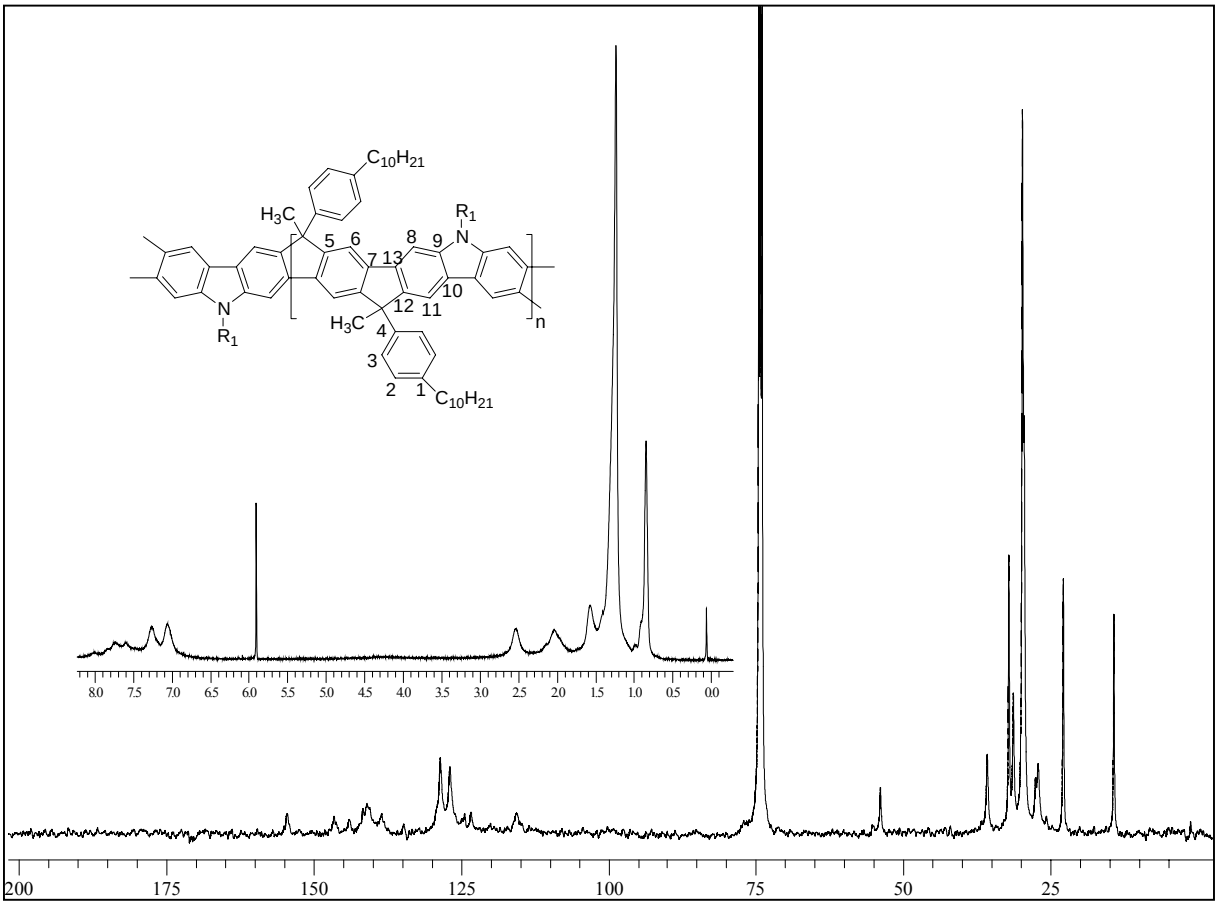

Figure 4.10: ^{1}H and ^{13}C NMR-spectra of LPPPC **8**

We have also synthesized LPPPC with different side chains by the using monomer N-3,7,11-trimethyldodecyl-2,7-bis(4′,4′,5′,5′-tetramethyl-1′,3′,2′-dioxaborolan-2′-yl)carbazole. The resulting ladder polymer LPPPC **15** (R_1= $C_{15}H_{31}$) shows a lower molecular weight ($\overline{M}_n$ = 10,940) as compared to LPPPC **8** (R_1 = C_8H_{17}) as shown in Table 4.1. This may be partially caused by the different monomer purity. The long alkyl chain substituted monomer still contains some remaining alkyl chloride, which may slightly affect the coupling reaction.

4.3.4 Synthesis of ladder-type poly(*para*-phenylene-3,6-carbazolylene) (LPPPMC)

The Suzuki coupling partners, N-octyl-3,6-bis(4′,4′,5′,5′-tetramethyl-1′,3′,2′-dioxaborolan-2′-yl)carbazole **43** and 1,4-bis(4′-decylbenzoyl)-2,5-dibromobenzene **22** were synthesized according to the literature[112,71]. The commercially available 3,6-dibromo-N-octylcarbazole **42** was treated with triethyl amine and 4,4,5,5-tetramethyl-1,3,2-dioxaborolane in presence of $PdCl_2$(dppf) as a catalyst (Fig. 4.11). Finally, N-octyl-3,6-bis(4′,4′,5′,5′-tetramethyl-1′,3′,2′-dioxaborolan-2′-yl)carbazole **43** was isolated in an acceptable yield (50 %) by purifying via column chromatography with 5 % ethyl acetate in hexane as a eluent. The final ladder polymer have been synthesized by following the already described procedure towards LPPPC **8** as shown in Figure 4.12. LPPPMC **46** is soluble in common organic solvents. The number average molecular weight ($\overline{M}_n$) of LPPPMC **46** was 6,800 with a polydispersity 1.58 as shown in Table 4.1. This lower molecular weight of ladder polymer **46** may be due to a lower reactivity of the bromo substituents at the electron-rich 3-and 6-positions of the carbazole ring in Suzuki-type couplings.

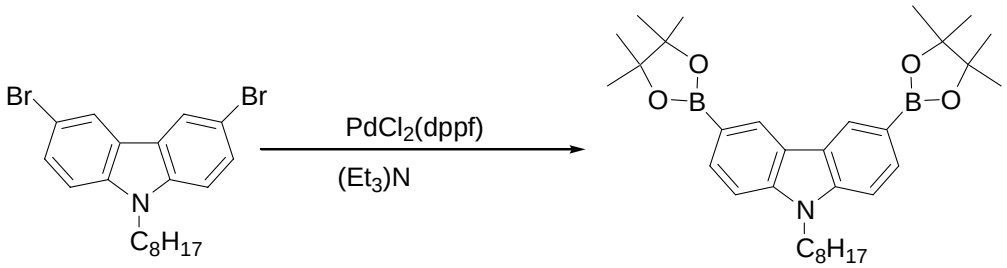

42 **43**

Figure 4.11 : Synthesis of N-octyl-3,6-bis(4′,4′,5′,5′-tetramethyl-1′,3′,2′-dioxaborolan-2′-yl)carbazole **43**

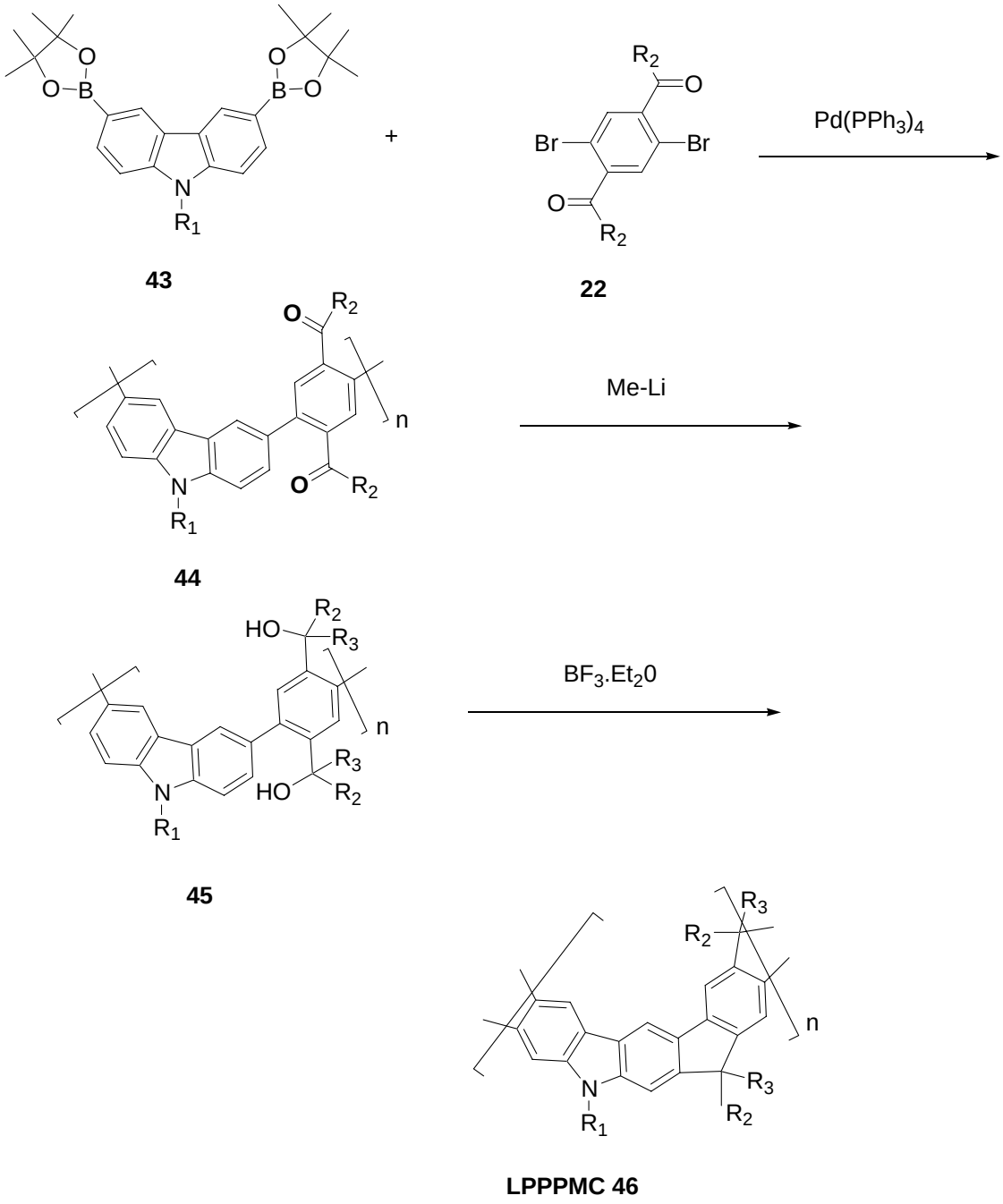

43 **22**

44

45

LPPPMC 46

R_1 = *n*-C_8H_{17}; R_2 = -1,4-C_6H_4-*n*-$C_{10}H_{21}$ and R_3 = CH_3

Figure 4.12: Synthesis of ladder-type poly(*para*-phenylene 3,6-carbazolyene) (LPPPMC)

4.4 Optical Characterization of LPPPC and LPPPMC

The room temperature absorption and photoluminescence (PL) spectra of LPPPC **8** in chloroform solution are shown in Figure 4.13. Both spectra reveal a characteristic structure.

The $S_0 \rightarrow S_1$ (0-0) transition is centered at 460 nm (2.64 eV), escorted by a vibronic feature displaced by 0.19 eV to higher energy. The PL spectrum of **8** is the mirror image of the absorption spectrum (λ_{max} = 468 nm), the small Stokes shift of 0.057 eV (460 cm^{-1}, upon excitation under non-siteselective conditions) in LPPPC **8** (Table 4.1) testifies the rigid geometry of this ladder polymer. The absorption and emission spectra of LPPPC **8** show a pronounced 0-0 transition, the absorption and emission maxima are slightly red shifted in relation to the corresponding nitrogen-free ladder polymer Me-LPPP (see Table 4.1) due to the presence of the electron-donating >NR substituents of the carbazole moieties within the conjugated main chain.

Polymer	$\overline{M}_n / \overline{M}_w$ (GPC, PS calibratation)	absorption maximum λ_{max} (nm) (in $CHCl_3$)	emission maximum λ_{max} (nm) (in $CHCl_3$)
Me-LPPP R_1 = *n*-C_6H_{13}; R_2 = -1,4-C_6H_4-*n*-$C_{10}H_{21}$ and $R_3 = CH_3$	38,500 / 76,100[a]	452	460
LPPPC 8 R_1 = *n*-C_8H_{17}; R_2 = -1,4-C_6H_4-*n*-$C_{10}H_{21}$ and $R_3 = CH_3$	35,300 / 69,100[a]	464	470
LPPPC 15 R_1 = *n*-$C_{15}H_{31}$; R_2 = -1,4-C_6H_4-*n*-$C_{10}H_{21}$ and $R_3 = CH_3$	10,940 / 20,620[a]	460	465
LPPPMC 46 R_1 = *n*-C_8H_{17}; R_2 = -1,4-C_6H_4-*n*-$C_{10}H_{21}$ and $R_3 = CH_3$	6,824 / 10,840[a]	411	460
PFCB 39 $R_1 = C_{15}H_{31}$	5,800 / 6,400	382	420

a) after removal of oligomers by extraction with acetone

Table 4.1: UV-Vis and photoluminescence data of Me-LPPP, LPPPC **8**, LPPPC **15**, LPPPMC **46,** and PFCB **39**

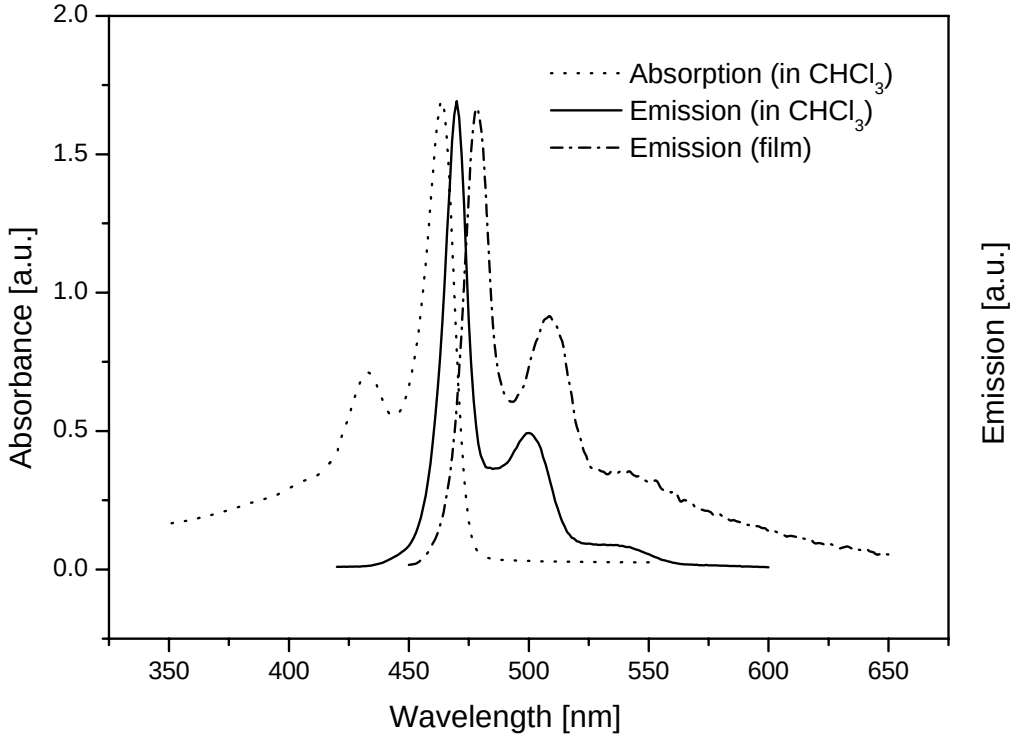

Figure 4.13: Absorption and emission spectra of LPPPC **8**.

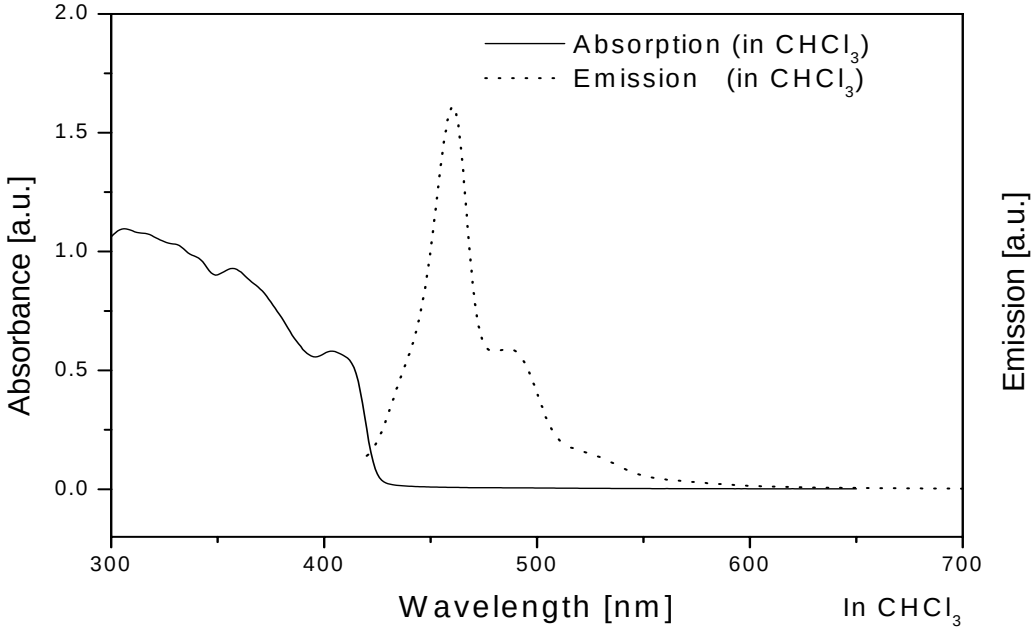

Figure 4.14: Absorption and emission spectra of LPPPMC **46** in chloroform

Figure 4.14 shows the absorption and emission spectrum of LPPPMC **46**. In comparison with LPPPC **8** the optical properties of LPPPMC **46** shows a hypsochromically shifted long wavelength absorption peak at 411 nm, and the emission maximum peak at 461 nm.

The low temperature fluorescence properties and thermally stimulated luminescence (TSL) measurements of LPPPC **8** have been done in collaboration with Dr. Andrey Kadashchuk, at Kiev and Marburg.

4.4.1 Low temperature fluorescence of LPPPC

The fluorescence spectrum of a frozen, diluted solution of LPPPC **8** measured at 4.2 K is substantially better resolved than at room temperature (Fig. 4.15) and consists of a main $S_1 \rightarrow S_0$ band at 484 nm (2.56 eV) followed by at least four well-resolved vibronic features displaced by about 80, 160 and 350 meV, accordingly. As expected, the low-temperature emission spectrum of a LPPPC **8** film is less resolved than that in solution (for instance, the emission band at 500 nm is no longer resolved in the film spectrum). Apart of the somewhat better resolved structure and the apparent red shift upon lowering temperature, the fluorescence spectrum of LPPPC **8** at 4.2 K is principally similar to that measured at room temperature (see fig. 4.13).

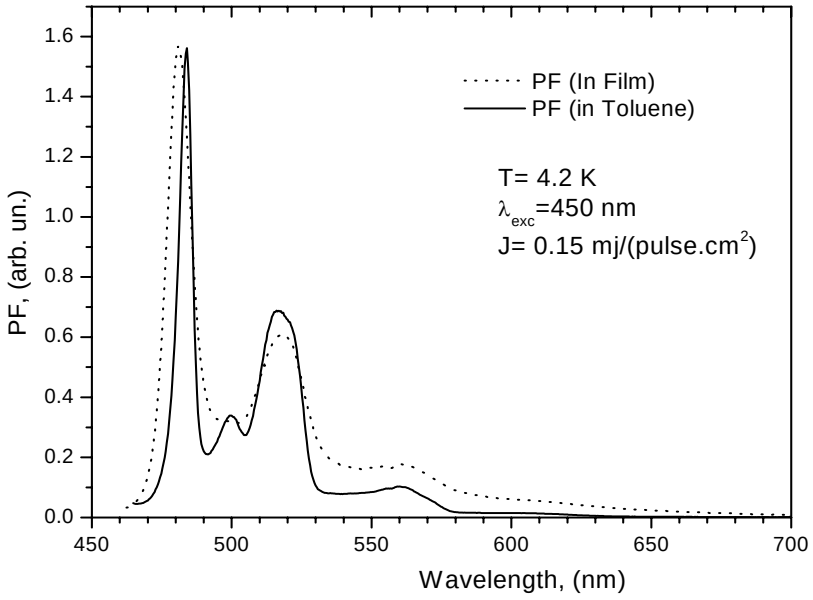

Figure 4.15: Low temperature fluorescence (PF) measured at 4.2 K in both frozen diluted solution (toluene) and in a film of LPPPC **8**.

4.4.2 Delayed fluorescence and phosphorescence in LPPPC

Delayed emission spectra [delayed fluorescence (DF) and phosphorescence (Ph)] measured at 4.2 K in frozen, diluted solution, and in LPPPC film are presented in Figure 4.16.

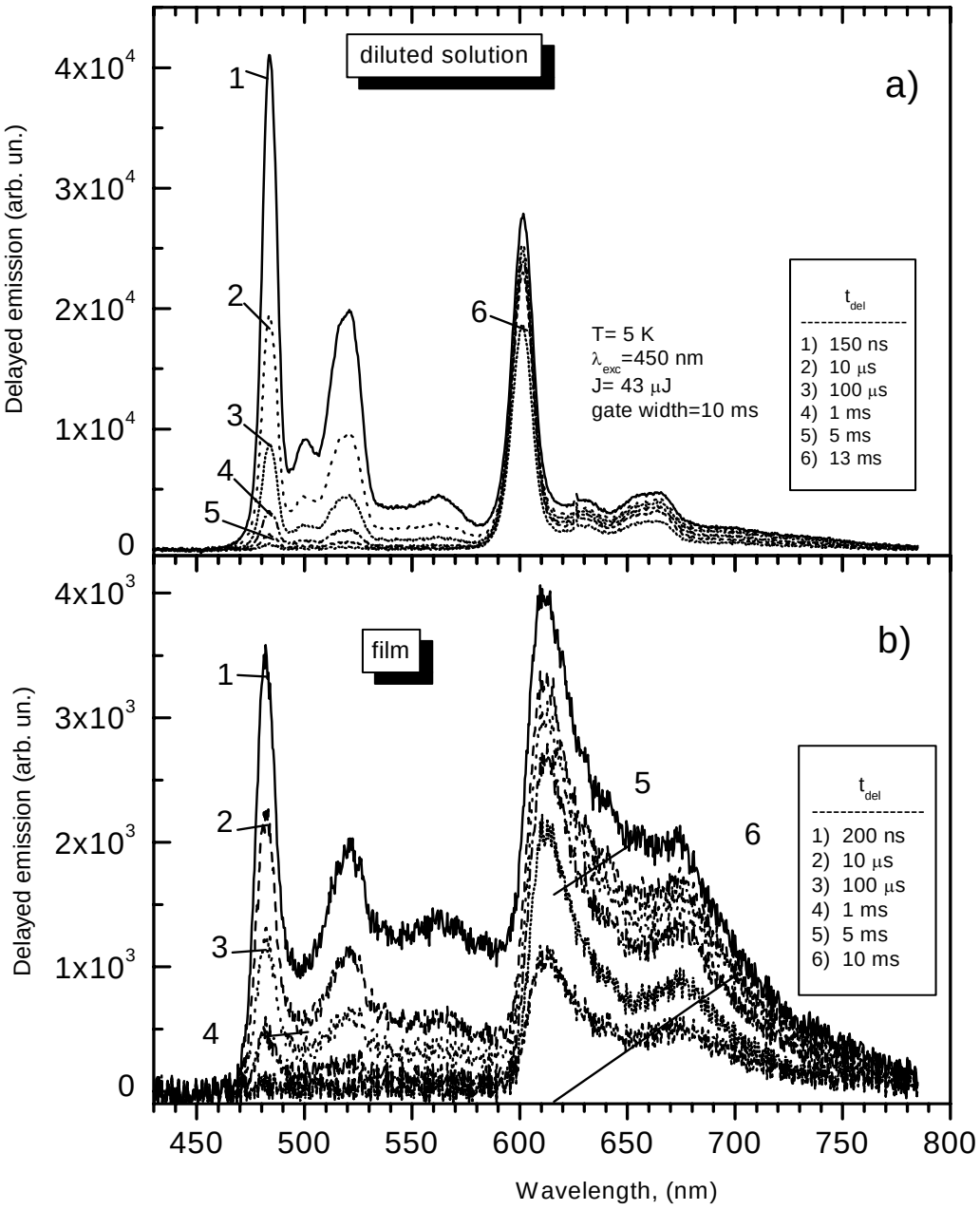

Figure 4.16: Delayed fluorescence (DF) and phosphorescence (Ph) measured at 4.2 K in frozen, dilute solution (a), and in a LPPPC film (b).

Low-temperature delayed emission spectra of LPPPC **8** were measured with different delay time (indicated in the figure) and the registration gate-width of 10 ms. The DF and Ph spectra are appeared to be much better resolved in diluted solution of LPPPC **8** than in the film. This is quite understandable that spectra of films are more broadened due to more efficient energy transfer in films comparing to solutions. Further, as one can see from Figure 4.15, phosphorescence dominates in the delayed emission in the milliseconds time domain and it decays notably slower in LPPPC **8** solution than in the film, that again can be readily explained by more efficient energy transfer in film resulting in nonradiative quenching of triplets on some sort of quenching centers.

In contrast to the low temperature (Fig. 4.15) spectra, the delayed emission from both LPPPC **8** solution (Fig. 4.16a) and film (Fig. 4.16b) exhibits two different sets of bands with different decay times and different spectral positions. The shorter wavelength part of the delayed emission of the dilute solution consists of four pronounced bands ranging from 470 to 570 nm (Fig. 4.16a) and is virtually identical to the low temperature spectrum of LPPPC **8** (Fig. 4.15). Thus it can be assigned to the delayed fluorescence (DF) from the S_1 state of LPPPC chain. The second slower decaying set of bands is shifted by 0.5 eV with respect to the first peak of DF, but has the same vibrational structure (Fig. 4.16a) as the fluorescence spectrum. It should be noted that this second series of bands can be seen only in the delayed emission and shows all generic signatures of phosphorescence, principally similar to that previously found in Me-LPPP[93]. Therefore this spectral part is assigned to phosphorescence from the T_1 state of LPPPC **8** featuring a singlet-triplet (S_1-T_1) splitting of about ΔE_{ST}=0.5 eV which probably is the smallest value observed so far in conjugated polymers. The above S_1-T_1 gap value for LPPPC **8** may be due to a large effective conjugation length in this polymer, as the gap decreases with increasing conjugation of the polymer backbone for PPP-type polymers[113].

4.5 Thermally stimulated luminescence in LPPPC

Thermally stimulated luminescence (TSL) has proved to be a suitable technique for studying the trapping effects in disordered organic materials[114,115]. TSL can provide important information on both the intrinsic density of states (DOS) and extrinsic deep trap distributions in conjugated polymers[116,117]. It also provides additional information on details of both photoluminescence mechanism and the geminate pair kinetics[118]. Recently, TSL was

studied in Me-LPPP[116]. One of the essential observations in Me-LPPP is that TSL in Me-LPPP occurs only at relatively low temperatures as expected in a material that reveals no charge-carrier trapping[119].

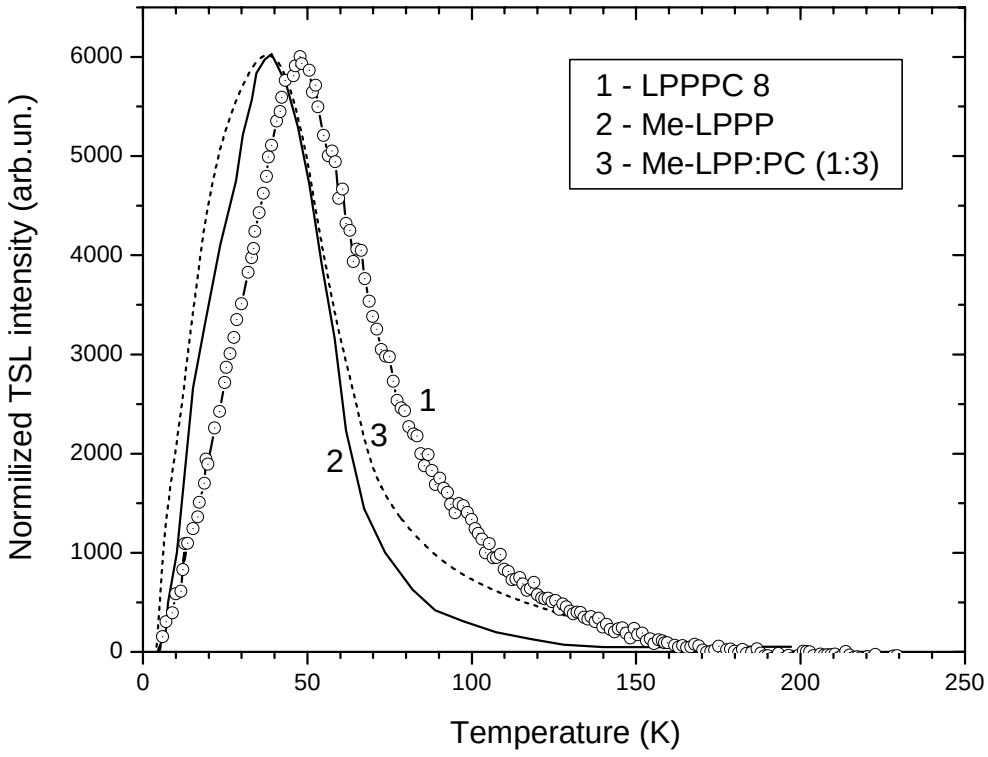

Figure 4.17: Typical TSL curve of LPPPC **8** (curve 1) and Me-LPPP films (curve 2) monitored under the same conditions. Curve 3 shows TSL for a blend of Me-LPPP/PC (1:3).

The TSL measurements were carried out using a home-built system operable from 4.2 to 350 K. TSL measurements after UV light excitation were performed with two different methodologies: uniform heating at a rate β = 0.15 K/s, and fractional heating. The latter procedure allows the determination of trap depth when different groups of traps are not well separated in energy or are continuously distributed. The fractional TSL technique[120], being an extension of the initial rise method, is based on cycling the sample with a large number of small temperature oscillations superimposed on a constant heating ramp. The main outcome of the fractional TSL is the temperature dependence of the mean activation energy, $\langle E \rangle (T)$[121].

Radiative recombination of sufficiently long range photogenerated off-chain geminate pairs of charge carriers has been identified as the origin of TSL in these materials. Figure 4.17 shows a typical TSL curve of a LPPPC **8** film (curve 1) after excitation at 4.2 K for a few min, the TSL of a Me-LPPP film monitored under the same conditions is given for comparison (Fig. 4.17, curve 2). TSL of LPPPC **8** represents a broad single peak with the maximum at $T_m \approx 50$ K. The TSL occurs only at relatively low-temperatures as expected for weakly disordered material devoid of deep traps[122]. However, as one can see from Fig. 4.17, the TSL glow curve of LPPPC **8** film is some what broader and notably extended to higher temperatures in comparison to that of Me-LPPP. This suggests a larger concentration of energetically "deeper" tail states and concomitantly somewhat larger energetic disorder of the charge transporting manifold in this material.

Analysis presented in Figure 4.17 clearly demonstrates the larger width of the charge-carrier DOS distribution in LPPPC **8** films. The notably broader DOS distribution of charge carriers in LPPPC **8** when compared to a Me-LPPP film is striking since the DOS distribution for neutral excitations shows the opposite trend. This effect can be explained with the presence of the permanent dipole moment of the carbazole moiety in LPPPC **8** (~2 D)[123] (in contrast to the almost unpolar Me-LPPP). It should be noted that similar effects were observed during the blending of dipolar additives into molecularly doped polymers (MDP)[124] or for the introduction of dipoles into σ-conjugated polysilanes[125] and polymers containing side-chain carbazole units [126].

To verify the dipolar disorder hypothesis TSL was also measured in Me-LPPP doped into bisphenol A-polycarbonate (PC), a polar polymer matrix which has a permanent dipole moment of about 2 D[127]. PC was used very extensively[128] to study the dipolar disorder effect in MDPs. Curve 3 in Figure 4.17 shows TSL measured in Me-LPPP doped into PC (1:3). The TSL curve is notably shifted to higher temperatures with respect to that of the pure Me-LPPP film (curve 2). That can be explained by the introduction of dipolar disorder due to the polar PC matrix.

Finally, the novel (LPPPC **8** and LPPMC **46**) ladder polymers containing carbazole units in the main chain have been synthesized successfully. LPPPC **8** is a very attractive material as far as its optical properties are concerned since the so-called "density of states" (DOS) in this polymer is very narrow. Especially LPPPC **8** is expected be useful for many

photonic applications (e.g. OFETs, polymer laser, two photon emission-etc). The permanent dipole moment within the repeat unit is expected to increase the two-photon absorption cross section. Two photon-pumped emission measurements are in progress. The outcome will be compared to the behaviour of well-known methyl substituted ladder-type poly(*para*-phenylene) Me-LPPP. The obtained results evidence a very low energetic disorder in LPPPC **8** presumably due to its regular intrachain structure and the low content of defects. It was found that although the DOS distribution for the neutral excitations is narrower than in Me-LPPP, the manifold of charge transporting localized states is substantially more energetically disordered due to the dipolar disorder contribution.

5. Carbazole-based copolymers

5.1 Introduction

As mentioned in chapter 4, poly(2,7-carbazole) homopolymer were recently developed and revealed interesting blue electroluminescence[56]. Considering the good hole-transporting properties of carbazole-based polymers, it would be advantageous to generate alternating copolymers with suited comonomers. The presence of alternating electron-acceptor and electron-donor moities in such copolymers should lower (HOMO-LUMO) the energy gap. Lower band gap emissive or non-emissive copolymers are valuable for several applications, particularly as red emitter in PLEDs or for polymer photovoltaic cells. We have synthesized two carbazole-based alternating copolymers containing electron-deficient benzothiadiazole moieties as well as bithiophene units, which could be useful for PLED or photovoltaic applications.

5.2 Synthesis of alternating copolymer:

5.2.1 Poly[N-octylcarbazole-2,7-diyl-*alt*-2,1,3-benzothiadiazole-4,7-diyl] (PCzBTDZ)

In creating polymers with unique properties the alternating copolymer approach has been applied succesfully. The choice of the comonomer has served as an excellent synthetic tool for designing polymers with well–balanced hole and electron-transport properties and colour control of emission. Benzothiadiazole (BT) is a electron-deficient building block. By incorporating an electron-deficient monomer, benzothiadiazole (BT), into the fluorene polymer, the resulting copolymer should possess a higher electron affinity and preferential electron-transporting properties e.g. compared to those of the poly(9,9-dioctylfluorene)[129]. By keeping in mind this advantage of benzothiadazole alternating carbazole-benzothiadazole copolymers have been synthesized. The synthesis of 4,7-dibromo-2,1,3-benzothiadiazole **49** monomer was carried out according to the literature[130] starting with 1,2-phenylenediamine **47** as shown in figure 5.2. Finally, 2,1,3-benzothiadiazole **48** was brominated by reacting with an execess of bromine in 83 % yield.

N-Octyl-2,7-bis(4′,4′,5′,5′-tetramethyl-1′,3′,2′-dioxaborolan-2′-yl)carbazole was synthesized in six steps (see page 39, figure 4.3). The final alternating copolymer poly[N-octylcarbazole-2,7-diyl-*alt*-2,1,3-benzothiadiazole-4,7-diyl] **50** was generated via Suzuki-type cross coupling by using an equimolar ratio of 4,7-dibromo-2,1,3-benzothiadiazole **49** and N-

octyl-2,7-bis(4′,4′,5′,5′-tetramethyl, 1′,3′,2′dioxaborolan-2′-yl)carbazole **38**. Polymerization was carried out in well degassed toluene/2M Na_2CO_3(aq.) with $Pd(PPh_3)_4$ as a catalyst at reflux for three days as shown in Figure 5.2. The Suzuki-type coupling is the prefered method for the synthesis of alternating copolymers because it allows to obtain an alternating copolymers in the case of AA/BB- type monomers[131].

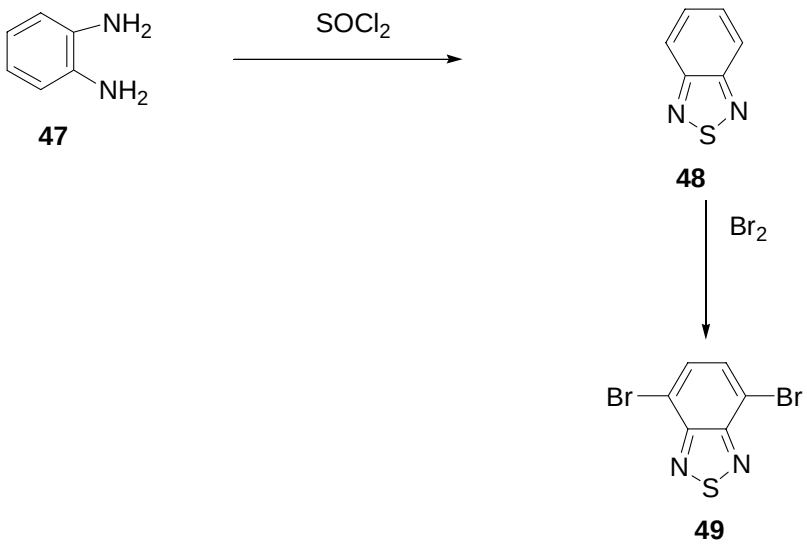

Figure 5.1 : Synthesis of 4,7-dibromo-2,1,3-benzothiadiazole

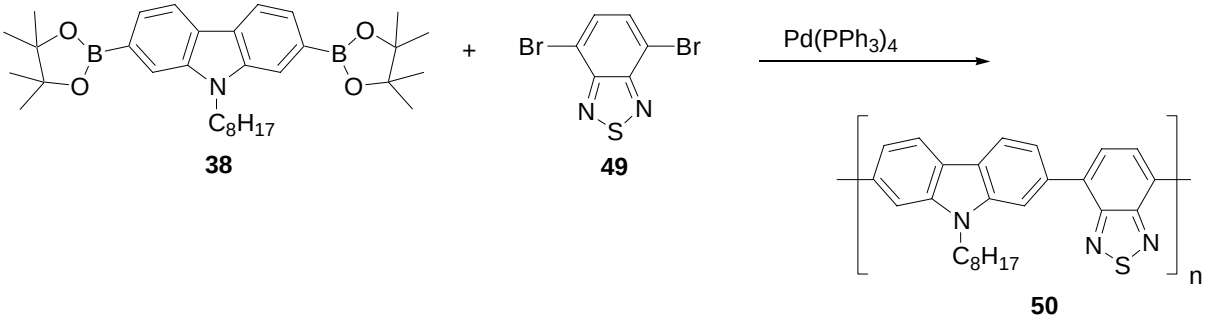

Figure 5.2 : Synthesis of poly[N-octylcarbazole-2,7-diyl-*alt*-2,1,3-benzothiadiazole-4,7-diyl]

The Suzuki-coupling of **38** with **49** leads to the final copolymer PCzBTDZ **50** with 56 % yield. The copolymer PCzBTDZ **51** is sparingly soluble in common organic solvents. The number average molecular weight $\overline{M}_n$ of the soluble part of this polymer (70 %) was

measured in THF with polystyrene as a standard and is found to 2,500 with a polydispersity of 1.2, corresponding to the degree of polymerization of ca. 8-10.

5.3 Optical characterization of Poly[N-octylcarbazole-2,7-diyl-*alt*-2,1,3-benzothiadiazole-4,7-diyl]

The UV-Vis absorption and photoluminescence (PL) spectra of PCzBTDZ **50** in thin film as well as in chloroform solution are as shown in Figure 5.3. The absorption maximum of PCzBTDZ **50** is centered at 450 nm, a second asorption peak occurs at 320 nm. The photoluminescence spectra of PCzBTDZ **50** is significantly red-shifted as compared to poly(N-alkyl-carbazole-2,7-diyl)s, the emission maximum occurs at 535 nm in chloroform solution.

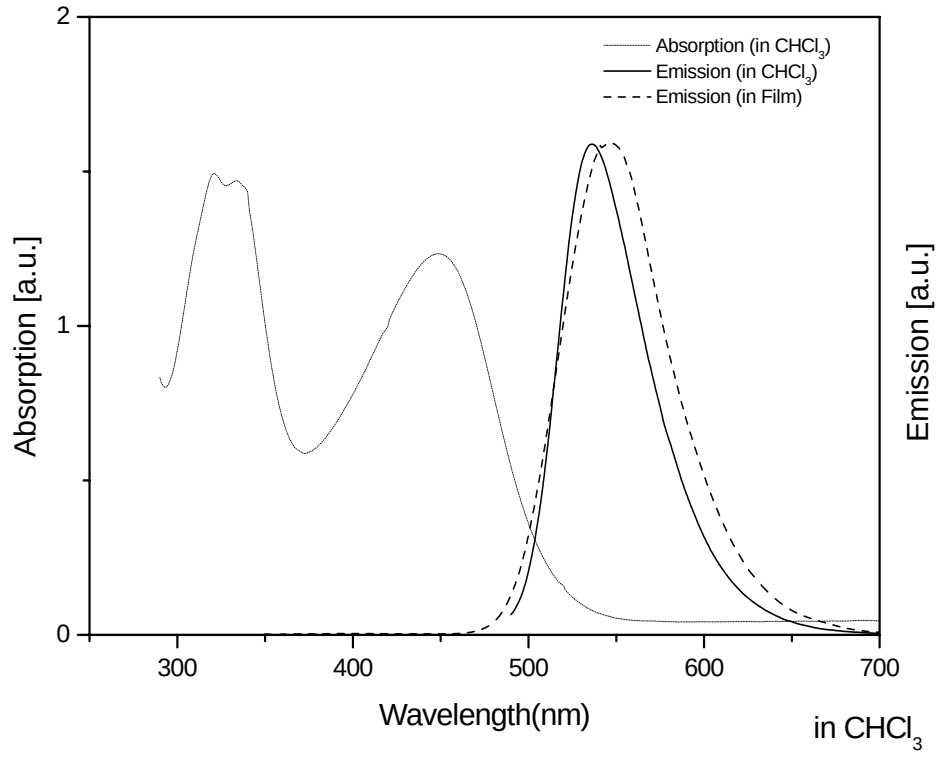

Figure 5.3 : Absorption and emission spectra of PCzBTDZ **50** in chloroform as well as in the solid state.

The photoluminescence spectrum of PCzBTDZ **50** in the solid state shows an emission maximum at 546 nm. The slight red-shift might be attributed to weak interchain interactions in the solid state.

A NMR analysis of PCzBTDZ **50** reveals a 1:1 composition corresponding to the feed ratio of the monomers. The ^{1}H NMR-spectrum of PCzBTDZ **50** shows peaks between 7.5 and 8.3 ppm for the protons of the carbazole and benzothiadiazole rings.

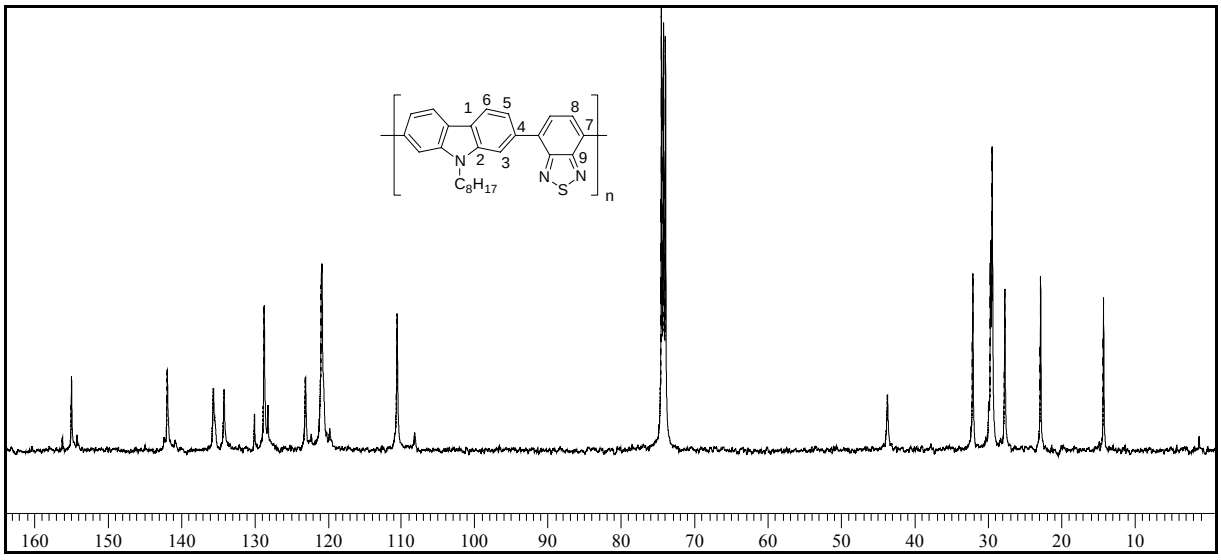

Figure 5.4 : ^{13}C NMR-spectrum of poly[N-octyl-carbazole-2,7-diyl-*alt*-2,1,3-benzothiadiazole-4,7-diyl]

The ^{13}C NMR-spectrum of PCzBTDZ **50** shows 9 peaks in the aromatic region for the 9 non-equivalent carbons of PCzBTDZ **50** as shown in the figure 5.4, accompanied by some minor peaks which are caused by end groups.

5.4 Poly[N-octylcarbazole-2,7-diyl-*alt*-2,2´-bithiophene-5,5´-diyl] (OCB2T)

It was recently found that thiophene diboronic acids were unstable under the basic conditions of the Suzuki-type cross coupling reactions[132]. Therefore we preceded to synthesize the bithiophene based alternating copolymer via a Stille-type cross coupling reaction. Stille-type cross-coupling reactions of aryl halides and aryl triflates with organotin compounds have been widely used for the construction of the aryl-aryl bonds in modern

synthesis[133]. Organotin compounds containing a variety of reactive functional groups can be prepared by a number of routes; fortunately these reagents are not particularly oxygen or moisture sensitive. N-octyl-2,7-bis(trifluoromethanesulfonyl)carbazole was synthesized in five steps (see page 39 fig. 4.3). 5,5′-Bis(trimethylstannyl)-2,2′-bithiophene was prepared by metalation of 2,2′-bithiophene with butyl lithium (*n*-Bu-Li) followed by treatment with trimethyl tin chloride (Fig. 5.5). This reaction affords the 5,5′-bis(trimethylstannyl)-2,2′-bithiophene in high yields after recrystallization from ethanol (70 %) as reported in the literature[134].

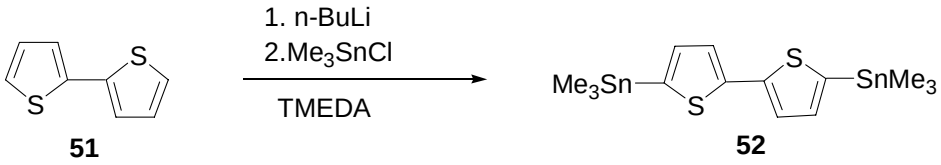

Figure 5.5: Synthesis of 5,5′-bis(trimethylstannyl)-2,2′-bithiophene

Poly[N-octylcarbazole-2,7-diyl-*alt*-2,2′-bithiophene-5,5′-diyl] **53** was generated via a Stille-type coupling of N-octyl-2,7-bis(trifluoromethanesulfonyl)carbazole **37** and 5,5′-bis(trimethylstannyl)-2,2′-bithiophene **52** using $Pd(PPh_3)_4$ as a catalyst in toluene as shown in figure 5.6. Polymer **53** was obtained in a low yield of 31 % caused by the limited solubility of the copolymer. The final alternating copolymers OCB2T **53** shows a very low solubility in common organic solvents. It was difficult to record NMR-spectra of this polymer. The number average molecular weight ($\overline{M}_n$) of the THF soluble part is ca. 2,000.

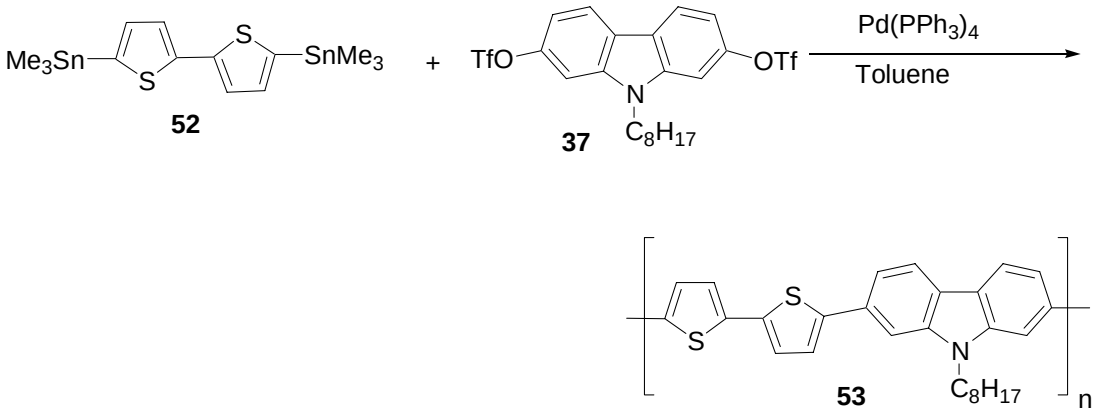

Figure 5.6 : Synthesis of poly[N-octyl-carbazole-2,7-diyl-*alt*-2,2′-bithiophene-5,5′-diyl)]

Finally, we have synthesized two novel carbazole-based copolymers by Suzuki-type as well as Stille-type coupling reactions. Particulary, PCzBTDZ **50** is a promising material as the electron transport should be greatly enhanced by the insertion of the benzothiadiazole units. The combination of carbazole units (as hole transporting moities) and benzothiadazole units (as electron transporting moities) should lead to a balanced charge carrier transport and consequently to high electroluminescence quantum yields.

6. Summary and Outlook

6.1 Summary

Semiconducting polymer electroluminescence (EL) has stimulated a lot of activities across a wide interdisciplinary reach within academic, industrial and governmental sectors. The enormous dynamics of the field have created the unique opportunity for synthetic chemists to develop high performance polymer materials in order to understand the underlying basic principles, necessary for a commercial success. In this thesis, the synthesis and characterization of new ladder-type poly(*para*-phenylene) (LPPP) derivatives has been investigated. The LPPP-type material have recently received much attention due to their potential applications in photonic devices such as electroluminescent diodes, two photon absorbers and solid state laser.

1. The work first introduces briefly conjugated polymers and their applications in display technology. The synthesis and spectroscopic behaviour of phenylene ladder polymers (LPPPs), especially so-called Me-LPPP, as a new class of well-defined conjugated polymers for applications in electronics and photonics (e.g. LEDs, polymer lasers) is discussed (chapter 1 and 2).

2. A novel structural analogue of Me-LPPP, a diaryl substituted phenylene ladder polymer (Ph-LPPP) was generated and showed for the first time intrinsic electrophosphorescence at room temperature (chapter 3). The synthetic approach to the ladder polymer (Ph-LPPP) is simple and efficient and leads to materials with fully reproducible properties. Hereby, the incorporation of a small amount of Pd centers (80-150 ppm) activates the phosphorescence channel, especially in the electrically pumped electrophosphorescence mode. To our knowledge, Ph-LPPP is the first polymer to show electrophosphorescence at room temperature without loosing the original electronic properties of LPPP-type polymers. Ph-LPPP demonstrates a novel principle for triplet harvesting in conjugated polymers by including a small amount of covalently bound heavy metal atoms (Pd) in the polymer backbone. The positions of the energetic levels (HOMO-LUMO) of the polymer are not affected by the isolated metal sites. The dramatically enhanced rate of radiative triplet decay provides a novel tool to study the energetic structure and dynamics of triplet excitations in conjugated polymers as well as their interaction with charge carriers[135].

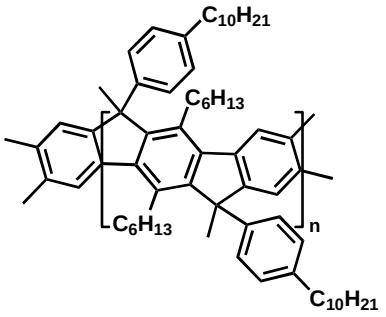

Me-LPPP

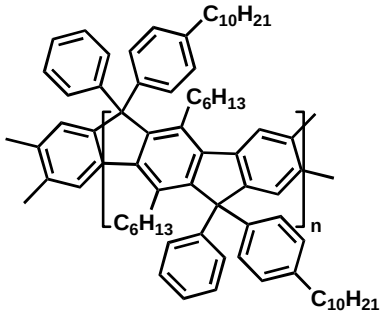

Ph-LPPP

In particular, the present results provide an important solution for the handling of triplet excitations in high excitation density applications such as polymer lasers. Triplet accumulation can often lead to a reduction in gain and undesirable thermal heating. A deactivation of the triplets by radiative means bypasses these parasitic effects and could help in the development of electrically driven polymer lasers or optically pumped steady state polymer lasers. It is believed that, this fundamental work will also help to improve the performance of polymer light emitting diodes. These unexpected results will contribute to the further development of these novel technologies.

3. Carbazole-based ladder polymers (e.g. LPPPC **8**) are novel semiconducting materials containing a polar carbazole group within the main chain. LPPPC is a very attractive material as far as its optical properties are concerned since the so-called "density of states" (DOS) in this polymer is very narrow (chapter 4). The latter is evidenced by a very small inhomogeneity of the absorption spectrum with a very small Stokes shift of ca. ≈460 cm^{-1} that is comparable to the value of 500 cm^{-1} reported for Me-LPPP[119], and a very well-resolved PL spectrum especially at low temperatures. The luminescence characterization of these polymers revealed no evidences for deep traps (defects). Absorption and PL spectra of LPPPC **8** as an amorphous conjugated polymers show remarkably narrow line widths for the allowed singlet exciton transitions, which is principally similar to that what was observed before for Me-LPPP[136]. The fabrication of electronic devices based on this material is in under progress.

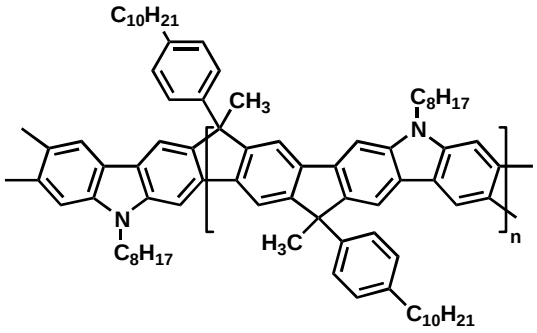

LPPPC **8**

4. Carbazole-based alternating copolymers are also attractive for optoelectronic applications. Especially the alternating carbazole/benzothiadiazole copolymer PCzBTDZ **50** with a backbone of alternating donor (carbazole) and acceptor (benzothiadiazole) units is particularly attractive for the application in photovoltaic cells (chapter 5). Promising initial results in collaboration with Siemens / Erlangen encourage for further investigations of this class of polymers. The measurements are in progress.

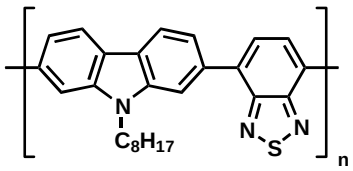

PCzBTDZ **50**

In conclusion, advances in materials development are a need for a further improvement of the polymer light emitting diode technology. With continuing the efforts of synthetic chemists to develop and improve these type of materials, the prospect for the PLED field should continue to brighten. The ease and low costs of making and processing these polymers can be exploited for future technologies and continued commercial applications.

6.2 Outlook:

The polymer light emitting device technology (PLED) faces a bright future in the display market. Eventually, the technology could be used to make screens large enough for laptop and desktop computers. PLED materials could someday be applied to create wall-size video panels, roll-up screens for laptops, or even head wearable displays. The potential of this technology is endless once certain technical problems can be overcome, including display uniformity, stability and colour rendition. Photo- and electrooxidative degradation processes can lead to low energy emission bands, especially in case of phenylene-based ladder polymers (Me-LPPP) or polyfluorenes (PF). Therefore, optimized semiconducting polymers showing a sufficient device stability have to be developed. Manufacturing is also critical although improvements in roll-to-roll processing or ink-jet deposition could significantly increase the efficiency thereby reducing costs. The commercial prospect of PLED also depends upon significant efficiency improvements in order to match the performance of inorganic semiconductors.

Despite the rapid progress of PLEDs and optically pumped lasers stimulated emission under electrical excitation has yet to be observed. Further experiments, however, have to clarify the role of charged excitations as well as the triplet excited states, which are inevitably present under electrical pumping. The present work described in chapter 3 outlines a new way to deal with triplets without loosing the intrinsic (original) electronic properties. From a synthetic point of view, optimized polymer materials for light emitting devices are a future need in order to grow this technology forward.

Generally, it can be stated that significant progress has been made during the last ten years and it is hoped that PLEDs may change the way in which we see things.

7 Experimental Section

7.1 Chemicals and Reagents:

All starting organic compounds which are commercially available were purchased from Aldrich Co. and used without further purification. The solvents were dried by conventional methods, freshly distilled and stored under argon. All reactions of air and water-sensitive materials were performed using standard Schlenck techniques.

7.2 General procedures and Instrumentation:

- ^{1}H and ^{13}C NMR (Nuclear magnetic resonance) spectra were acquired on a Bruker AMX 300 and Bruker ARX 400. Where appropriate, chemical shifts are reported in ppm relative to $(CH_3)_4Si$ as an internal standard. In all cases individual peaks are reported as chemical shift, multiplicity (s=singlet, d=doublet, dd=doublet of doublets, t=triplet, q=quartet, m=multiplet), relative integrated intensity, and coupling constants.

- Gel permeation chromatography (GPC) were performed on
  (1) Spectra 100, Column: MZ sdv-Gel (5 μm particle, Size: 10^5, 10^4, 500 Å)
  Detector: Spectra System UV-2000, Shodex RI-71
  Calibration with polystyrene standard (PSS)
  Solvent: THF
  (2) Jasco AS950, Column: MZ lineal mixed bed
  Detector: Jasco UV-2070, Jasco RI-930
  Calibration with polystyrene standard (PSS)
  Solvent: THF

- Mass spectra (MS) were determined using a Zab 2 SE FPD Bruker Reflex II spectrometer.
  Reported as *m*/*z* and percent relative intensity.

- Absorption spectra were recorded on Jasco V-550 and Shimadzu UV-2101PC

- Photoluminescence spectra were recorded on Fluoromax 3, Fluorescence Spectrophotometer F2500

ICP-OES

- Palladium content were analyzed by inductively coupled plasma optical emission spectroscopy (**ICP-OES or ICP-AES**). This is a major technique for elemental analysis. The sample to be analyzed, if solid, is normally first dissolved and then mixed with water before being fed into the plasma. Atoms in the plasma emit light (photons) with characteristic wavelengths for each element. This light is recorded by one or more optical spectrometers and when calibrated against standards the technique provides a quantitative analysis of the original sample. This analysis have been carried out at Terracon "Laboratorium für Umwelt und Pestizidanalytik GmbH" Am Reitstadion, Jüterberg.

7.3 Monomers

7.3.1 Synthesis of 2,5-dihexylbenzene-1,4-bisboronic acid

7.3.1.1 2,5-Dihexylbenzene [M1]

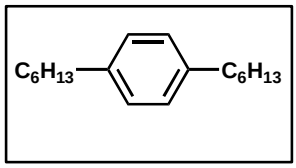

Step 1: Preparation of Grignard Reagent

A three-necked 500 ml flask charged with magnesium turnings (24.3 g; 100 mmol) containing 200 ml ether. Then 2 ml of the hexyl bromide [165.08 g (140 ml); 100 mmol] was injected to the reaction mixture to start the reaction. After 10 minutes the rest of the hexyl bromide in ether was added drop by drop to the reaction mixture via a dropping funnel. The above mixture was stirred at room temperature for 30 min and stored in a same flask under inert atmosphere for the next step of the reaction.

Step 2: Carbon-Carbon Coupling

A flame dried separate flask was charged with 1,4-dichlorobenzene (59 g; 100.4 mmol) and Ni(dppp)Cl_2 (250 mg; 45 mmol) in a 350 ml dry ether. The reaction mixture was cooled to 0 ^{o}C. The freshly prepared Grignard reagent was added to the reaction mixture within 15 minutes and stirred at room temperature for 30 minutes. The mixture was refluxed overnight and cooled down to room temperature. The organic layer was washed with 50 ml water, the organic layer separated and dried with $MgSO_4$. The title product was distilled out at 108 °C under 10^{-3} mbar pressure.

Yield: 86 g (86.26 %)

^{1}H-NMR (200 MHz, d_6-DMSO):

δ(^{1}H) [ppm]: 7.10 (s, 4H, ar-H), 2.65 (t, 4H, α-CH_2), 1.48 (m, 4H, β-CH_2), 1.28, 0.86 (18H alkyl-H)

^{13}C-NMR (50 MHz, d_6-DMSO):

δ(^{13}C) [ppm]: 140.1, 132.3, 35.2, 32.3, 31.2, 28.8, 22.0, 14.0

FD-Mass-spectra: m/z = 246.1 (M^+)

Elemental Analysis: ($C_8H_4O_4Br_2$)

Cal.(%): C: 87.73; H: 12.27

Found(%): C: 87.17; H: 11.95

7.3.1.2 2,5-Dibromo-1,4-di-*n*-hexylbenzene [M2]

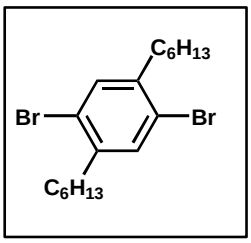

A two-necked flame-dried flask was charged with dihexylbenzene (29.52 g; 120 mmol) and iodine (0.152 g; 60 mmol). The reaction mixture was cooled at 0 ^{o}C. Bromine (41.54 gm = 13.5 ml; 26 mmol) was added within 30 minutes to the above reaction mixture. The flask was rapped with aluminum foil to avoid light. The reaction mixture was stirred overnight at room temperature. The excess bromine was destroyed by the addition of 20 % aqueous KOH solution and stirred until the brown colour disappeared. The organic phase was separated and washed with water. The solvent was evaporated till dryness, the product recrystallized from ethanol.

Yield: 40.4 g (85.2 %)

^{1}H-NMR (200 MHz, d_6-DMSO):

δ(^{1}H) [ppm]: 7.14 (s, 2H, ar-H), 2.65 (t, 4H, α-CH_2), 1.48 (m, 4H, β-CH_2),1.26,0.86, (18H alkyl-H))

^{13}C-NMR (50 MHz, d_6-DMSO):

δ(^{13}C) [ppm]: 140.1, 133.3, 122.2, 35.2, 32.3, 31.2, 28.8, 22.0, 14.0

FD-Mass-spectra: m/z = 404.1 (M^{+})

Elemental Analysis: ($C_8H_4O_4Br_2$)

Cal.(%):	C: 53.48; H: 6.98; Br: 39.53
Found(%):	C: 53.29; H: 6.72; Br: 38.95

7.3.1.3 2,5-dihexylbenzene-1,4-bisboronic acid [M3]

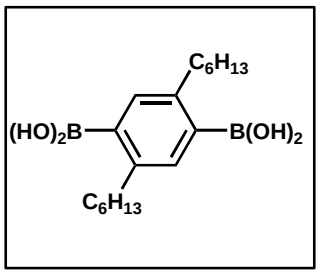

To a refluxing solution of 1,4-dibromo-2,5-dihexylbenzene (23.15 g; 57.25 mmol) in dry hexane (200 ml) was added slowly a 1.6M solution of butyl lithium in hexane (95 ml; 152 mmol). This mixture was refluxed for 24 h, cooled to –70 °C and, after the addition of undiluted trimethyl borate (50 g; 0.48 mol) is stirred for 10 h at 20 °C. Then 2M HCl (200ml) was added and the mixture was stirred until the precipitation of the product was finished. This takes approximately 24 h. The crystalline mass was recovered on a Büchner funnel and washed with hot water two to three times to remove the excess of boronic acid, dried in high vacuum. The material was recrystallized from hot acetone.

Yield: 6.5 g (34 %)

Melting Point: 172 °C

^{1}H-NMR (200 MHz, d_6-DMSO):

δ(^{1}H) [ppm]: 7.85 [s, 4H, -$B(OH)_2$], 7.14 (s, 2H, ar-H), 2.65 (t, 4H, α-CH_2), 1.48 (m, 4H, β-CH_2), 1.26, 0.86 (18H alkyl-H)

^{13}C-NMR (50 MHz, d_6-DMSO):

δ(^{13}C) [ppm]: 141.8, 133.3, 128.7, 35.2, 32.3, 31.2, 28.8, 22.0, 14.0

FD-Mass-spectra: m/z = 334.5 (M^+)

Elemental Analysis : ($C_8H_4O_4Br_2$)

Cal.(%):	C: 64.72; H: 9.65
Found(%):	C: 64.10; H: 9.28

7.3.2 Synthesis of 1,4-bis(4´-decylbenzoyl)-2,5-dibromobenzene

7.3.2.1 2,5-Dibromoterephthalic acid [M4]

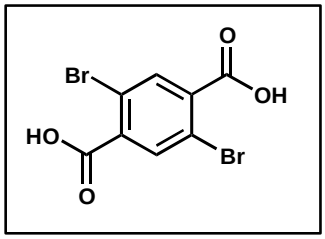

A flame-dried three-necked flask containing 500 ml of half concentrated HNO_3 was charged with 200 g dibromo-p-xylol (0.75 mol, M = 263.97 g/mol). The orange suspension was refluxed for 5 days, three times additional 50 ml of HNO_3 were added. The product starts to precipitate after five days. The reaction mixture was cooled down and neutralize with aqueous KOH solution. Then 300.0 g of $KMnO_4$ (1.9 mol, M = 158.03 g/mol) were added and the mixture refluxed for 24 h. The reaction mixture was charged again with 50.0 g of $KMnO_4$ (0.32 mol, M = 158.03 g/mol) and refluxed for further 3 h. The reaction mixture was cooled down to room temperature and acidified with 50% H_2SO_4 (pH = 1). Simultaneously sodium sulphite (Na_2SO_3) was added until the solution becomes clear. The colourless precipitate was washed 2-3 times with water. The product was dried under high vacuum.

Yield: 175 g (71.80 %)

Melting Point: >250 °C

^{1}H-NMR (200 MHz, d_6-DMSO):

δ(^{1}H) [ppm]: 13.74 (s, COOH, 2H), 8.02 (s, ar-H, 2H)

^{13}C-NMR (50 MHz, d_6-DMSO):

δ(^{13}C) [ppm]:165.8, 137.3, 135.2, 119.0

FD-Mass-spectra: m/z = 323.5 (M^+)

Elemental Analysis: ($C_8H_4O_4Br_2$)

Cal.(%): C: 29.66; H: 1.24; Br: 49.34

Found(%): C: 29.17; H: 1.08; Br: 49.10

7.3.2.2 2,5-Dibromoterephthaloyl dichloride [M5]

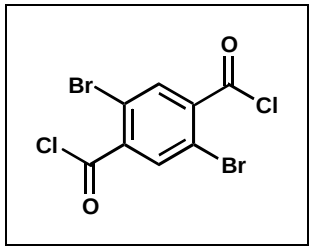

A flame-dried two-necked flask was charged with 25.88 g of 2,5- dibromoterephthalic acid (0.08 mol, M = 323.93 g/mol) and 52.4 g thionylchloride (0.44 mol, M = 118.97 g/mol) and refluxed for 6 h. The excess of thionylchloride was distilled off and the residue recrystallized from heptane (200 ml).

Yield: 26.0 g (90.40 %)

Melting Point: 90 °C

^{1}H-NMR (200 MHz, d_6-DMSO):

δ(^{1}H) [ppm]: 8.17 (s, ar-H, 2H)

^{13}C-NMR (50 MHz, d_6-DMSO):

δ(^{13}C) [ppm]: 165.6, 137.2, 135.3, 119.1

FD-Mass-spectra: m/z = 360.50 (M^+)

Elemental Analysis:($C_8H_2O_2Cl_2Br_2$)

Calc.(%): C: 26.63; H: 0.56

Found (%): C: 26.17; H: 0.40

7.3.2.3 1,4-Bis(4-decylbenzoyl)-2,5-dibromobenzene [M6]

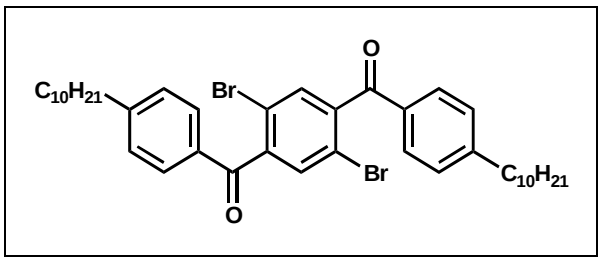

To a solution of 2,5-dibromoterephthaloyl dichloride (3.96 g; 11 mmol, M = 360.81 g/mol) in 100 ml dichloromethane was added aluminium trichloride (3.4 g; 26 mmol; M = 133.05 g/mol) for 15 minutes at 0 °C. A mixture of phenyldecan (9.37 g; 43 mmol, M = 218.05 g/mol) and 30 ml dichloromethane was then added. The reaction mixture was stirred overnight at room temperature. The aluminium complex was destroyed by addition of 10 ml of water and 20 ml aqueous HCl. The organic phase was separated and washed with water. The solvent evaporated till dryness and the product recrystallized from acetone.

Yield: 6.2 g (78.20 %)

Melting Point: 253 °C

^{1}H-NMR (250 MHz, $CDCl_3$):

δ(^{1}H) [ppm]: 7.86 (s, ar-H, 2H), 7.65 (d, ^{3}J = 13.15, ar-H, 4H), 7.22 (d, ^{3}J = 13.15, ar-H, 4H), 2.55 (t, ^{3}J = 7.3, ar-CH_2-, 4H), 1.58-1.21 (m, 32H), 0.96 (t, ^{3}J = 5.3, -CH_3, 6H)

^{13}C-NMR (62.5 MHz, $CDCl_3$):

δ(^{13}C) [ppm]: 187.0, 147.0, 143.1, 135.3, 135.0, 129.9, 128.0, 123.4, 35.8, 32.5, 32.4, 30.3, 23.1, 14.0

FD-Mass-spectra: m/z = 724.50 (M^+)

Elemental Analysis: ($C_{40}H_{52}O_2Br_2$)

Cal.(%): C: 66.30; H: 7.23; Br: 22.05

Found (%): C: 65.95; H: 6.90; Br: 21.89

7.3.3 Hydrogenation and bromination of aliphatic alcohols

7.3.3.1 3,7,11-Trimethyldodecan-1-ol [M7]

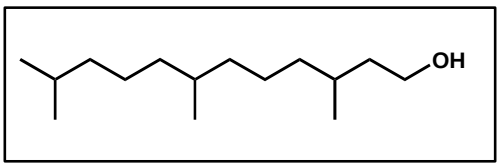

A three-necked 1000 ml flask was charged with 3,7,11-trimethyldodecan-2,6,10-trien-1-ol (12.68 g; 57.05 mmol) and PtO_2*H_2O (78 mg; 0.32 mmol) in 1000 of ml ethyl acetate. The reaction mixture was purged with argon for 10 minutes. Then hydrogen gas was bubbled through the mixture for 6 days at room temperature with constant stirring. The reaction mixture was filtered through a Millipore®-filter (PTFE, SLCR025NB, 0.2 μm) to get rid of the catalyst. The final product was purified by steam distillation.

Yield: 11.5 g (88 %)

^{1}H-NMR (400 MHz, $CDCl_3$):

δ(^{1}H) [ppm]: 3.65 (m, 2H, -CH_2OH), 1.90 (m, 1H, -CH-), 1.57 (m, 2H, -CH_2-), 1.35 (dq, 1H, J=8.0 Hz, -CH_2(-CH_3)$_2$), 1.21-0.90 (m, 13H, -CH_2-), 0.87 (t, 6H, J= 8.0Hz,-CH_3), 0.87 (t, 6H, J = 6.66 Hz, -CH_3).

^{13}C-NMR (100 MHz, $CDCl_3$):

δ(^{13}C) [ppm]: 61.2, 40.0, 39.9, 39.3, 37.5, 37.4, 32.8, 29.5, 27.9, 24.8, 24.3, 22.7, 22.6, 19.7, 19.6

FD-Mass-spectra : m/z = 228.4 (M^+)

7.3.3.2 1-Bromo-3,7,11-trimethyldodecane [M8]

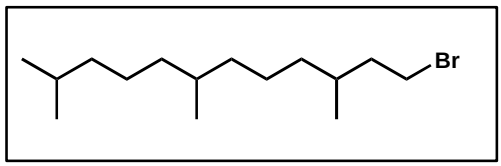

A flame-dried flask was charged with 3,7,11-trimethyldodecane-1-ol (20 g; 87.55 mmol) and triphenylphosphine (25.2 g; 96.85 mmol) in 50 ml of CH_2Cl_2 and the reaction mixture was cooled to 0 °C. N-Bromosuccinimide (18.6 g; 92.1 mmol) was added to the reaction mixture, the mixture was stirred at room temperature for 16 h. The reaction mixture was dissolved in hexane and filtered to get rid of succinimide by-product. The organic phase was vacuum distilled at 95 °C and $5*10^{-3}$ mbar pressure.

Yield: 22 g (84 %)

^{1}H-NMR (400 MHz, $CDCl_3$):

δ(^{1}H) [ppm]: 3.34 (m, 2H, -CH_2Br), 1.80 (m, 1H, -CH-), 1.58 (m, 2H, -CH_2), 1.42 (dq, 1H, J=6.59 Hz, -CH(-CH_3)$_2$, 1.21-0.90 (m, 13H, -CH_2-), 0.78 (t, 6H, J=6.59 Hz,-CH_3), 0.76 (t, 6H, J=6.38 Hz, -CH_3)

^{13}C-NMR (100 MHz, $CDCl_3$):

δ(^{13}C) [ppm]: 40.1, 39.3, 37.3, 37.2, 36.7, 32.7, 31.7, 31.6, 27.9, 24.8, 24.2, 22.7, 22.6, 19.7, 18.9

FD-Mass-spectra: m/z = 291.3 (M^+)

Elemental Analysis: ($C_{15}H_{31}Br$)

Cal.(%):	C: 61.85; H: 10.73; Br: 27.42
Found(%):	C: 61.37; H: 10.46; Br: 26.85

7.3.4 Synthesis of N-Octyl-2,7-bis(4´,4´,5´,5´-tetramethyl-1´,3´,2´-dioxaborolan-2´-yl) Carbazole

7.3.4.1 1-Methoxy-4(4´-methoxyphenyl)-2-nitrobenzene [M9]

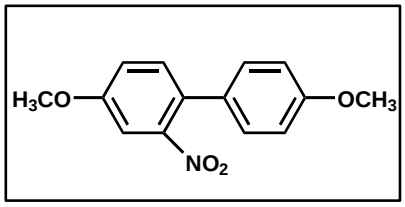

In a 100 ml flask charged with methoxyphenylboronic acid (4.0 g, 26.3 mmol), 4-bromo-3-nitroanisol (5.50 g, 25.0 mmol), 30 ml benzene and 20 ml of 2M aqueous K_2CO_3 solution. The resulting solution was degassed with a vigorous flow of argon. 0.5-1.0 mol % $Pd(PPh_3)_4$ was then added under argon and the mixture was refluxed for 2 h. The mixture was filtered through a Büchner funnel and the filtrate was extracted with three portions of diethyl ether. The combined organic fractions were washed with brine and dried over magnesium sulfate. The solvent was removed under reduced pressure and the residue was recrystallized with a mixture of ethyl acetate and hexane to provide the title product as a yellow solid.

Yield: 5.0 g (81.43 %)

Melting Point: 123-125 °C

^{1}H-NMR (400 MHz, $CDCl_3$):

δ(^{1}H) [ppm]: 7.32 (m, 2H), 7.21 (d, 2H, J = 8.8 Hz), 7.13(dd, 1H, J = 5.9 & 2.2 Hz), 6.94 (d, 2H, J = 8.8 Hz), 3.88 (s, 3H), 3.83 (s, 3H).

^{13}C-NMR (100 MHz, $CDCl_3$):

δ(^{13}C) [ppm]: 159.4, 158.8, 149.7, 132.8, 129.4, 129.2, 128.2, 118.6, 114.1, 108.9, 55.9, 55.3

FD-Mass-spectra: m/z = 259.05 (M^+)

Elemental Analysis: ($C_{14}H_{13}NO_4$)

Cal.(%): C: 64.86; H: 5.05; N: 5.40

Found (%): C: 64.25; H: 4.90; N: 4.91

7.3.4.2 2,7-Dimethoxycarbazole [M10]

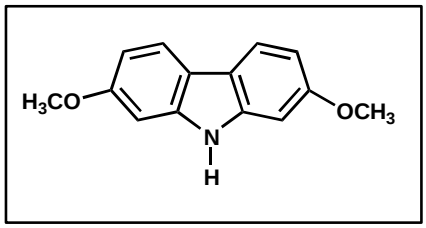

A 50 ml flask was charged with (4.5 g; 17.35 mmol) of 1-methoxy-4(4′-methoxybenzene)-2-nitrobenzene, and 20 ml triethylphosphite. The resulting mixture was refluxed under argon for 5 h. The excess of triethylphosphite was removed under reduced pressure (40 °C, 0.25 mm Hg) and the crude product was recrystallized from hot hexane to provide the title product as a pale yellow solid.

Yield: 3.0 g (76.14 %)

^{1}H-NMR (400 MHz, $CDCl_3$):

δ(^{1}H) [ppm]: 8.02 (s, 1H), 7.68 (dd, 2H), 6.80 (m, 4H), 3.95 (s, 6H)

^{13}C-NMR (100 MHz, $CDCl_3$):

δ(^{13}C) [ppm]: 156.5, 135.8, 120.3, 117.2, 109.5, 97.0, 55.6

FD-Mass-Spectra: m/z = 227.0 (M^+)

Elemental Analysis: ($C_4H_{13}NO_2$)

Cal.(%):	C: 73.99; H: 5.77; N: 6.16
Found(%):	C: 73.26; H: 5.35; N: 5.95

7.3.4.3 N-Octyl-2,7-dimethoxycarbazole [M11]

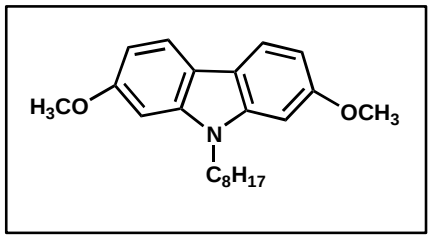

A 50 ml flask was charged with 2,7-dimethoxycarbazole (2.5g; 11 mmol), 1-bromoocatne (4.25 g; 22 mmol), sodium hydroxide reagent grade (0.89 g; 22 mmol), and tetrabutylamonium hydrogensulfate (TBAH) 134 mg (0.39 mmol) in 25 ml of anhydrous acetone. The resulting mixture was refluxed under argon for 24 h and then poured into 100 ml of distilled water. The aqueous layer was extracted three times with diethyl ether. The combined organic fractions were dried over magnesium sulfate and the solvent was removed under reduced pressure. The residue was purified by column chromatography (silica gel, 5% ethyl acetate in hexane as eluent) to provide the title product as white fluffy solid.

Yield: 5.0 g (94.79 %)

Melting Point: 63-64 °C

^{1}H-NMR (400 MHz, $CDCl_3$) :

δ(^{1}H) [ppm] : 7.88 (dd, 2H, J = 5.9 and 1.5 Hz), 6.84 (m, 4H), 4.17 (t, 2H, J = 7.4 Hz), 3.95 (s, 6H), 1.86 (m, 2H), 1.35 (m, 10H), 0.92 (t, 3H, J = 4.4 Hz).

^{13}C-NMR (100 MHz, $CDCl_3$):

δ(^{13}C) [ppm]: 158.2, 141.9, 120.1, 117.1, 106.6, 93.6, 55.7, 43.0, 31.8, 29.4, 29.2, 28.7, 27.3, 22.6, 14.1

FD-Mass- Spectra: m/z = 339.50 (M^+)

Elemental Analysis: ($C_{22}H_{29}NO_2$)

Cal.(%):	C: 77.84; H: 8.61; N: 4.13
Found (%):	C: 77.26; H: 8.40; N: 3.95

7.3.4.4 N-Octyl-2,7-hydroxycarbazole [M12]

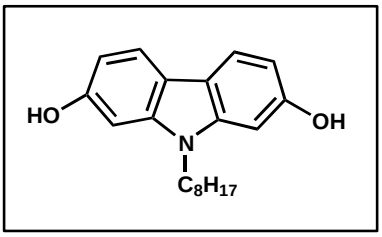

A 250 ml flask dried flask was charged with N-octyl-2,7-dimethoxycarbazole (4.0 g; 11.71 mmol) and 100 ml of anhydrous methylene chloride. The solution was cooled to –78 °C and 25 ml (50 mmol) of boron tribromide (1M in methylene chloride) was added over 0.5 h. The resulting mixture was stirred under argon at –78 °C for 3 h and at room temperature for 12 h. The mixture was quenched slowly with 50 ml of aqueous HCl (10 % v/v) to destroy the excess of boron tribromide and extracted three times with methylene chloride. The combined organic fractions were dried over magnesium sulfate and the solvent removed under reduced pressure. Recrystallization from toluene / hexane obtained the title product.

Yield: 2.0 g (54.64 %)

Melting Point: 144-145 °C

^{1}H-NMR (400 MHz, $CDCl_3$):

δ(^{1}H) [ppm]: 8.22 (s, 2H), 7.76 (d, 2H, J = 8.8 Hz), 6.88 (d, 2H, J = 2.2 Hz), 6.70 (dd, 2H, J = 8.8 and 2.2 Hz), 4.19 (t, 2H, J = 7.4 Hz), 1.82 (m, 2H), 1.31 (m, 10H); 0.86 (t, 3H, J = 6.6 Hz).

^{13}C-NMR (100 MHz, $CDCl_3$):

δ(^{13}C) [ppm]: 156.3, 142.8, 120.3, 117.1, 108.4, 95.7, 43.2, 32.2, 29.8, 29.2, 28.9, 27.2, 23.1, 14.2.

FD-Mass- Spectra: m/z = 311.50

Elemental Analysis: ($C_{20}H_{25}NO_2$)

Cal. (%): C: 77.14; H: 8.09; N: 4.50

Found (%): C: 76.90; H: 7.80; N: 4.17

7.3.4.5 N-Octyl-2,7-bis(trifluoromethanesulfonyl)carbazole [M13]

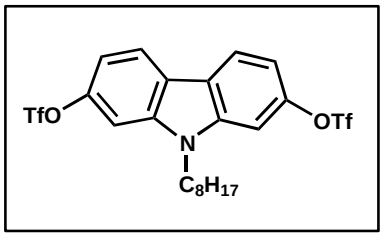

A 50 ml flask was charged with N-octyl-2,7-hydroxycarbazole, 1.5 g (4.8 mmol), dimethylaminopyridine (DMAP) 520 mg (4.8 mmol) and 16 ml of anhydrous pyridine. The mixture was cooled to 0 °C and trifluoromethanesulfonic anhydride, 4.06 g (14.40 mmol) was added drop wise. After 10 minutes 4 ml of pyridine were added to dissolve the white precipitate formed during the addition of the anhydride. The mixture was stirred at 0 °C for 1 h and at room temperature for 24 h. The excess of anhydride was destroyed via slow addition of 25 ml of distilled water. The mixture was extracted three times with 25 ml of diethyl ether. The combined organic fractions were washed successively with five 50 ml portions of distilled water, five 50 ml portions of 0.1M aqueous $CuSO_4$, three 50 ml portions of brine and again with 50 ml portions of distilled water. The mixture was dried over magnesium sulfate and the solvent was removed under reduced pressure. The crude product was purified by column chromatography (silica gel, 5 % ethyl acetate in hexane as eluent) to provide the title product as a red oil.

Yield : 2.0 g (72.20 %)

^{1}H-NMR (400 MHz, $CDCl_3$):

δ(^{1}H) [ppm] : 8.00 (d, 2H, J=8.8 hz,), 7.28 (d, 2H, J =2.2 Hz), 7.13 (dd, 2H, J = 8.8 and 2.2 Hz), 4.17 (t, 2H, J = 7.4 Hz), 1.83 (m, 2H), 1.30 (m, 10H), 0.89 (t, 3H, J = 6.6 Hz).

^{13}C-NMR (100 MHz, $CDCl_3$):

δ(^{13}C) [ppm]: 148.6, 141.8, 122.1, 121.4, 113.3, 103.0, 43.6, 31.6, 29.2, 29.0, 28.6, 27.1, 22.5, 13.9.

FD-Mass- Spectra: m/z = 575.50 (M^+)

Elemental Analysis: ($C_{22}H_{23}F_6NO_6S_2$)

Cal. (%):	C: 45.91; H: 4.03; N: 2.43; S: 11.14
Found (%):	C: 45.40; H: 3.80; N: 2.10; S: 10.80

7.3.4.6 N-Octyl-2,7-bis(4´,4´,5´,5´-tetramethyl-1´,3´,2´-dioxaborolan-2´-yl) carbazole [M14]

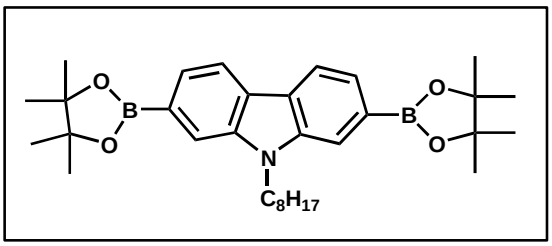

A flame-dried 50 ml flask was charged simultaneously with 1.5 g (2.61 mmol) of the bistriflate (M13) 25 ml of dioxane, 38 mg (0.05 mmol) of $PdCl_2$(dppf), 2.5 ml of triethylamine and 1.14 ml (7.8 mmol) of 4,4,5,5-tetramethyl-1,3,2-dioxaborolane. The mixture was stirred under argon for 24 h at 80 °C and then poured in 50 ml of distilled water. The aqueous layer was extracted with three portions of chloroform. The combined organic layers were dried over magnesium sulfate and the solvent was removed under reduced pressure. The crude dark red oil was purified by column chromatography (triethyl amine pre-treated silica gel with 5 % ethyl acetate in hexane as eluent) to provide the title product as a white solid.

Yield: 850 mg (61.59 %)

Melting Point: 168-170 °C

^{1}H-NMR (400 MHz, $CDCl_3$):

δ(^{1}H) [ppm]: 8.13 (d, 2H, J = 7.4 Hz), 7.89 (s, 2H), 7.69 (d, 2H, J = 7.4 Hz), 4.40 (t, 2H, J = 7.4 Hz), 1.90 (m, 2H), 1.32 (m, 24H), 1.30 (m, 10H), 0.88 (t, 3H, J = 6.6 Hz).

^{13}C-NMR (100 MHz, $CDCl_3$):

δ(^{13}C) [ppm]: 140.4, 125.0, 124.8, 120.0, 115.2, 83.8, 42.9, 31.8, 29.3, 29.2, 29.1, 27.1, 24.9, 22.6, 14.1

FD-Mass- Spectra: m/z = 531.50 (M^+)

Elemental Analysis: ($C_{32}H_{47}B_2NO_4$)

Cal. (%)	C: 72.33; H: 8.92; N: 2.64
Found (%)	C: 71.89; H: 8.40; N: 2.28

7.3.5 Synthesis of N-octyl-2,7-dichlorocarbazole

7.3.5.1 1-Chloro-4-(4´-chlorophenyl)-2-nitrobenzene [M15]

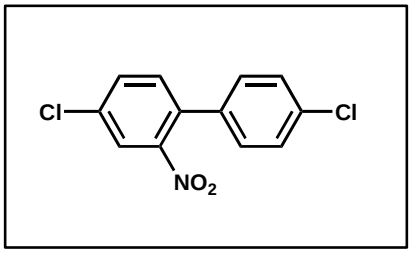

In a 100 ml flask, 4-chlorophenylboronic acid (4.0 g; 25.6 mmol), 1-bromo-4-chloro-2-nitrobenzene (5.44 g; 23 mmol), 40 ml of benzene and 25 ml of 2M aqueous K_2CO_3 were mixed. The resulting solution was degassed with a vigorous flow of argon. Tetrakis(triphenylphosphino) Pd(0) (0.5 mol%) was then added under argon and the mixture was refluxed for 2 h. The mixture was filtered through a Büchner funnel and the filtrate was extracted three times with diethyl ether. The combined organic fractions were washed with brine and dried over magnesium sulfate. The solvent was removed under reduced pressure and the residue was purified by column chromatography (silica gel, hexane as eluent) to provide the title product as a yellow solid.

Yield : 6.10 g (97.91 %)

Melting Point: 88-89 °C

^{1}H-NMR (400 MHz, $CDCl_3$):

δ(^{1}H) [ppm]: 8.06 (d, 1H, J =2.2 Hz), 7.82 (dd, 1H, J = 5.9 and 2.2 Hz), 7.61 (d, 1H, J = 5.9 Hz), 7.52 (dd, 2H, J = 8.8 and 2.2 Hz), 7.40 (dd, 2H, J = 8.8 and 2.2 Hz).

^{13}C-NMR (100 MHz, $CDCl_3$):

δ(^{13}C) [ppm]:136.0, 134.9, 134.6, 134.0, 133.5, 130.4, 129.6, 124.8

FD-Mass- Spectra: m/z = 267 (M^+)

Elemental Analysis: ($C_{12}H_7Cl_2NO_2$)

Cal.(%):	C: 53.76; H: 2.63; N: 5.22
Found (%):	C: 53.40; H: 2.50; N: 5.10

7.3.5.2 2,7-Dichlorocarbazole [M16]

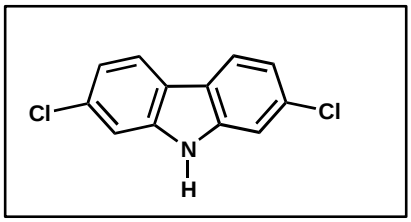

A 25 ml flask was charged with 5.0 g (18.65 mmol) of 1-chloro-4-(4´-chlorophenyl)-2-nitrobenzene and 25 ml triethylphosphite. The resulting mixture was refluxed under argon for 5 h. The excess of triethyl phosphate was removed by washing the crude product with hexane provides title product.

Yield: 3.10 g (70.50 %)

Melting point: 188-189 °C

^{1}H-NMR (400 MHz, $CDCl_3$):

δ(^{1}H) [ppm]: 8.02 (s, 1H), 7.91 (d, 2H, J = 8.8 Hz), 7.38 (d, 2H, J = 1.5 Hz), 7.22 (dd, 2H, J = 8.8 and 1.5 Hz) .

^{13}C-NMR (100 MHz, $CDCl_3$):

δ(^{13}C) [ppm]: 140.1, 131.8, 121.4, 121.1, 120.6, 110.8

FD-Mass- Spectra: m/z = 235 (M^+)

Elemental Analysis: $C_{12}H_7Cl_2N$

Cal. (%): C: 61.05; H: 2.99; Cl: 30.03; N: 5.93

Found (%): C: 60.90; H: 2.70; Cl: 29.80; N: 5.47

7.3.5.3 N-Octyl-2,7-dichlorocarbazole [M17]

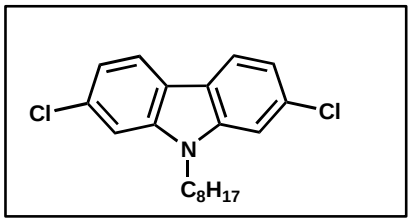

To a solution of 2,7-dichlorocarbazole (2.5 g; 10.63 mmol) in 30 ml DMF were added 2.93 g (21.26 mmol) of anhydrous K_2CO_3. The mixture was stirred at 80 °C for 2 h under argon after 4.10 g (21.20 mmol) of 1-bromooctane were added. The mixture was stirred at 80 °C for 24 h and then quenched with 40 ml of water. The aqueous layer was extracted three times with 50 ml of diethyl ether. The organic layer was dried over magnesium sulfate and the solvent was removed under vacuum. The residue was purified by column chromatography (silica gel, hexane as eluent) to give the title product as a white solid.

Yield: 3.2 g (86.40 %)

^{1}H-NMR (400 MHz, $C_2D_2Cl_4$):

δ(^{1}H) [ppm]: 7.80 (d, 2H, J = 8.8 Hz), 7.30 (d, 2H, J= 2.2 Hz), 7.19 (dd, 2H, J =8.8 and 2.2 Hz), 4.07 (t, 2H, J = 7.4 Hz), 1.86 (m, 2H), 1.35 (m, 10H), 0.92 (t, 3H, J = 4.4 Hz).

^{13}C-NMR (100 MHz, $C_2D_2Cl_4$):

δ(^{13}C) [ppm]: 141.7, 131.7, 121.0, 120.8, 119.8, 109.2, 43.2, 32.2, 29.8, 29.2, 28.9, 27.2, 23.1, 14.2

FD-Mass-Spectra: m/z = 347.5 (M^+)

Elemental Analysis: ($C_{20}H_{23}Cl_2N$)

Cal. (%):	C: 68.97; H: 6.66; Cl: 20.36; N: 4.02
Found (%):	C: 68.35; H: 6.25; Cl: 20.17; N: 3.95

7.3.5.4 N-3,7,11-trimethyldodecyl-2,7-dichlorocarbazole [M18]

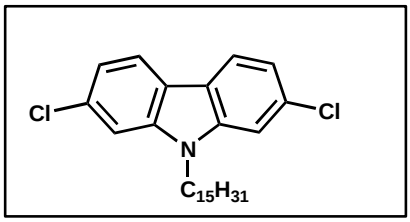

To a solution of 2,7-dichlorocarbazole (2.5 g; 10.63 mmol) in 30 ml DMF were added 2.93 g (21.26 mmol) of anhydrous K_2CO_3. The mixture was stirred at 80 °C for 2 h under argon after 5.82 g (20 mmol) of 1-bromo-3,7,11-trimethyldodecane were added. The mixture was stirred at 80 °C for 24 h and then quenched with 40 ml of water. The aqueous layer was extracted three times with 50 ml of diethyl ether. The organic layer was dried over magnesium sulfate and the solvent was removed under vacuum. The residue was purified by column chromatography (silica gel, hexane as eluent) to give the title product as a white solid.

Yield: 3.7 g (78 %)

^{1}H-NMR (400 MHz, $C_2D_2Cl_4$):

δ(^{1}H) [ppm]: 7.80 (d, 2H, J = 8.8 Hz), 7.30 (d, 2H, J= 2.2 Hz), 7.19 (dd, 2H, J =8.8 and 2.2 Hz), 4.07 (t, 2H, J = 7.4 Hz), 1.58 (m, 2H), 1.34-1.04 (m, 15H), 0.98 (d,6H, -CH_3), 0.81 (t, 6H, -$(CH_3)_2$)

^{13}C-NMR (100 MHz, $C_2D_2Cl_4$):

δ(^{13}C) [ppm]: 141.7, 131.7, 121.0, 120.8, 119.8, 109.2, 39.2, 38.2, 37.8, 37.5, 37.4, 33.0, 32.7, 28.2, 25.0, 24.6, 22.7, 19.7, 19.5, 23.1, 14.2

FD-Mass-Spectra: m/z = 445.5 (M^+)

Elemental Analysis: ($C_{20}H_{23}Cl_2N$):

Cal. (%):	C: 72.63; H: 8.35; Cl: 15.88; N: 3.14
Found (%):	C: 72.17; H: 8.16; Cl: 15.29; N: 2.98

7.3.6 Synthesis of N-octyl-3,6-bis(4´,4´,5´,5´-tetramethyl-1´,3´,2´-dioxaborolan-2´-yl)carbazole

7.3.6.1. N-Octyl-3,6-dibromocarbazole [M19]

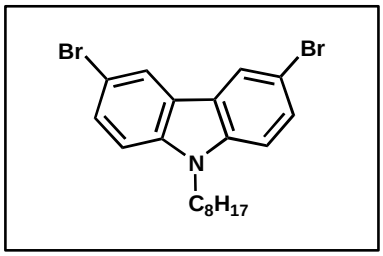

A 50 ml flask was charged with 3,6-dibromocarbazole (4.25 g;13.2 mmol), 1-bromooctane (5.10 g; 26.40 mmol), 1.06 g (26.40 mmol) of sodium hydroxide reagent grade, tetrabutylammonium hydrogensulfate (TBAH) (134 mg; 0.39 mmol) and 25 ml of anhydrous acetone. The resulting mixture was refluxed under argon for 24 h and then poured into 100 ml of distilled water. The aqueous layer was extracted three times with diethyl ether. The combined organic fractions were dried over magnesium sulfate and the solvent was removed under reduced pressure. The residue was purified by column chromatography (silica gel, 5 % ethyl acetate in hexane as a eluent) to provide the title product as white fluffy solid.

Yield: 5.0 g (87.10 %)

^{1}H-NMR (400 MHz, $C_2D_2Cl_4$):

δ(^{1}H) [ppm]: 8.14 (s, 2H), 7.57 (d, 2H, J=6.6 Hz), 7.32 (d, 2H, J=6.6 Hz), 4.17 (t, 2H, J = 7.4 Hz), 1.86 (m, 2H), 1.35 (m, 10H), 0.92 (t, 3H, J = 4.4 Hz).

^{13}C-NMR (100 MHz, $C_2D_2Cl_4$):

δ(^{13}C)[ppm]: 140.2, 129.7, 124.1, 123.9, 112.5, 111.4, 43.2, 32.4, 29.8, 29.2, 28.9, 27.2, 23.1, 14.2

FD-Mass-Spectra: 435.5 (M^+)

Elemental Analysis: ($C_{20}H_{23}Br_2N$)

Cal. (%):	C: 54.94; H: 5.30; Br: 36.55; N: 3.20
Found (%):	C: 54.50; H: 5.17; Br: 36.10; N: 2.95

7.3.6.2 N-Octyl-3,6-bis(4´,4´,5´,5´-tetramethyl-1´,3´,2´-dioxaborolan-2´-yl) carbazole [M20]

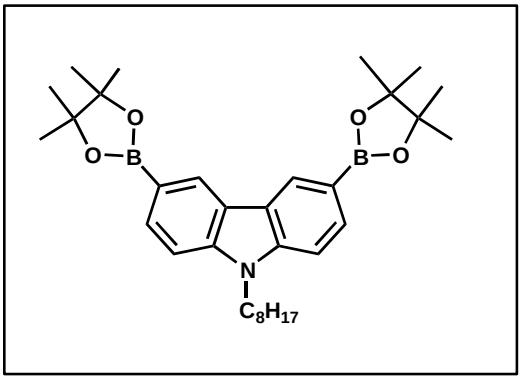

A flame-dried 50 ml flask was charged simultaneously with N-octyl-3,6-dibromocarbazole (2.0 g; 4.6 mmol), 25 ml of dioxane, 38 mg (0.05 mmol) of $PdCl_2$(dppf), 2.5 ml of triethylamine and 1.38 ml (9.2 mmol) of 4,4,5,5-tetramethyl-1,3,2-dioxaborolane. The mixture was stirred under argon for 24 h at 80 °C and then poured into 50 ml of distilled water. The aqueous layer was extracted with three portions of chloroform. The combined organic layers were dried over magnesium sulfate and the solvent was removed under reduced pressure. The crude dark red oil was purified by column chromatography (Triethyl amine pre-treated silica gel 5 % ethyl acetate in hexane as eluent) to provide the title product as a white solid.

Yield: 1.2 g (49.18 %)

^{1}H-NMR (400 MHz, $C_2D_2Cl_4$):

δ(^{1}H) [ppm]: 8.60 (s, 2H), 7.86 (d, J=6.9 Hz, 2H), 7.44 (d, J=6.9 Hz, 2H), 4.40 (t, 2H, J = 7.4 Hz), 1.90 (m, 2H), 1.41 (m, 24H), 1.30 (m, 10H), 0.88 (t, 3H, J = 6.6 Hz).

^{13}C-NMR (100 MHz, $C_2D_2Cl_4$):

δ(^{13}C) [ppm]: 143.4, 132.7, 128.4, 123.4, 111.4, 109.0, 84.4, 42.91, 31.84, 29.37, 29.20, 29.17, 27.12, 24.95, 22.64, 14.11

FD-Mass-Spectra: m/z = 531.5 (M^+)

Elemental Analysis ($C_{34}H_{51}B_2NO_4$):

Cal. (%):	C: 73.00; H: 9.19; N: 2.50
Found(%):	C: 72.49; H: 8.98; N: 2.08

7.3.7 Synthesis of 5,5´-bis(trimethylstannyl)-2,2´-bithiophene

7.3.7.1 5,5´-bis(trimethylstannyl)-2,2´-bithiophene [M21]

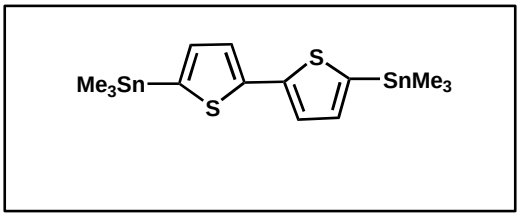

A flame-dried flask was charged with 2,2´-bithiophene (1.162 g; 7 mmol) and N,N,N´,N´-tetramethylethylenediamine (TMEDA) (2.34 ml; 15.59 mmol) in anhydrous hexane-THF (10:20 ml). The mixture was cooled down to –50 °C and n-BuLi (1.6 M in hexane) (10.21 ml; 16.35 mmol) was added dropwise via a syringe. The mixture was heated to reflux for 45 minutes and then cooled to –78 °C. Trimethyltinchloride (16.35 ml; 16.35 mmol) was added dropwise via a syringe, and the mixture was stirred for 2 h at room temperature. The solution was than poured into aq. NH_4Cl (2M). The aqueous layer was extracted with ether. The combined organic layers were washed with H_2O, dried on $MgSO_4$ and the solvent was removed. The resulting residue was recrystallized from ethanol.

Yield: 2.47 g (72 %)

^{1}H-NMR (400 MHz, $C_2D_2Cl_4$):

δ(^{1}H) [ppm]: 7.20 (d, J=3.3 Hz, 2H,), 7.02 (d, J=3.3 Hz, 2H,), 0.31 (s, 18 H)

^{13}C-NMR (100 MHz, $C_2D_2Cl_4$):

δ(^{13}C) [ppm]:143.1, 137.6, 136.3, 125.1, 7.71

FD-Mass-Spectra: m/z = 491.5 (M^+)

Elemental Analysis ($C_{14}H_{22}S_2Sn_2$):

Cal. (%):	C: 34.19; H: 4.51; S: 13.04; Sn: 48.27
Found(%):	C: 34.08; H: 4.26; S: 12.80

7.3.8 Synthesis of 4,7-dibromo-2,1,3-benzothiadiazole

7.3.8.1 2,1,3 –Benzothiadiazole [M22]

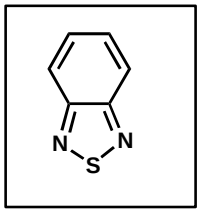

A flame-dried round bottom flask was charged with *ortho*-phenylenediamine (5.0 g; 46.29 mol) in a mixture of pyridine and methylene chloride. The mixture was vigorously stirred at –20 °C during dropwise addition of thionyl chloride (6.64 ml; 92.58 mol in 25 ml CH_2Cl_2) over 30 minutes. The orange mixture was warmed to 25 °C and the solvent removed at a pressure of 0.02 mm. The dry solid was washed with water several times and dried with high vacuum pump.

Yield: 4.96 g (79 %)

Melting Point: 44 °C

FD-Mass-Spectra: m/z = 136.0

^{1}H-NMR (400 MHz, $CDCl_3$)

δ(^{1}H) [ppm]: 7.96 (d, 2H), 7.52 (d, 2H)

^{13}C-NMR (100 MHz, $CDCl_3$)

δ(^{13}C) [ppm]: 121.5, 129.2, 154.7

Elemental Analysis:

Cal. (%):	C: 52.92; H: 2.96; N: 20.57; S: 23.55
Found(%):	C: 52.50; H: 2.61; N: 20.16; S: 23.13

7.3.8.2 4,7-Dibromo-2,1,3-benzothiadiazole: [M23]

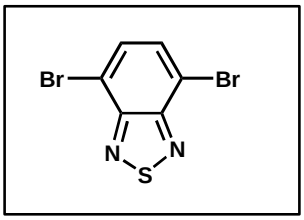

A mixture of 2,1,3- benzothiadiazole (2.20 g; 16.2 mmol) in 20 ml of conc. hydrobromic acid (47 %) was heated under reflux with vigorous stirring, while 2.67 ml (48.6 mmol) of bromine was added slowly within 30 minutes. Towards the end of the addition, the reaction mixture became a viscous suspension. In order to facilitate stirring, another 100 ml of 47 % hydrobromic acid was added and the mixture was heated under reflux for 2.5 hours after completion of the bromine addition . The mixture was filtered while hot, cooled, filtered again and washed with water and dried gave the title product.

Yield: 5.0 g (83.89 %)

Melting Point: 185 °C

FD-Mass-Spectra: m/z = 293.0

^{1}H-NMR (400 MHz, $C_2D_2Cl_4$)

δ(^{1}H) [ppm]: 7.78 (s, 2H)

^{13}C-NMR (100 MHz, $C_2D_2Cl_4$)

δ(^{13}C) [ppm]: 152.9, 132.24, 113.83

Elemental Analysis:

Cal.(%): C: 24.51; H: 0.69; Br: 54.36; N: 9.53; S: 10.91

Found (%): C: 24.11; H: 0.48; Br: 54.17; N: 9.14; S: 10.65

7.4 Homopolymers

7.4.1 Poly[N-(3,7,11-trimethyldodecyl)carbazole-2,7-diyl] [PFCB 39]

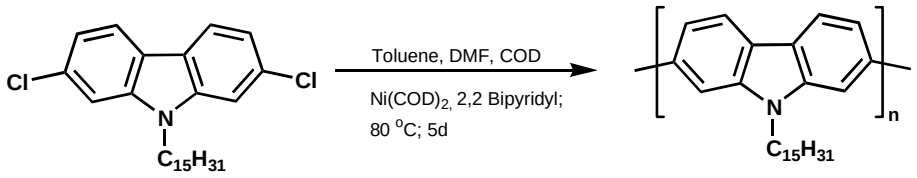

Two Schlenk tubes (100 ml and 50 ml) both sealed with rubber stopper and equipped with a stirring bar are evacuated under high vacuum and dried thoroughly with a heat gun several times. The small Schlenck tube was flushed with argon and N-(3,7,11-trimethyldodecyl)-2,7-dichlorocarbazole (0.890 g; 2.0 mmol) has been charged under a light stream of argon. The solid monomer was completely dissolved using an ultrasonic bath in 15 ml toluene.

The large 100 ml-Schlenck tube was transferred into a glove box and flushed with the inert atmosphere. The tube was charged with $Ni(COD)_2$ (1.265 g; 4.6 mmol) and 2,2`-bipyridyl (0.718 g; 4.6 mmol) and sealed again with a rubber stopper. The tube was taken outside the glove box and dry 15 ml DMF and 45 ml toluene are added by syringe. The solution turns into a deep blue colour after a while. The tube was put into ultrasonic bath for one minute and wrapped completely with aluminium foil to exclude light. The large tube was transferred into an oil bath (80 °C) under vigorous stirring and 1,5 cyclooctadiene (COD) (0.313 g; 2.9 mmol) injected by syringe. The solution was stirred at this temperature for 30-45 min. The monomer solution was transferred from the small schlenck tube into the catalyst mixture using a syringe. The polycondensation reaction is carried out at 80 °C for 3-7 days. When using an additional monofunctional end capper one can limit the reaction time to 2-3 days.

The reaction is quenched by adding ca. 10 ml of a 4M-solution of HCl in Dioxane, again the reaction mixture is stirred for 15 minutes at 80 °C. The reaction mixture was then transferred into a separating funnel with 200 ml chloroform. The organic phase was washed with 100 ml aqueous 2N HCl and 100 ml of a saturated Na_2-EDTA solution. Finally the

organic phase was washed with 100 ml of a saturated $NaHCO_3$-solution and treated once again with 100 ml Na_2-EDTA solution. The organic phase was then filtered through a column with a small layer of Celite 545, a considerable amount of silica gel and a thin layer of sand. The solvent was evaporated until the solution becomes viscous. Then the polymer was precipitated into a mixture of acetone and aqueous 2N HCl. The polymer was collected by filtration and dried under high vacuum.

Yield: 525 g (70.18 %)

GPC (THF): $\overline{M}_n$ = 5,800 g/mol; $\overline{M}_w$ = 6,400 g/mol; D = 1.11

UV/Vis-absorption (in $CHCl_3$): $\lambda_{max,}$ Abs. (nm) = 382 nm

(Solid state): λ_{max}, Abs. (nm) = 371 nm

Photoluminescence (in $CHCl_3$): λ_{max}, PL (nm) = 420 nm

(Solid state): $\lambda_{max,}$ PL (nm) = 429 nm

7.5 Synthesis of ladder polymers

7.5.1 Poly[2,5-bis(4´-decylbenzoyl)-1,4-phenylene-*co*-2,5-dihexyl-1,4-phenylene] [23]

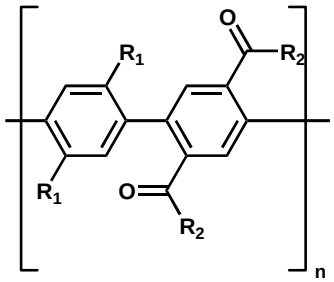

R_1 = *n*-C_6H_{13}; R_2 = -1,4-C_6H_4-*n*-$C_{10}H_{21}$

A flame-dried two-necked flask charged with 1,4-bis(4´-decylbenzoyl)-2,5-dibromobenzene (0.725 g; 1 mmol), 2,5-dihexyl-1,4-phenylenediboronic acid (0.334 g; 1 mmol), 5 ml of an aqueous 1 M sodium carbonate solution and in 25 ml of toluene. The mixture was refluxed and 35 mg of tetrakis(triphenylphosphino)palladium(0) in 5 ml toluene were added . The mixture was refluxed for 3 days under argon. The mixture was filtered through Büchner funnel and the filtrate was washed three times with water and aqueous 2N HCl. The combined organic phases were dried over magnesium sulphate and the solvent removed under reduced pressure till a viscous solution remain in the flask. The viscous solution of the polymer was precipitated into a mixture of acetone and aqueous 2N HCl. The solid material was recovered by filtration through a Büchner funnel and dried under reduced pressure.

Yield: 550 mg (68.1 %)

GPC (THF): $\overline{M}_n$ = 8,500 g/mol; $\overline{M}_w$ = 16,800 g/mol; D = 1.97

^{1}H-NMR (400 MHz, $C_2D_2Cl_4$):

δ(^{1}H) [ppm]: 7.60, 7.40, 7.22, 6.93, 6.65, 2.55 (4H), 2.35 (4H), 1.3 (48H), 0.95 (12H)

^{13}C-NMR (100 MHz, $C_2D_2Cl_4$):

δ(^{13}C) [ppm]: 190.8, 142.7, 140.5, 137.8, 136.2, 135.2, 131.8, 130.3, 129.7, 128.0, 35.8, 32.5, 31.8, 31.6, 30.3, 29.5, 29.3, 23.1, 22.5, 14.0

7.5.2 Poly[2,5-bis(4´-decylphenyl-phenylhydroxy-methyl)-1,4-phenylene-*co*-2,5-dihexyl –1,4-phenylene] [24]

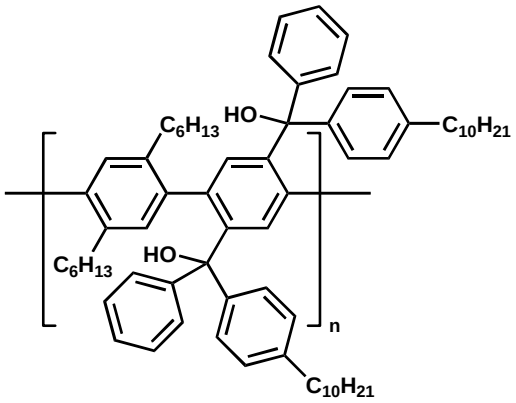

To a solution of polyketone **23** (400 mg; 0.495 mmol) in toluene and tetrahydrofuran (1:1), Ph-Li (5 mmol) 2 ml of 2N solution in diethyl ether was added under argon . The solution was stirred for 30 minutes at room temperature and carefully quenched with ethanol, water and 2N aqueous hydrochloric acid. The organic layer was washed with water, dried and concentrated to dryness. The polymer was dried thoroughly under high vacuum for 24 h.

Yield: 350 mg (73.34 %)

^{1}H-NMR (400 MHz, $C_2D_2Cl_4$):

δ(^{1}H) [ppm]: 7.56,7.20, 7.01, 6.98, 6.7, 5.03, 2.0, 1.3, 0.95 (12H)

^{13}C NMR (100 MHz, $C_2D_2Cl_4$):

δ(^{13}C) [ppm]: 142.0, 141.2, 140.3, 139.0, 138.5, 137.3, 129.2,128.5, 128.2,127.0, 126.5, 125.5, 72.8, 35.9, 32.6, 31.8, 29.5, 29.3, 22.5, 14.0

7.5.3 Diphenyl-substituted *para*-phenylene ladder polymer) [Ph-LPPP]

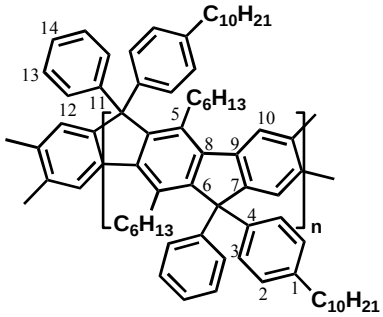

A solution of polymer **24** (290 mg; 0.312 mmol) in 50 ml dichloromethane was treated with boron trifluoride etherate (2.896 g; 20.37 mmol). The solution was stirred for 30 min at room temperature. Then, 20 ml of ethanol were added followed by 50 ml of water to quench excess of boron trifluoride. The organic layer was carefully washed with water, dried and concentrated. Precipitation into acetone gave Ph-LPPP as a bright yellow powder.

Yield: 250 mg (89.60 %)

GPC (THF): $\overline{M}_n$ = 10,700 g/mol; $\overline{M}_w$ = 15,100 g/mol; D = 1.41

Palladium content : 80 ppm

UV/VIS-Absorption (in $CHCl_3$): $\lambda_{max,}$ Abs. (nm) = 425, 455

(solid state): λ_{max}, Abs. (nm) = 420, 446

Photoluminescence (in $CHCl_3$): $\lambda_{max,}$ PL (nm) = 459, 520

(solid state): $\lambda_{max,}$ PL (nm) = 460, 524

^{1}H-NMR (400 MHz, $C_2D_2Cl_4$):

δ(^{1}H) [ppm]: 7.62, 7.26, 7.14, 7.07, 6.91, 2.56, 1.62, 1.3 (48H), 0.95 (12H)

^{13}C-NMR (100 MHz, $C_2D_2Cl_4$):

δ(^{13}C) [ppm]: 155.8, 151.0, 148.1, 143.0, 141.5, 140.0, 139.1, 134.8, 129.0, 126.0, 64.5, 36.1, 32.4, 32.0, 30.0, 23.1, 14.0

7.6 Synthesis of carbazole-based ladder polymers

7.6.1 Poly[2,5-bis(4´-decylbenzoyl)-1,4-phenylene-*co*-*N*-octylcarbazole-2,7-diyl] [40]

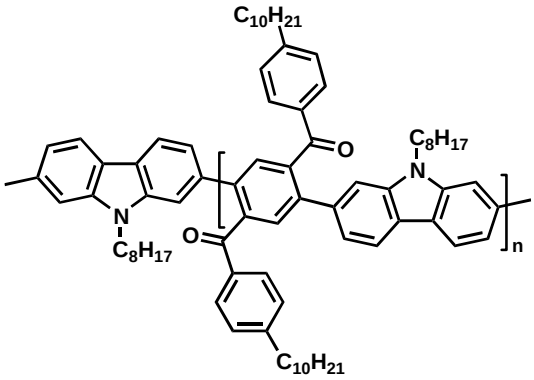

A flame-dried 100 ml two-neck flask was charged with N-octyl-2,7-bis(4´,4´,5´,5´-tetramethyl-1´,3´,2´-dioxaborolan-2´-yl)carbazole (531 mg; 1 mmol) and 1,4-bis(4´-decylbenzoyl)-2,5-dibromobenzene, (724 mg; 1 mmol) dissolved in 20 ml of toluene. Then, 35 mg $Pd(PPh_3)_4$, 1 g Na_2CO_3 in 5 ml of distilled water, and 5 ml of *n*-butanol were added. The mixture was refluxed under argon for 3 days. The resulting white suspension was poured into cold methanol, and the precipitate collected by filteration. After being dried under high vacuum for 24 h a light yellowish solid was obtained.

Yield: 570 mg (67.8 %).

GPC (THF): $\overline{M}_n$ = 10,200 g/mol ; $\overline{M}_w$ = 20,300 g/mol; D = 1.99

^{1}H-NMR (400 MHz, $C_2D_2Cl_4$):

δ(^{1}H) [ppm]: 7.8 –7.0, 3.9, 2.4, 1.5-1.1, 0.9-0.8

^{13}C-NMR (100 MHz, $C_2D_2Cl_4$):

δ(^{13}C) [ppm]: 198.1, 149.6, 149.2, 141.4, 140.4, 139.8, 137.4, 135.3, 130.5, 132.5, 128.7, 120.8, 122.3, 110.2, 36.4, 32.1, 29.7, 27.5, 25.9, 22.9, 21.4, 14.32

7.6.2 Poly[2,5-bis(4´-decylphenyl-hydroxymethyl)-1,4-phenylene-co-*N*-octylcarbazole-2,7-diyl] [41]

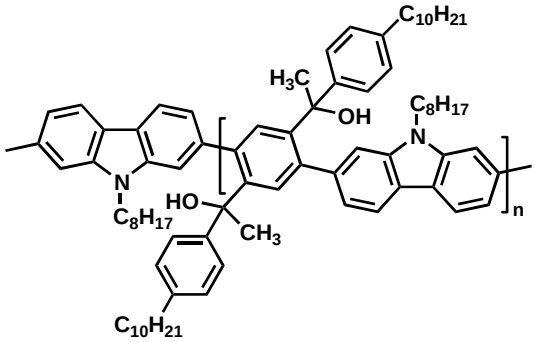

To a solution of polyketone **40** (400 mg; 0.476 mmol) in a mixture of toluene and tetrahydrofuran (1:1) Me-Li (200 mg; 10 mmol, 1.6M solution in diethyl ether) was added under argon. The solution was stirred for 30 minutes at room temperature and carefully quenched with ethanol, water and 2N aqueous hydrochloric acid. The organic layer was washed with water, dried and concentrated to dryness. The polymer was dried thoroughly under high vacuum for 24 h.

Yield: 310 mg (74.6 %).

^{1}H NMR (400 MHz, $C_2D_2Cl_4$):

δ(^{1}H) [ppm] : 7.4-7.0, 3.85, 2.4, 2.0-1.1, 0.9

^{13}C NMR (100 MHz, $C_2D_2Cl_4$):

δ(^{13}C) [ppm] : 149.6, 149.2, 141.4, 140.4, 139.8, 137.4, 135.3, 130.5, 132.5, 128.7, 75.8, 36.4, 32.1, 29.7, 27.5, 25.9, 22.9, 21.4, 14.32

7.6.3 Ladder-type poly(*para*-phenylene carbazole-2,7-diyl) [LPPPC 8]

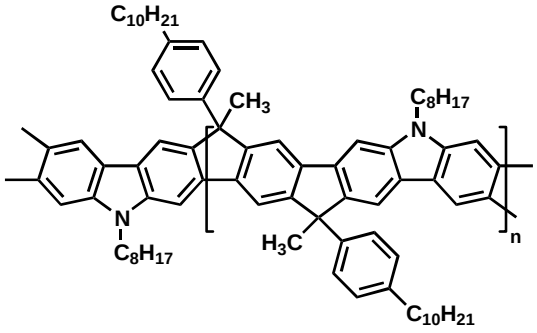

A solution of polyalcohol **41** (250 mg, 0.286 mmol) in 50 ml dichloromethane was treated with boron trifluoride etherate (2.896 g, 20.37 mmol). The solution was stirred for 30 minutes at room temperature. Then, 20 ml of ethanol were added, followed by 50 ml of water to quench the excess of boron trifluoride. The organic layer was carefully washed with water, dried and concentrated. Precipitation into acetone gave LPPPC as a yellow powder.

Yield: 200 mg (83.5 %).

GPC (THF): $\overline{M}_n$ = 35,300 g/mol; $\overline{M}_w$ = 69,100 g/mol; D = 1.95

UV/VIS-Absorption (in $CHCl_3$): λ_{max}, Abs. (nm) = 433, 464

(solid state): λ_{max}, Abs. (nm) = 434, 465

Photoluminescence (in $CHCl_3$): λ_{max}, PL (nm) = 470, 501

(solid state): λ_{max}, PL (nm) = 478, 553

^{1}H-NMR (400 MHz, $C_2D_2Cl_4$):

δ(^{1}H) [ppm]: 7.8-7.7, 7.3-7.2 (broad), 2.6, 2.0, 1.6, 1.4 , 1.3 ,0.9

^{13}C-NMR (100 MHz, $C_2D_2Cl_4$):

δ(^{13}C) [ppm]: 154.0, 146.0, 143.5, 141.09, 140.4, 140.1, 137.9, 134.19, 128.0, 126.6,123.8
115.2, 53.3, 35.2, 31.5, 30.7, 29.2, 28.9, 26.5, 25.0, 22.3, 13.7

7.6.4 Poly[2,5-bis(4´-decylbenzoyl)-1,4-phenylene-*co*-*N*-(3,7,11-trimethyldodecyl) carbazole-2,7-diyl]

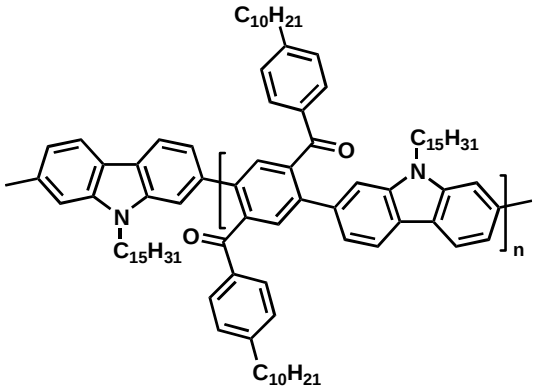

This polymer has been synthesized similar to **40**

Reagents:

N-(3,7,11-trimethyldodecyl)-2,7-bis(4´,4´,5´,5´-tetramethyl-1´,3´,2´-dioxaborolan-2´-yl)carbazole (629.2 mg; 1 mmol)

1,4-bis(4´-decylbenzoyl)-2,5-dibromobenzene (724 mg; 1 mmol)

$Pd(PPh_3)_4$, (35 mg) Na_2CO_3 (1 g) in 5 ml of distilled water, and 5 ml of *n*-butanol.

Yield: 750 mg (79.9 %)

GPC (THF): $\overline{M}_n$ = 3,700 g/mol; $\overline{M}_w$ = 5,600 g/mol; D = 1.50

^{1}H-NMR (400 MHz, $C_2D_2Cl_4$):

δ(^{1}H) [ppm]: 7.8 –7.0, 3.85, 1.73, 1.83, 1.6-1.0

^{13}C-NMR (100 MHz, $C_2D_2Cl_4$):

δ(^{13}C) [ppm]: 198.1, 149.6, 149.2, 141.4, 140.4, 139.8, 137.4, 135.3, 130.5, 132.5, 128.7, 120.8, 122.3, 110.2, 55.9, 39.7, 36.4, 37.5, 32.1, 29.7, 28.5, 25.9, 22.9, 20.1, 19.8

7.6.5 Poly[2,5-bis(4´-decylphenyl-hydroxymethyl)-1,4-phenylene-*co*-*N*-(3,7,11-trimethyldodecyl)carbazole-2,7-diyl]

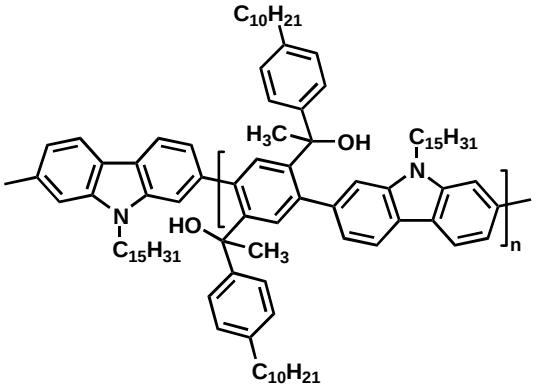

This polymer has been synthesized similar to **41** by using 650 mg of the corresponding polyketone.

Yield: 580 mg (86.3 %)

^{1}H-NMR (400 MHz, $C_2D_2Cl_4$):

δ(^{1}H) [ppm]: 7.4-7.0, 3.85, 1.73, 1.83, 1.6-1.1

^{13}C NMR (100 MHz, $C_2D_2Cl_4$):

δ(^{13}C) [ppm]: 149.6, 149.2, 141.4, 140.4, 139.8, 137.4, 135.3, 130.5, 132.5, 128.7, 120.8, 122.3, 110.2, 75.8, 39.7, 36.4, 37.5, 32.1, 29.7, 28.5, 25.9, 22.9, 20.1, 19.8

7.6.6 Ladder-type poly(*para*-phenylene carbazole-2,7-diyl) [LPPPC 15]

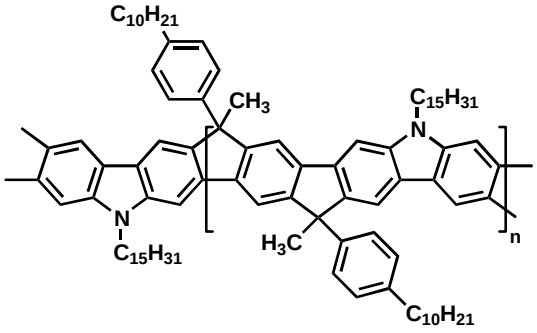

This polymer has been synthesized similar to **LPPPC 8** by using 500 mg of the corresponding polyalcohol

Yield: 410 mg (85 %).

GPC (THF): $\overline{M}_n$ = 10,900 g/mol; $\overline{M}_w$ = 20,600 g/mol; D = 1.88

UV/VIS-Absorption (in $CHCl_3$): $\lambda_{max,}$ Abs. (nm) = 432, 460

(solid state): λ_{max}, Abs. (nm) = 434, 465

Photoluminescence (in $CHCl_3$): λ_{max}, PL (nm) = 465, 495

(solid state): λ_{max}, PL (nm) = 467, 541

^{1}H-NMR (400 MHz, $C_2D_2Cl_4$):

δ(^{1}H) [ppm]: 7.8-7.7, 7.3-7.2 (broad), 3.85, 1.73, 1.83, 1.6-1.1

^{13}C-NMR (100 MHz, $C_2D_2Cl_4$):

δ(^{13}C) [ppm]: 154.0, 146.0, 143.5, 141.09, 140.4, 140.1, 137.9, 134.19, 128.0, 126.6, 123.8
22.7, 115.2, 53.3, 39.7, 36.4, 37.5, 32.1, 29.7, 28.5, 25.9, 22.9, 20.1, 19.8

7.6.7 Poly[2,5-bis(4´-decylbenzoyl)-1,4-phenylene-*co*-*N*-octylcarbazole-3,6-diyl] [44]

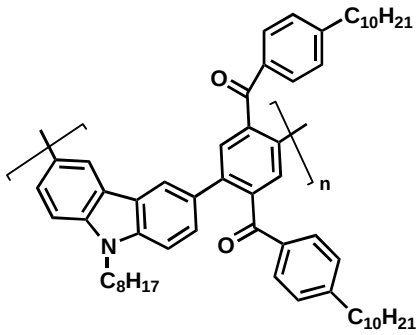

This polymer has been synthesized similar to **40**

Reagents:

N-octyl-3,6-bis(4´,4´,5´,5´-tetramethyl-1´,3´,2´-dioxaborolan-2´-yl)carbazole (501 mg; 1 mmol)

1,4-bis(4´-decylbenzoyl)-2,5-dibromobenzene (724 mg; 1 mmol)

$Pd(PPh_3)_4$, (35 mg) Na_2CO_3 (1 g) in 5 ml of distilled water, and 5 ml of *n*-butanol.

Yield: 550 mg (65.4 %)

GPC (THF): $\overline{M}_n$ = 4,500; $\overline{M}_w$ = 6,000; D = 1.33

^{1}H-NMR (400 MHz, $C_2D_2Cl_4$):

δ(^{1}H) [ppm]: 8.36 – 6.87 (m, ar-H, 16H), 3.85, 2.4, 2.0-1.1, 0.9

^{13}C-NMR (100 MHz, $C_2D_2Cl_4$):

δ(^{13}C) [ppm]: 196.2, 148.2, 143.0, 141.4, 137.7, 137.0, 130.2, 127.9, 127.0, 125.9, 113.4, 36.4, 32.1, 29.7, 27.5, 25.9, 22.9, 21.4, 14.32

7.6.8 Poly[2,5-bis(4´-decylphenyl-hydroxymethyl)-1,4-phenylene-*co*-*N*-octylcarbazole-3,6-diyl] [45]

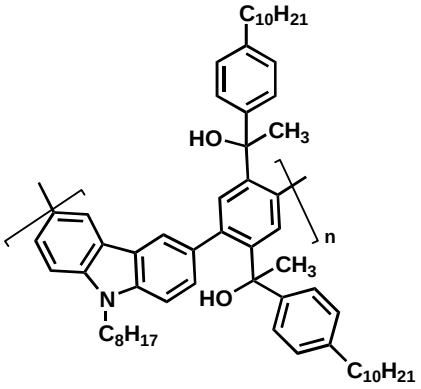

This polymer has been synthesized similar to **41** by using 400 mg (0.476 mmol) polyketone of the corresponding polyketone.

Yield: 320 mg (77.1 %)

^{1}H-NMR (400 MHz, $C_2D_2Cl_4$):

δ(^{1}H) [ppm]: 7.30 – 6.87 (m, ar-H, 16H), 3.85, 2.4, 2.0-1.1, 0.9

^{13}C-NMR (100 MHz, $C_2D_2Cl_4$):

δ(^{13}C) [ppm]: 141.4, 137.7, 137.0, 130.2, 128.9, 128.0, 125.9, 113.4, 75.20, 36.4, 32.1, 29.7, 27.5, 25.9, 22.9, 21.4, 14.32

7.6.9 Ladder-type poly(*para*-phenylene carbazole-3,6-diyl) [LPPPMC 46]

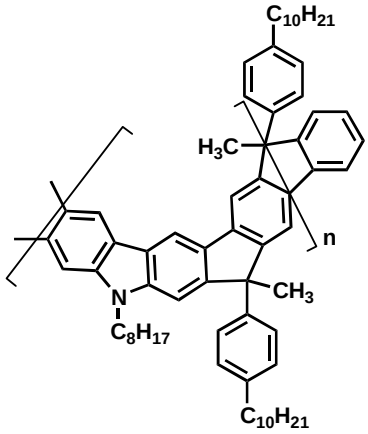

This polymer has been synthesized similar to **LPPPC 8** by using 250 mg (0.286 mmol) of the corresponding polyalcohol.

Yield: 200 mg (83.4 %).

GPC (THF): $\overline{M}_n$ = 6,800 g/mol; $\overline{M}_w$ = 10,800 g/mol; D = 1.58

UV/VIS-Absorption (in $CHCl_3$): $\lambda_{max,}$ Abs. (nm) = 361, 411

Photoluminescence (in $CHCl_3$): λ_{max}, PL (nm) = 460, 491

^{1}H-NMR (400 MHz, $C_2D_2Cl_4$):

δ(^{1}H) [ppm]: 8.32 – 6.58 (m, ar-H, 14H), 2.6, 2.0, 1.6, 1.4,1.3, 0.9

^{13}C-NMR (100 MHz, $C_2D_2Cl_4$):

δ(^{13}C) [ppm]: 150.2, 146.1, 144.9, 141.6, 140.6, 136.4, 128.6, 128.2, 115.3, 35.2, 31.5, 30.7 , 29.2 , 28.9 , 26.5 , 25.0 , 22.3, 13.7

7.7 Synthesis of alternating copolymers

7.7.1 Poly[N-octylcarbazole-2,7-diyl-*alt*-2,1,3-benzothiadiazole-4,7-diyl] [PCzBTDZ 50]

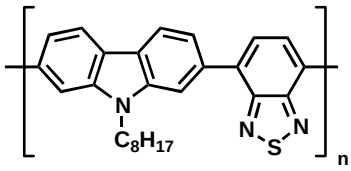

A flame-dried 100 ml three-necked flask was charged with N-octyl-2,7-bis (4′,4′,5′,5′-tetramethyl-1′,3′,2′-dioxaborolan-2′-yl)carbazole (531 mg; 1mmol) and 4,7-dibromo-2,1,3-benzothiadiazole (291.8 mg; 1mmol) dissolved in 20 ml of dry toluene. Then, 35 mg $Pd(PPh_3)_4$, 1 g Na_2CO_3 in 5 ml of distilled water, and 5 ml of *n*-butanol were added. The mixture was refluxed under argon for 3 days. After cooling to room temperature 50 ml of chloroform and 50 ml aq. HCl (2M) was added to the mixture. The organic layer was isolated, washed with HCl (2M) and saturated aq. $NaHCO_3$. The organic phase was dried over $MgSO_4$ and concentrated. The polymer was precipitated into a mixture of MeOH-acetone-aq. HCl (2M) (10:2:1 v/v/v). The solid material was extracted for 5-7 days in a soxhlet apparatus with acetone to remove short chain oligomers. The resulting polymer was collected and dried under vacuum.

Yield: 250 mg (60.8 %).

GPC (THF): $\overline{M}_n$ = 2,400 g/mol; $\overline{M}_w$ = 2,900 g/mol; D = 1.21

UV/VIS-Absorption (in $CHCl_3$): λ_{max}, Abs. (nm) = 320, 450

Photoluminescence (in $CHCl_3$): λ_{max}, PL (nm) = 535

(in solid state): λ_{max}, Abs. (nm) = 549

^{1}H-NMR (400 MHz, $C_2D_2Cl_4$):

δ(^{1}H) [ppm]: 8.2-7.8 (m, ar-H, 10H), 4.4, 2.0, 1.5, 1.4, 1.2, 0.8

^{13}C-NMR (100 MHz, $C_2D_2Cl_4$):

δ(^{13}C) [ppm]: 154.8, 141.8, 135.5, 134.0, 129.9, 122.9, 120.7, 110.5, 108.1, 43.2, 32.0, 29.4, 27.7, 22.7, 14.2

7.7.2 Poly[N-octylcarbazole-2,7-diyl-*alt*-2,2´-bithiophene-5,5´-diyl] [OCB2T 53]

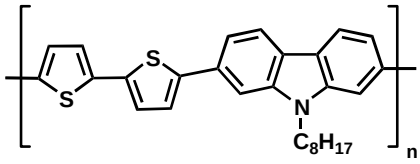

A flame dried 100 ml three-necked flask was charged with N-octyl-2,7-bis(trifluoromethanesulfonyl)carbazole (575.5 mg; 1 mmol), 5,5´-bis(trimethylstannyl)-2,2´-bithiophene (493 mg; 1 mmol), 35 mg $Pd(PPh_3)_4$ in 50 ml anhydrous toluene. The mixture was refluxed under argon for 3 days. After cooling to room temperature 50 ml chloroform and 50 ml aq. HCl (2M) was added to the mixture. The organic layer was isolated, washed with HCl (2M) and saturated aq. $NaHCO_3$. The organic phase was dried over $MgSO_4$ and concentrated. The polymer was precipitated into a mixture of MeOH-acetone-aq. HCl (2M) (10:2:1 v/v/v). The solid material was extracted for 5-7 days in a soxhlet apparatus with acetone to remove short chain oligomers. The resulting polymer was collected and dried under vacuum.

Yield: 150 mg (34 %)

GPC (THF): $\overline{M}_n$ = 2,000 g/mol; $\overline{M}_w$ = 2,500 g/mol D = 1.25

UV/VIS-Absorption (in $CHCl_3$): λ_{max}, Abs. (nm) = 325, 448

Photoluminescence (in $CHCl_3$): λ_{max}, PL (nm) = 502

8. References

[1] L. Salem, *The Molecular Orbital Theory of Conjugated Systems,* W. A. Benjamin Inc., *New York,* **1966.**

[2] G. Natta, G. Mozzanti, P. Corradini, *Atti Accad. Naz. Lincei, Cl. Sci. Fis. Mat. Nat. Rend.,* **1958,** *25,* 3.

[3] C. K. Chiang, C. R. Fincher, Y. W. Park, A. J. Heeger, H. Shirakawa, E. J. Louis, S. C. Gau, A. G. MacDiarmid, *Phys. Rev. Lett.,* **1977,** *39,* 1098.

[4] H. Shirakawa, E. J. Louis, A.G. MacDiarmid, C. K. Chiang, A. J. Heeger, *J. Chem. Soc. Chem. Commun.,* **1977**, *578*.

[5] J. Roncali. *Chem. Rev.,* **1992,** *92,* 711.

[6] A. J. Heeger, S. Kivelson, J. R. Schrieffer, W. P. Su, *Rev. Mod. Phys.,* **1988,** *60,* 781.

[7] A. J. Epstein, *Conjugated polymers* (J. L. Bredas and R. Silbey, Eds.), Kluver, Dordrecht, The Netherlands, **1991,** *p. 211.*

[8] A. J. Heeger *Synth. Met.,* **1993,** *55,* 3471.

[9] G. B. Street, *Polypyrrole: from powders to plastics, in Handbook of Conducting Polymers*, Vol. 1 (T. J. Skotheim Eds.), Marcel Dekker, New York, **1986**, *p.265*.

[10] A. J. Epstein, J. Joo, C. Y. Wu, A. Benatar, C. F. Faisst, J. Zegarski, A. G. MacDiarmid, *Polyaniline: Recent advances in processing and applications to welding of plastics in intrinsically conducting polymers:* An Emerging Technology (M. Aldissi, ed.), NATO ASI Series E, Vol. 246, Kluwer, Dordrecht, **1993,** *p.165*.

[11] P. M. Grant, T. Tani, W. D. Gill, M. Kroubni, T. C. Clarke, *J. Appl. Phys.,* **1981,** *52,* 869.

[12] E. Ebisawa, T. Kurokawa, S. Nara, *J. Apply. Phys.,* **1983,** *54,* 3255.

[13] J. Kanicki, *Polymeric semiconductor contacts and photovoltaic applications, in Handbook of Conducting Polymers,* Vol.1 (T.J. Skothem, eds.), Marcel Dekker, New York, **1986** *p. 544*.

[14] W. Helfrich, W. Schneider, *Phy. Rev. Lett.,* **1965,** *14,* 229.

[15] C. W. Tang, S. W. vanSlyke, *Appl. Phys. Lett.,* **1987,** *51,* 913.

[16] C. Adachi, T. Tsutsui, S. Saito, *Appl. Phys. Lett.,* **1990,** *56,* 799.

[17] C. Adachi, S. Tokito, T. Tsutsui, S. Saito, *Jpn. J. Appl. Phys.,* **1998,** *28,* L269.

[18] J. H. Burroughes, D. D. C. Bradley, A. R. Brown, R. N. Marks, K. Mackay, R. H. Friend, J. P. Calbert, *Nature*, **1990,** *347,* 539.

[19] In order to know current status of PLED research visit http://www.dow.com/dow_news/feature

[20] N. C. Greenham, R. H. Friend, *Solid State Phys.,* **1995,** *49,* 1.

[21] J. Grüner, F. Cacialli, R. H. Friend, *J. Appl. Phys.,* **1996,** *80,* 207.

[22] I. Murase, T. Ohnishi, T. Noguchi M. Hirooka, *Poly. Commun.,* **1984,** *25,* 327.

[23] D. R. Gagnon, J. D. Capistran, F. E. Karasz, R. W. Lenz, *Poly. Bull.,* **1984,** *12,* 293.

[24] P. L. Burn, D. D. C. Bradley, R. H. Friend, D. A. Halliday, A. B. Holmes, R. W. Jackson, A. M. Kraft, *J. Chem. Soc. Perkin Trans 1,* **1992,** 3225.

[25] (a) S. Miyata, H. S. Nalwa*, Organic Electroluminescent Materials and Devices, Gordon and Breach Publishers, Amsterdam,* **1997**; (b) H. Bässler*, Poly. Adv. Technol.,* **1998,** 9, 402.

[26] (a) R. O. Garay, U. Baier, C. Bubeck, K. Müllen, *Adv. Mater.,* **1993,** *5,* 561; (b) J. Morgado, F. Cacialli, J. Grüner, N. C. Greenham, R. H. Friend, *J. Appl. Phys.,* **1999,** *85,* 1784.

[27] (a) J. D. Hong, D. Kim, K. Cha, J. I. Jin, *Synth. Met.,* **1997,** *84,* 815; (b) M. Gao, B. Richter, S. Kirstein, H. Möhwald, *J. Phys. Chem. B,* **1998,** *102,* 4096.

[28] (a) A. Wu, M. Kakimoto, M. Jikei, Y. Imai, S. Ukishima, Y. Takahashi, *Chem. Lett.,* **1994,** 2319; (b) A. Wu, M. Kakimoto, *Adv. Mater.,* **1995,** *7,* 812.

[29] C. Braun, A. J. Heeger, *Appl. Phys. Lett.,* **1991,** *58,* 1982.

[30] (a) M. R. Anderson, G. Yu, A. J. Heeger, *Synt. Met.,* **1997,** *85,* 1275; (b) B. J. Schwartz, F. Hide, M. R.Anderson, A. J. Heeger, *Chem. Phys. Lett.,* **1997,** *265,* 327.

[31] K. L. Brandon, P. G. Bentley, D. D. C. Bradley, D. A. Dunmur, *Synt. Met.,* **1997,** *91,* 305.

[32] C. T. Wong, W. K. Chan, *Adv. Mater.,* **1999,** *11,* 455.

[33] M. Hamaguchi, K. Yoshino, *Jpn. J. Appl. Phys.,* **1995,** *34,* L712.

[34] J. Salbeck, *Ber. Bunsenges, Phys. Chem.,* **1996,** *100,* 1666.

[35] M. Grell, D. D. C. Bradley, *Adv. Mater.,* **1999,** *11,* 895.

[36] M. Herold, J. Gemeiner, W. Riess, M. Schwoerer, *Synt. Met.,* **1996,** *76,* 109.

[37] N. C. Greenham, S. C. Moratti, D. D. C. Bradley, R. H. Friend, A. B. Holmes, *Nature,* **1993,** *365,* 628.

[38] D. Y. Kim, H. N. Cho, C. Y. Kim, *Prog. Polym. Sci.,* **2000,** *25,* 1089.

[39] G. Grem, G. Leditzky, B. Ullrich, G. Leising, *Synth. Met.,* **1992,** *51,* 383.

[40] Y. Yang, Q. Pei, A. J. Heeger, *J. Appl. Phys.,* **1996,** *79,* 934.

[41] Y. Yang, Q. Pei, A. J. Heeger, *Synth. Met.,* **1996,** *78,* 263.

[42] S. A. Chen, C. I. Chao, *Synth. Met.,* **1996,** *79,* 93.

[43] A. Edwards, S. Blumstengel, I. Sokolik, R. Dorsinville, H. yun, T. K. Kwei, Y. Okamoto, *Appl. Phys. Lett.,* **1997,** *70*, 298.

[44] V. N. Blinznyuk, S. A. Carter, J. C. Scott, G. Klärner, R. D. Miller, D.C. Miller, *Macromol.,* **1999,** *32,* 361.

[45] Q. Pei, Y. J. Yang, *J. Am. Chem. Soc.,* **1996,** *118,* 7416.

[46] Y. Ohmori, M. Uccida, K. Muro, K. Yoshino, *Jpn. J. Appl. Phys.,* **1995,** *34,* L587.

[47] Y. Ohmori, N. Tada, A. Fujii, H. Ueta, T. Sawatani, K. Yoshino, *Thin Solid Films,*

1998, *331,* 89.

[48] J. S. Kim, R. H. Friend, F. Cacialli, *Appl. Phys. Lett.,* **1999,** *74,* 3084.

[49] D. Sainova, T. Miteva, H. G. Nothofer, U. Scherf, I. Glowacki, J. Ulanski, H. Fujikawa, D. Neher, *Appl. Phys. Lett.,* **2000,** *76,* 1810.

[50] E. J. W. List, R. Guentner, P. Scandiucci de Freitas, U. Scherf, *Adv. Mater.,* **2002,** *14,* 374.

[51] A. Itaya, K. Okamoto, S. Kusabayashi, *Bull. Chem. Soc. Jpn.,* **1979,** *52,* 2218.

[52] J. M. Pearson, *Encyclopaedia of polymer science and Enggnering* Wiley, New York, **1989**, *P. 257.*

[53] F. Bai, M. Zheng, G. Yu, D. Zhu, *Thin Solid Films,* **2000,** *363,* 118.

[54] O. Stephan, J. C. Vial, *Synth. Met.,* **1999,** *106,* 115.

[55] J. F. Morin, M. Leclerc, *Macromol.,* **2001,** *34,* 4680.

[56] J. F. Morin, S. Beaupre, M. Leclerc, I. Levesque, M. D´lorio, *Appl. Phys. Lett.,* **2002,** *80,* 341.

[57] U. Scherf, K. Müllen, *Adv. Polym. Sci.,* **1995,** *123.*

[58] D. S. Boudreaux, R. R. Chance, J. F. Wolf, L. W. Shacklette, J. L. Bredas, B. Themans, J. M. Andre, R. J. Silbey, *Chem. Phys.,* **1986,** *85,* 4584.

[59] J. K. Stille, E. L. Mainen, *Macromol.,* **1968,** *1,* 36.

[60] F. E. Arnold, R. L. VanDeussen, *J. Appl. Poly. Sci,.* **1971,** *15,* 2035.

[61] A. J. Sicree, F. E. Arnold, R. L. Van Deusen, *J. Polym. Sci. Polym. Chem. Ed.,* **1974,** *12,* 265.

[62] A-D Schlüter, *Adv. Mater.,* **1991,** *3,* 282.

[63] U. Scherf, K. Müllen, *Polymer,* **1992,** *33,* 2443.

[64] J. M. Tour, J. J. S. Lamba, *J. Am. Chem. Soc.* **1993,** *115,* 4935.

[65] G. K. Noren, J. K. Stille, *Macromol. Rev.,* **1971,** 5, 385.

[66] R. H. Baughman, J. L. Bredas, R. R. Chance, R. I. Elsenbaumer, L. W. Shacklette, *Chem. Rev.,* **1982,** *82*, 209.

[67] M. Rehahn, A. D. Schlüter, G. Wegner, W. J. Feast, *Polymer,* **1989,** *30,* 1060.

[68] M. Rehahn, A. D. Schlüter, G. Wegner, W. J. Feast, *Polymer,* **1989,** *30,* 1054.

[69] A-D. Schlüter, *Acta Polym.,* **1993,** *44,* 59.

[70] A-D. Schlütter, *Synthesis of poly(para-phenylene) in Handbook of Conducting Polymers* (T. Skothem, eds.), Marcel Dekker, New york, **1998,** *p.209*.

[71] U. Scherf, K. Müllen, *Makromol. Chem. Rapid Comm.,* **1991,** *12,* 489.

[72] N. Miyaura, A. Suzuki, *Chem. Rev.,* **1995,** *95,* 2457.

[73] W. Graupner, S. Eder, S. Tasch, G. Leising, G. Lanzani, M. Nisoli, S. de Silvestri, U. Scherf, *J. Fluorescence,* **1995,** *7,* 195.

[74] U. Scherf, E. J. W. List, *Adv. Mater.,* **2002,** *14,* 477.

[75] G. Green, G. Leising, *Synth. Met.,* **1993,** *55-57*, 4105.

[76] J. Pan, U. Scherf, A. Schreiber, R. Bilke, D. Haarer, *Synth. Met.,* **2000,** *115,* 79.

[77] S. Tasch, A. Niko, G. Leising, U. Scherf, *Appl. Phys. Lett.,* **1996,** *68,* 1090.

[78] D. Hertel, H. Bässler, U. Scherf, *Adv. Mater.,* **1998,** *10,* 1119.

[79] S. Barth, H. Bässler, U. Scherf, K. Müllen, *Chem. Phys. Lett.,* **1998,** *288,* 147.

[80] H. P. Weber, R. Ulrich, *Appl. Phys. Lett.,* **1971,** *19,* 38.

[81] M. D. McGehee, A. J. Heeger, *Adv. Mater.*, **2000,** *12,* 1655.

[82] W. Graupner, G. Leising, G. Lanzani, M. Nisoli, S.de Silvestri, U. Scherf, C*hem. Phys. Lett.,* **1995,** *246,* 95.

[83] A. Haugeneder, M. Neges, C. Kallinger, W. Spirkl, U. Lemmer, J. Feldmann, U. Scherf. *J. Appl. Phys.,* **1999,** *85,* 1124.

[84] C. Zenz, W. Graupner, S. Tasch, G. Leising, K. Müllen, U. Scherf, *Appl. Phys. Lett.,* **1997,** *71,* 2566.

[85] C. Kallinger, M. Hilmer, A. Haugeneder, M. Perner, W. Spirkl, U. Lemmer, J. Feldmann, U. Scherf, K. Müllen, A. Gombert, V. Wittwer, *Adv. Mater.,* **1998,** *10,* 920.

[86] A. Köhler, J. Grüner, R. H. Friend, K. Müllen, U. Scherf, *Chem. Phys. Lett.,* **1995,** *243,* 456.

[87] A. Hohenau, C. Cagran, G. Kranzelbinder, U. Scherf, G. Leising, *Adv. Mater.,* **2001**, *13,* 1303.

[88] J. Grimme, M. Kreyenschmidt, F. Uckert, K. Müllen and U. Scherf, *Adv. Mater.,* **1995,** *7,* 3.

[89] U. Lemmer, S. Heun, R. F. Mahrt, U. Scherf, M. Hopmeier, U. Siegner, E. O. Göbel, K. Müllen, H. Bässler, *Chem. Phys. Lett.,* **1995,** 240, 373.

[90] M. A. Baldo, D. F. O'Brien, Y. You, A. Shoustikov, S. Sibley, M. E. Thompson, S.R. Forrest, *Nature,* **1998,** *395,* 151.

[91] R. H. Friend, D. Bradley, A. B. Holmes, *Physics World,* **1999,** *10,* 4246.

[92] R. H. Friend, R. W. Gymer, A. B. Holmes, J. H. Burroughes, R. N. Marks, C. Taliani, D. D. C. Bradley, D. A. Dos Santos, J. L. Brédas, M. Lögdlund, W. R. Salaneck, N*ature,* **1999,** *397,* 121.

[93] Y. V. Romanovskii, A. Gerhard, B. Schweitzer, U. Scherf, R. I. Personov, H. Bässler, *Phys. Rev. Lett.,* **2000,** *84,* 1027.

[94] V. Cleave, G. Yahioglu, P. Le Barny, D. H. Hwang, A. B. Holmes, R. H. Friend, N. Tessler *Adv. Mater.,* **2001,** *13*, 44.

[95] X. Gong, J. C. Ostrowski, G. C. Bazan, D. Moses, A. J. Heeger, M. S. Liu, A. K.-Y. Jen, *Adv. Mater.,* **2003**, *15*, 45.

[96] J. Stampfi, W. Graupner, G. Leising, U. Scherf, *J. Lumin.,* **1995,** 63, 117.

[97] J. M. Lupton, A. Pogantsch, T. Piok, E. J. W. List, S. Patil, U. Scherf, *Phys. Rev.*

Lett., **2002,** *89,* 167401.

[98] M. Catellani, E. Motti, L. Paterlini, *J. Organomet. Chem.,* **2000,** *594,* 240.

[100] A. P. Monkman, H. D. Burrows, I. Hamblett, S. Navaratnam, *Chem. Phys. Lett.,* **2001,** *340,* 467.

[100] R. F. Mahrt, U. Siegner, U. Lemmer, U. Hopmeier, U. Scherf, S. Heun, E. Göbel, K. Müllen, H. Bässler, *Chem. Phys. Lett.,* **1995,** *240,* 373.

[101] J. S. Wilson, A. S. Dhoot, A. J. A. B. Seeley, M. S. Khan, A. Köhler, R. H. Friend *Nature,* **2001,** *413,* 828.

[102] J. S. Wilson, N. Chawdhury, M. R. A. Al-Mandhary, M. Younus, M. S. Khan, P. R. Raithby, A. Kohler, R. H. Friend, *J. Am. Chem. Soc.,* **2001,** *123*, 9412.

[103] B. Kippelen, A. Golemme, E. Hendrickx, J. F. Wang, S. R. Marder, N. Peyghambarian; *Photorefractive Polymers and Polymer-Dispersed Liquid Crystals, in Field Responsive Polymers: Electroresponsive, Photoresponsive and Stimuli responsive polymers in Chemistry and Biology,* ACS Symposium Series; I. M. Kahn, J. S. Harrison, Eds; American Chemical Society: Washington DC, **1999**; *726,* p. 204.

[104] C. Xia, R. C. Advincula, *Macromol.,* **2001,** *34,* 5854.

[105] H. Kimura-Suda, Y. Zhang, T. Sassa, T. Wada, H. Sasabe, *Adv. Mater.,* **2000,** *12,* 1196.

[106] W. Y. Wong, D. L. Lu, K. H. Choi, J. X. Shi, *Macromol.,* **2002,** *35,* 5317.

[107] J. Kido, K. Hongawa, K. Okuyama, K. Nagai, *Appl. Phys. Lett.,* **1994,** *64,* 815.

[108] A. Suzuki, *J. Organomet. Chem.,* **1999,** *576,* 147.

[109] V. Cimrova, M. Remmes, D. Neher, G. Wegner, *Adv. Mater.,* **1996,** *8,* 146.

[110] S. Schlüter, J. Frahn, B. Karakaya, A.-D. Schlüter, *Macromol. Chem. Phys.,* **2000,** *201,* 139.

[111] U. Asawapirom, R. Güntner, R. Forster, T. Farrell, U. Scherf, *Synthesis,* **2002,** 1136.

[112] G. Zotti, G. Schiavon, S. Zecchin, J. F. Morin, M. Leclerc, *Macromol.,* **2002,** *35,* 2122.

[113] D. Hertel, S. Setayesh, H.-G. Nothofer, U. Scherf, K. Müllen, H. Bässeler, *Adv. Mater.,* **2001,** *13,* 65.

[114] A. Kadashchuk, D. S. Weiss, P. M. Borsenberger, S. Nespuarek, N. Ostapenko, V. Zaika, *Chem. Phys.,* **1999,** *247,* 307.

[115] A. Kadashchuk, N. Ostapenko, V. Zaika, S. Nespuarek, *Chem. Phys.,* **1998,** *234,* 285.

[116] A. Kadashchuk, Yu. Skryshevski, A. Vakhnin, N. Ostapenko, V. I. Arkhipov, H. Bässler, *Phys. Rev. B,* **2001,** *63,* 115205.

[117] V. I. Arkhipov, E. V. Emelianova, A. Kadashchuk, H. Bässler, *Chem. Phys.,* **2001,** *266,* 97.

[118] F. Stolzenburg, H. Bässeler, *Mol. Cryst. Liq. Cryst.,* **1989,** *175,* 147.

[119] D. Hertel, H. Bässeler, U. Scherf, H. H. Hörhold, *J. Chem. Phys.,* **1999,** *110,* 9214.

[120] I. A. Tale, *Phys. Status Solidi A,* **1981,** *66,* 65.

[121] P. I. Butlers, I. A. Tale, J. Pospisil, S. Nespuarek, *Prog. Colloid Polym. Sci.,* **1988,** *78,* 93.

[122] S. Patil**,** U. Scherf, A. Kadashchuk, *Adv. Funct. Mater.,* **2003**, *13*, 609.

[123] A. L. McClellan, *Tables of Experimental Dipole moments, Freeman, San Francisco, CA* **1963.**

[124] R. F. Young, *Philos. Mag. B.,* **1995,** *72,* 435.

[125] S. Nespuarek, J. Sworakowaski, A. Kadashchuk, *IEEE Trans. Dielectr. Electr. Insul.,* **2001,** *8,* 432.

[126] A. Kadashchuk, N. Ostapenko, N. Lukashenko, *Adv. Mater. Opt. Electron.,* **1997,** *7,* 99.

[127] P. M. Borsenberger, H. Bässeler, *J. Chem. Phys.,* **1991,** *95,* 5327.

[128] P. M. Borsenberger, D. S. Weiss, *Organic photoreceptors for Xerography,* Marcel Dekker, New York **1998.**

[129] A. J. Campbell, D. D. C. Bradley, H. Antoniadis, *Appl. Phys. Lett.,* **2001,** *79,* 2133.

[130] K. Pilgram M. Zupan, R. J. Skiles*, J. Heterocycl. Chem.,* **1970,** *7,* 629.

[131] J. Huang, Y. Niu, W. Yang, Y. Mo, M. Yuan, Y. Cao, *Macromol.,* **2002,** *35,* 6080.

[132] M. Jayakannan, J. L. J. van Dongen, R. A. J. Janssen, *Macromol.,* **2001,** *34,* 5386.

[133] J. K. Stille, *Angew. Chem. Int. Ed. Engl.,* **1986,** *25,* 508.

[134] B. Tsuie, J. L. Reddinger, G. A. Sotzing, J. Soloducho, A. R. Katritzky, J. R. Reynolds, *J. Mater. Chem.,* **1999,** *9,* 2189.

[135] J. O. Romano, M. Hoffmann, M. P. De Haas, L. D. A. Siebbeles, J. M. Warman, *Nature,* **1998,** *392,* 54.

[136] M. G. Harrison, S. Möller, G. Weiser, U. Urbasch, R. F. Mahrt, H. Bässeler, U. Scherf, *Phys. Rev. B,* **1999,** *60,* 8650.

9. List of publications

1. New Conjugated Ladder Polymer Containing Carbazole Moieties
   S. Patil, U. Scherf, A. Kadashchuk,
   Advanced Functional Materials, **2003**, *13*, 609-614.
2. Intrinsic Room Temperature Electrophophoresence from conjugated polymer
   J. M. Lupton, A. Pogantsch, T. Piok, E. J. W. List**, S. Patil**, U. Scherf,
   Phyical Review Letters, **2002,** *89,* 16740.
3 Semiconducting Polymer Nanospheres in Aqueous Dispersion Prepared by a Miniemulsion Process
   K. Landfester, R. Montenegro, U. Scherf, R. Güntner, U. Asawapirom, **S. Patil**, D. Neher, Thomas Kietzke
   Advanced Materials, **2002,***14,* 651-654.
4 Organic Light Emitting Devices Fabricated from Semiconducting Nanospheres
   T. Piok, S.Gamerith, C. Gadermaier, **S. Patil**, R.Montenegro, T. Kietzke, U. Scherf, K. Landfester, D. Neher, E.J.W. List
   Advanced Materials, **2003,** *15,* 800-804.
5. Crossover from diffusion to annihilation limited phosphorescence in conjugated polymers
   M. Reufer, F. Schindler, **S. Patil**, U. Scherf, J. M. Lupton
   Chemical Physics Letters, **2003,** *381,* 60-66.
6. Self-absorption effects in a LEC with low Stokes shift
   F. P. Wenzl, P. Pachler, E. J. W. List, D. Somitsch, P. Knoll, **S. Patil**, R. Guentner, U. Scherf, G. Leising
   Physica A, **2002** 1251-1254.
7. A detailed study of the photophysics of organic semiconducting nanospheres
   T. Piok, L. Romaner, C. Gadermaier, F. P. Wenzl, **S. Patil,** R.Montenegro, K. Landfester, G. Lanzani, G. Cerullo, U. Scherf, E. J. W. List
   Synthetic Metals, **2003,** *139*, 609-612.

10. Acknowledgment

I owe a huge debt of gratitude to my advisor Prof. Ullrich Scherf for his continuous support and fruitful discussion during this work. He is not only a great scientist with deep vision but also a kind person. In every sense, none of this work would have been possible without him. I am deeply thankful to Dr. S. Radhakrishnan (NCL, Pune India). He introduced me to the world of conjugated polymers and his approach to research, broad-minded tolerance, intuitive discussions helped me significantly during my Ph.D. work. I am grateful to all my co-workers Roland Güntner, Askin Bilge, Frank Galbrecht, Benjamin Nehls, Eduard Preis, Sascha Prentzel, Daniel Krüger Dr. Bernhard Köhler, Dr. Deqing Gao for their assistance and companionship throughout my stay in the Scherf group. I am grateful to Dr. Udom Asawapirom and Torsten Bünnagel for their assistance with computer related problems while preparing this thesis. Special, thanks goes to Dr. Tony Farrell and Dr. Michael Forster for progressive comments on my research work as well as my thesis. I am also thankful to my friends Swapna and Jitendra for giving me good company in office as well as in laboratory. Special thanks goes to Swapna for providing good Indian food, so I never felt I am away from home. I am thankful to our group secretary Bianca Enz for always being there to solve my all administrative problems. I would like to thank many people who have collaborated with me and contributed to various parts of this research, in particular: Dr. John Lupton, Dr. Emil List for electroluminescence measurement data, Dr. Andrey Kadashchuk is gratefully acknowledged for TSL measurement data. I wish to express my warm and sincere thanks to Prof. Markus Antonietti for giving me permission to carry out analytical measurements (NMR, GPC, Elemental analysis-etc) in the Max-Planck Institute of colloids and interface, Potsdam. My warm thanks to Olaf Niemeyer, Sylvia Pirok, Anke Helfer for GPC and NMR measurements. I feel a deep sense of gratitude for my wonderful parents. For always being there when I needed them most, and never once complaining about how infrequently I make telephone calls, they deserve far more credit than I can ever give them. My final, and most heartfelt, acknowledgment must go to my wife Bhagyashree for her support, encouragement, and companionship which has turned my life journey into a pleasure. Finally, I would like to thank all whose direct and indirect support helped me completing my thesis in time.